

## **Distribution Agreement**

In presenting this thesis or dissertation as a partial fulfillment of the requirements for an advanced degree from Emory University, I hereby grant to Emory University and its agents the non-exclusive license to archive, make accessible, and display my thesis or dissertation in whole or in part in all forms of media, now or hereafter known, including display on the world wide web. I understand that I may select some access restrictions as part of the online submission of this thesis or dissertation. I retain all ownership rights to the copyright of the thesis or dissertation. I also retain the right to use in future works (such as articles or books) all or part of this thesis or dissertation.

Signature:

---

Sarah E. Anderson

---

Date

Copy Number of an Antibiotic Resistance Locus Controls Aminoglycoside Heteroresistance and  
a Virulence Switch in *Acinetobacter baumannii*

By

Sarah E. Anderson

Doctor of Philosophy

Graduate Division of Biological and Biomedical Sciences

Microbiology and Molecular Genetics

---

Philip N. Rather, Ph.D.  
Advisor

---

Joanna B. Goldberg, Ph.D.  
Committee Member

---

William M. Shafer, Ph.D.  
Committee Member

---

Charles P. Moran, Ph.D.  
Committee Member

---

David S. Weiss, Ph.D.  
Committee Member

Accepted:

---

Lisa A. Tedesco, Ph.D.  
Dean of the James T. Laney School of Graduate Studies

---

Date

Copy Number of an Antibiotic Resistance Locus Controls Aminoglycoside Heteroresistance and  
a Virulence Switch in *Acinetobacter baumannii*

By

Sarah E. Anderson

B.S., University of North Carolina, 2013

Advisor: Philip N. Rather, Ph.D.

An abstract of

A dissertation submitted to the Faculty of the

James T. Laney School of Graduate Studies of Emory University

in partial fulfillment of the requirements for the degree of

Doctor of Philosophy

in Graduate Division of Biological and Biomedical Sciences

Microbiology and Molecular Genetics

2019

## Abstract

### Copy Number of an Antibiotic Resistance Locus Controls Aminoglycoside Heteroresistance and a Virulence Switch in *Acinetobacter baumannii*

By: Sarah E. Anderson

*Acinetobacter baumannii* is a Gram-negative opportunistic pathogen. This bacterium is a significant public health threat, in part due to the high levels of antibiotic resistance exhibited by many strains of this pathogen. Therefore, more research is needed into the identification of novel *A. baumannii* drug targets, as well as a more complete understanding of the antibiotic resistance mechanisms employed by this species. This work is focused on aminoglycoside heteroresistance and colony opacity variation in the multidrug-resistant *A. baumannii* strain AB5075. Heteroresistance is a phenomenon wherein a subpopulation of cells within an isogenic bacterial strain exhibit increased resistance to an antimicrobial. Colony opacity variation refers to the production of opaque and translucent colony types by a bacterium; in *A. baumannii* this involves a high-frequency switch between virulent opaque (VIR-O) and avirulent translucent (AV-T) colonies. Here, we establish that both aminoglycoside heteroresistance and opacity switching are controlled by copy number of a horizontally-acquired antibiotic resistance locus. AB5075 spontaneously gives rise to cells with RecA-dependent high-copy amplifications of this locus, which includes the aminoglycoside resistance gene *aadB*. This leads to increased *aadB* expression in a subset of cells, which results in heteroresistance to tobramycin and gentamicin. Variations in copy number of this locus also result in changes in the frequency of VIR-O to AV-T switching in AB5075. Opaque cells exhibiting a single copy of this locus switch to AV-T at a low frequency, a phenotype designated as low-switching opaque (LSO). Duplications of this locus lead to nearly three-log fold increases in switching to AV-T. The element responsible for controlling switching is encoded at the 5' end of the *aadB* gene, and our evidence suggests that this element is an sRNA. We further determined that LSO variants exhibit decreased virulence relative to normal VIR-O cells carrying the duplication, possibly due to decreased expression of virulence genes in the LSO variant. This work establishes the important role of gene duplications and amplifications in mediating phenotypic heterogeneity in *A. baumannii*. This research also increases our understanding of a complex virulence switch, which could eventually lead to the development of novel virulence-targeted therapeutics for this pathogen.

Copy Number of an Antibiotic Resistance Locus Controls Aminoglycoside Heteroresistance and  
a Virulence Switch in *Acinetobacter baumannii*

By

Sarah E. Anderson

B.S., University of North Carolina, 2013

Advisor: Philip N. Rather, Ph.D.

A dissertation submitted to the  
Faculty of the James T. Laney School of Graduate Studies of Emory University  
in partial fulfillment of the requirements for the degree of  
Doctor of Philosophy  
in Graduate Division of Biological and Biomedical Sciences  
Microbiology and Molecular Genetics

2019

## Acknowledgements

I would like to thank my advisor, Dr. Phil Rather, for his excellent mentoring over the past three years. I am so grateful to him for taking a chance on me and welcoming me into his lab when my first thesis lab didn't work out. Thank you for your scientific guidance, flexibility as a mentor, and support of me and my goals. I would also like to thank the rest of my thesis committee for their support and advice throughout my graduate career. I am particularly grateful to Dr. Bill Shafer for mentoring me through ARTDTP, and for providing me with excellent advice at some critical junctures of my PhD.

I would like to thank my lab mates for their moral support, camaraderie, and help throughout the years. A particular thank you to Aimee Tierney, who has been a consistent source of laughs and encouragement. Thank you also to our Weiss lab collaborators, Chui Yoke Chen and Edgar Sherman, for your scientific expertise and help in fleshing out the stories presented here.

I would also like to thank all my loved ones. Thank you to my parents, for encouraging me to pursue my dreams, and for always listening and offering support when I was discouraged that those dreams seemed out of reach. I quite literally wouldn't be here without you, and I love you both. Thank you to my brother, my grandmother, and the rest of my family for all your love and support. Thank you to my friends for all the trips, visits, and fun, and for reminding me that life isn't just about science. Thank you in particular to Margaret Neville; I can't imagine what my life would be like without you as my best friend. Thank you for listening every time I called you to rant about grad school, even if you frequently had no idea what I was saying. Finally, I want to thank my girlfriend, Kenley Patanella, for helping me to be more fully myself and for being so supportive, sweet, and wonderful. I love you and I'm so glad we found each other.

## Table of Contents

Abstract

Acknowledgements

Table of Contents

List of Tables and Figures

Chapter 1: Introduction.....1

Chapter 2: Aminoglycoside Heteroresistance in *Acinetobacter baumannii* AB5075.....38

Chapter 3: Copy Number of an Integron-Encoded Antibiotic Resistance Locus Regulates a  
Virulence and Opacity Switch in *Acinetobacter baumannii* AB5075.....81

Chapter 4: Distinguishing Colony Opacity Variants and Measuring Opacity Variation in  
*Acinetobacter baumannii*.....153

Chapter 5: Discussion.....166

## Tables and Figures

### Chapter 2

Table 1: The tobramycin-resistant subpopulation exhibits increased cross-resistance to gentamicin but not other antimicrobials

Table 2: HetR-O2 and hetR-T1 exhibit gene amplifications that include *aadB*

Table 3: *aadB* copy number in the presence and absence of antibiotic selection

Table 4: Relative copy number of *aadB* in *recA::Tc* isolates with increased tobramycin resistance

Figure 1: AB5075 produces a subpopulation of cells with increased resistance to tobramycin

Figure 2: Characterization of tobramycin heteroresistance in AB5075

Figure 3: Increased expression of *aadB* in cells with increased tobramycin resistance

Figure 4: Amplified region in p1AB5075 that includes *aadB*

Supplemental Figure S1: Complementation of *recA* leads to increased heteroresistance in the *recA::Tc* mutant

Supplemental Figure S2: Characterization of tobramycin heteroresistance in a *recA* mutant

Supplemental Table 1: Oligonucleotides used in this study

### Chapter 3

Figure 1: Wild-type AB5075 produces at least two subpopulations of opaque variants

Figure 2: Copy number of an antibiotic resistance locus positively correlates with switching frequency to AV-T

Figure 3: p1AB5075 carrying two copies of the duplicated region is sufficient to cause increased switching to AV-T

Figure 4: Overexpression of the *aadB* region is sufficient to stimulate switching

Figure 5: The element responsible for stimulating switching is encoded towards the 5' end and upstream of *aadB*

Figure 6: Data suggest that the element controlling switching is a functional sRNA

Figure 7: The LSO variant exhibits decreased virulence in a mouse pneumonia infection model

Supplemental Table S1: The LSO variant exhibits decreases in antimicrobial resistance relative to the normal VIR-O

Supplemental Table S2: Oligonucleotides used in this study

Supplemental Figure S1: Overexpression of the entire duplicated region increases switching to the same level as overexpression of *aadB* alone

Supplemental Figure S2: AadB protein production is not required for stimulation of switching by the *aadB* region

Supplemental Figure S3: Transposon insertions blocking switching do not localize to any predicted ORFs encoded in the *aadB* upstream region

Supplemental Data File S1: RNA-seq results comparing the normal VIR-O and LSO

## **Chapter 4**

Figure 1: Examples of stereo microscopes with oblique illumination that can be used to visualize colony opacity

Figure 2: Examples of translucent (AV-T), opaque (VIR-O), and switching VIR-O colonies.

## Chapter 1: Introduction

### *Acinetobacter baumannii*

*Acinetobacter baumannii* is a highly antibiotic resistant bacterium and an emerging public health threat. In a 2013 report, the CDC estimated that *A. baumannii* was responsible for 12,000 infections in the United States each year (1). As an opportunistic pathogen, *A. baumannii* is capable of causing a variety of infections, including pneumonia, catheter-associated urinary tract infections, meningitis, bloodstream infections, and wound infections (2). *A. baumannii* is generally considered to be a nosocomial pathogen; however, it can also cause severe community-acquired infections, particularly in tropical regions (3). This pathogen was also commonly associated with combat wound infections during Operation Iraqi Freedom (4-7). Treatment of *A. baumannii* infections is complicated by widespread antibiotic resistance in this species, which is often associated with the horizontal acquisition of mobile resistance elements (8, 9). The CDC has estimated that nearly two-thirds of *A. baumannii* infections exhibit multidrug resistance (1). In 2017, the World Health Organization named carbapenem-resistant *A. baumannii* as its most critical priority for research and development of new antibiotics (10). This announcement underscores the urgent need for novel drug targets and treatment strategies for this pathogen.

*Acinetobacter* was first isolated from soil in 1911 by Dutch microbiologist M. W. Beijerinck (2, 11). Originally named *Micrococcus calcoaceticus*, *Acinetobacter* was rediscovered and renamed at least 15 times over the course of the next several decades (2, 11, 12). The genus *Acinetobacter* was finally proposed by Brisou and Prevot in 1954 (2, 13), and was comprehensively defined by Baumann *et al* in 1968 (12). Members of the genus *Acinetobacter* are Gram-negative, obligately aerobic coccobacilli (2, 12). Members of *Acinetobacter* were originally also defined as being nonmotile due to their lack of flagella (2,

12), but it is now known that *Acinetobacter* species do exhibit motility (14-16). While Baumann *et al* were unable to conclusively assign *Acinetobacter* isolates to species based on phenotypic traits (12), members of this genus were later divided into several species, including *A. baumannii*, based on DNA hybridization studies (17). Although other species of *Acinetobacter* are capable of causing opportunistic infections, *A. baumannii* is the one of the most clinically important members of this genus (17, 18). *A. baumannii* is a diverse species, and several genetically distinct strains of this bacterium have been used in laboratory studies. This dissertation utilizes the recently described strain AB5075, which is genetically tractable, multidrug resistant, hypervirulent in animal models, and is thought to be representative of modern strains of this bacterium (19, 20).

A number of virulence factors have been identified in various strains of *A. baumannii*. Unlike for some other bacterial pathogens, virulence of *A. baumannii* is not due to the production of a single toxin; rather multiple determinants are required for the bacterium to survive within the host and cause disease (21, 22). Several *A. baumannii* surface features have been implicated in virulence, including capsule, lipopolysaccharide (LPS), outer membrane proteins, and pili. All of these features are encoded by strain AB5075 (20, 23). Multiple mutations affecting capsule production have been shown to affect virulence in different *A. baumannii* strains and infection models (24-27). Capsule contributes to virulence by mediating resistance against complement-mediated killing and host antimicrobials (25, 26, 28-30). Complement resistance is also mediated by LPS (31). LPS further contributes to *A. baumannii* virulence by eliciting a pro-inflammatory immune response, which is associated with worsened infection outcomes (32). OmpA, the most abundant outer membrane protein in *A. baumannii*, has been implicated in virulence in multiple studies, and is thought to help mediate interactions between *A. baumannii*

and host cells, including host cell cytotoxicity (23, 27, 33, 34). In addition to being found on the cell surface of *A. baumannii*, OmpA is also secreted from cells in outer membrane vesicles (35, 36). Similarly to OmpA, a second outer membrane protein known as Omp34 has also been shown to have pro-apoptotic activity (37). Finally, *A. baumannii* Csu pili are thought to enhance disease by contributing to biofilm formation (38).

Aside from these surface features, *A. baumannii* exhibits additional factors that contribute to virulence. *A. baumannii* encodes a number of secretion systems, including members of types I, II, IV, V, and VI (39). Of these, the type II and type V secretion systems have been directly implicated in virulence (40-43). Metal acquisition systems, particularly for iron, but also zinc and manganese, are considered virulence factors because they contribute to the growth of *A. baumannii in vivo* (44-52). Phospholipases have also been shown to contribute to *A. baumannii* virulence by facilitating the degradation of host phosphatidylcholine (53-55). Further proposed virulence factors in *A. baumannii* include the GigAB signaling proteins, the DNA repair protein RecA, the GacSA two-component system, the *aba* quorum sensing system, and the phenylacetic acid catabolic pathway (27, 52, 56-60). In addition to these specific virulence factors, many strains of *A. baumannii* have been shown to undergo a high-frequency phenotypic switch controlling both colony opacity and virulence (61, 62), which is discussed in more detail in subsequent sections. Despite the breadth of pathogenesis research that has been performed on this bacterium, more work is still needed to develop a comprehensive understanding of *A. baumannii* virulence.

In addition to virulence, antibiotic resistance is also a clinically important feature of *A. baumannii*. As a Gram-negative bacterium, *A. baumannii* exhibits intrinsic antibiotic resistance due to its low outer membrane permeability. Even for a Gram-negative bacterium, *A. baumannii*

is unusually impenetrable, due to the low permeability of its major outer membrane porin, OmpA (63, 64). Intrinsic antibiotic resistance in this species can also be due to the production of two chromosomal  $\beta$ -lactamases (65, 66), as well as the expression of endogenous efflux pumps, including AdeABC and AdeIJK (67, 68). Resistance mediated by these enzymes and pumps can be increased in individual strains by mutations in regulators of these genes, or by introduction of insertion element-encoded promoters upstream of these genes (69-72). Increased expression of *adeABC* can lead to resistance to aminoglycosides and tigecycline, both of which are used to treat carbapenem-resistant *A. baumannii* (22, 67, 69, 72). *A. baumannii* can also acquire resistance through random mutations resulting in modifications of drug targets, as has been observed for fluoroquinolones (which target gyrase and topoisomerase IV) and the last-line therapy colistin (which targets the bacterial cell membrane) (73-76). However, much of the resistance observed in *A. baumannii* is due to horizontally acquired resistance genes.

*A. baumannii* strains exhibit widespread acquisition of mobile resistance elements. *A. baumannii* is both naturally competent and capable of generalized transduction (77-81), which aid in the ability of this bacterium to take up exogenous DNA. Horizontally acquired resistance genes in *A. baumannii* are associated with a number of mobile elements, including insertion sequences, transposons, integrons, and plasmids (82, 83). In *A. baumannii*, resistance genes frequently cluster in large transposons known as resistance islands (20, 84-87). *A. baumannii* strains commonly accumulate resistance genes targeting  $\beta$ -lactams (including carbapenems, which are the preferred treatment option for *A. baumannii*) and aminoglycosides, among others (20, 22, 83, 88-90). This acquisition of resistance has led to the increasing use of last-line therapies to treat *A. baumannii* infections, and underscores the need for new antimicrobials for this pathogen.

Further complicating our view of *A. baumannii* antibiotic resistance, the present work demonstrates that aminoglycoside resistance levels vary between cells in populations of AB5075, a phenomenon termed heteroresistance. This work further establishes that aminoglycoside heteroresistance is linked to virulence, as the integron-encoded locus that controls heteroresistance also controls the frequency of the opacity and virulence switch. The remainder of this introduction will focus on aminoglycoside resistance and integrons, heteroresistance, and the opacity/virulence switch.

### **Aminoglycoside Resistance and Integrons**

Aminoglycosides are broad-spectrum antimicrobials that target the bacterial ribosome. The first aminoglycoside, streptomycin, was isolated in the 1940s from *Streptomyces griseus* (91). Since then, several naturally occurring and semi-synthetic aminoglycosides have been introduced to clinical use (92). Aminoglycosides function by binding to rRNAs in the bacterial 30S ribosome, resulting in conformational changes to the ribosomal A site (92, 93). These changes lead to the incorporation of noncognate tRNAs, resulting in a loss of translational fidelity and the production of incorrect proteins, which ultimately causes cell death (92). Although aminoglycosides are active against a variety of non-anaerobic bacteria, they can also cause serious side-effects, including oto- and nephrotoxicity (92). With the rise of resistance to less toxic antimicrobials, the clinical importance of aminoglycosides as alternative therapies has increased. However, resistance to aminoglycosides is also threatening their utility in the clinic.

Resistance to aminoglycosides generally occurs by one of three mechanisms. The first is drug inactivation, which relies on the production of aminoglycoside modifying enzymes (AMEs), including aminoglycoside acetyltransferases (AACs), phosphotransferases (APHs), and nucleotidyltransferases (ANTs). All three of these classes catalyze the covalent modification of

aminoglycosides, blocking the ability of these enzymes to bind their rRNA targets. AACs catalyze the transfer of the acetyl group from acetyl-CoA to one of four amino groups on aminoglycosides (94). APHs phosphorylate aminoglycosides using either ATP or GDP as a donor (92). ANTs transfer AMP onto hydroxyl groups in aminoglycosides, using ATP as a substrate (94). The second type of aminoglycoside resistance, ribosomal protection, involves methylation of 16S rRNA, which blocks binding of aminoglycosides (95). 16S ribosomal methylases were once rare outside of aminoglycoside-producing bacteria, but have recently also been spreading in Gram-negative pathogens (95-99). Finally, aminoglycoside resistance can also be conferred by increased efflux or decreased drug uptake. Aminoglycoside efflux is mediated by members of the resistance-nodulation-division (RND), major facilitator (MFS), and multidrug and toxic compound extrusion (MATE) superfamilies of pumps (67, 100-103). Decreased uptake of aminoglycosides can occur through modifications decreasing the negative charge of the cell surface, which inhibits binding by positively-charged aminoglycosides, or by disruption of proton-motive force, which blocks the active import of these drugs (92, 104-106). All three of these mechanisms can cause aminoglycoside resistance in *A. baumannii*.

Aminoglycoside resistance in *A. baumannii* is associated with many different genes. Aminoglycoside resistance due to ribosomal protection in *A. baumannii* is mediated by *armA*, which was originally identified as a plasmid-borne ribosomal methylase gene in *Klebsiella pneumoniae* (8, 99). *armA* is now widely distributed in *A. baumannii* strains from diverse geographic locations, where it causes high-level resistance to a variety of aminoglycosides, including tobramycin, amikacin, and gentamicin (8, 88, 107, 108). Aminoglycoside resistance has also been associated with both RND (AdeABC, ArpAB) and MATE (AbeM) efflux pumps in *A. baumannii* (67, 101, 103, 109, 110). However, drug inactivation is considered the most

prevalent mechanism of aminoglycoside resistance in *A. baumannii*. AMEs of all three classes have been detected in *A. baumannii* strains (8). Each AME mediates resistance to only a subset of aminoglycosides (111), but *A. baumannii* strains can achieve resistance to wide range of these drugs by acquiring multiple AME genes. For example, AB5075 encodes six horizontally acquired AMEs, including one AAC (*aacA4*), three APHs (*strA*, *strB*, and *aphA6*), and two ANTs (*aadB* and *aadA1*) (20). As a result, this strain is resistant to many clinically relevant aminoglycosides, particularly amikacin, gentamicin, streptomycin, and tobramycin (19). Although AMEs can be horizontally acquired by many mechanisms, they are frequently associated with class 1 integrons in *A. baumannii*, including AB5075 (20, 112, 113).

Integrons mediate horizontal gene transfer by facilitating the incorporation of exogenous gene cassettes into host genomes. By this mechanism, integrons are capable of generating large arrays of antibiotic resistance cassettes. Uptake of cassettes is catalyzed by an integron-encoded integrase (IntI), which is a member of the tyrosine recombinase family (114). IntI mediates site-specific recombination between a defined integron sequence (*attI*) and a cassette sequence (*attC*) (115, 116). Integrons are split into five classes based on their *intI* sequences (117, 118). The most common, well studied, and clinically relevant class of integrons is class 1 (117, 118). In addition to encoding *intI* and *attI*, clinical class 1 integrons also encode *sulI*, which mediates sulfonamide resistance, and *orf5*, which has an unknown function (117-119). Class 1 integrons also encode complex promoter regions, which include binding sites for the DNA binding proteins FIS, LexA, IHF, and H-NS (120); a gene encoding a small peptide (ORF-11), which enhances translation of cassette genes (121); and three promoters—one for *intI* ( $P_{intI}$ ), and two for cassette genes ( $P_c$  and  $P_2$ ) (120, 122-124). In some class 1 integrons,  $P_2$  is mutated and possesses negligible activity (120). Class 1 integrons have also been proposed to encode a

riboswitch that responds to aminoglycosides (125-127); however, the existence of this element is controversial (128). While not mobile on their own, class 1 integrons can be mobilized by transposons and plasmids (118). This appears to be the case for a large integron in AB5075.

AB5075 encodes a resistance island (RI-2) containing a large composite integron that mediates resistance to several antimicrobials, including aminoglycosides. RI-2 is flanked by miniature inverted-repeat transposable element (MITE) sequences, which suggest that it can be mobilized by transposition (20). It is also inserted into a large transmissible plasmid, p1AB5075 (20, 129, 130). RI-2 is a composite integron, meaning that it is actually made up of two fused class 1 integrons (20, 131). One integron encodes an intact *intI* gene, the AME genes *aadB*, *aadA2*, and *strAB*, as well as the chloramphenicol resistance gene *cmlA* (20). The second integron encodes a pseudogene *intI*, the beta-lactamase gene *bla<sub>GES-14</sub>*, the AME gene *aacA4*, and the trimethoprim resistance gene *dfrA7*, in addition to the typical *sulI* and *orf5* genes (20). Although unusual, this composite integron is not unique to AB5075, and has also been found in *A. baumannii* strains AP (isolated in France in 2010) and Ab8098 (isolated in Tunisia in 2008) (130, 131). Despite mutations rendering one integrase gene nonfunctional, the two copies of *intI* found in RI-2 are highly homologous (99% nucleic acid identity across 1062 bp), and flank *aadB*, *cmlA*, *aadA2*, and *strAB* (20). In this work, we present evidence that these flanking *intI* genes are important for mediating aminoglycoside heteroresistance in AB5075.

## **Heteroresistance**

Heteroresistance is a phenomenon wherein subpopulations of cells in a clonal bacterial population exhibit increased resistance to an antimicrobial. In these strains, resistant subpopulations are frequently unstable in the absence of selection, demonstrating that this resistance is not due to acquisition of stable point mutations (132). Although the frequencies of

resistant cells in heteroresistant strains vary, frequencies are often quite low (between  $10^{-7}$  and  $10^{-3}$ ) (132). Because of these low frequencies, heteroresistance is often not detectable by standard clinical susceptibility testing (133, 134). In cases where the majority population is clinically sensitive to an antibiotic, resistant subpopulations are thought to contribute to treatment failure. This has been demonstrated in humans (135-140), animal models (133, 134), and through mathematical modeling (141).

Heteroresistance to a variety of antimicrobials has been reported in several pathogens (132), but the mechanisms underlying this phenomenon are not understood in all systems. In *A. baumannii*, heteroresistance has been described to colistin (142-145), polymyxin B (146), carbapenems (141, 147-149), cephalosporins (141), trimethoprim/sulfamethoxazole (141), and aminoglycosides (141, 150). While the mechanisms underlying *A. baumannii* heteroresistance to polymyxins and  $\beta$ -lactams have not been thoroughly investigated, heteroresistance to trimethoprim/sulfamethoxazole and aminoglycosides has been shown to occur through unstable tandem gene amplifications of known antibiotic resistance genes (141, 150). Gene amplifications leading to unstable drug resistance in *A. baumannii* have been shown to occur through both homologous recombination and transposition (150, 151). *A. baumannii* aminoglycoside heteroresistance has also been associated with random non-duplicative mutations that result in a high fitness cost, leading to instability of the resistance phenotype (141). Tandem duplications and costly mutations have also been shown to underlie heteroresistance in other Gram-negative species (141, 152). Non-mutational mechanisms for unstable heteroresistance have also been proposed. Variations in expression of the regulatory protein MarA were shown to contribute to transient differences in antimicrobial susceptibility in *Escherichia coli* (153), and differential expression of the outer membrane porin OmpA has been

implicated in heteroresistance to kanamycin in *Salmonella enterica* (154). However, more research is needed to fully understand the contributions of different mechanisms to this phenomenon, as the mechanisms underlying many cases of heteroresistance have not been determined.

### **Colony Opacity Variation and Virulence**

Many bacterial species have been shown to undergo colony opacity variation wherein strains yield both opaque and translucent/transparent colonies, with cells that are capable of interconverting between the two states. In many species, this phenomenon is important for virulence or survival in different niches. In addition to *A. baumannii*, this phenomenon has also been described in *Neisseria gonorrhoeae* and *meningitidis* (155, 156), *Streptococcus pneumoniae* (157), and *Haemophilus influenzae* (158), as well as in species from the *Mycoplasma* (159-161), *Pseudomonas* (162, 163), and *Vibrio* (164-166) genera. Of these, the mechanisms of opacity variation in *Neisseria* and *S. pneumoniae* are best characterized.

In *Neisseria*, opacity is conferred by outer membrane lipoproteins known as Opa proteins (156, 167). *N. gonorrhoeae* encodes up to eleven *opa* genes, whereas *N. meningitidis* encodes four (168-170). Opacity variation in *Neisseria* is due to phase-variable translation of *opa* genes caused by slipped-strand mispairing in a pentameric repeat track at the 5' end of each gene (167, 171). While the *opa* genes are transcribed constitutively, variations in the number of pentameric repeats move the downstream portions of the coding regions in and out of frame, turning on and off protein production (167, 171). Expression of Opa proteins leads to increased adherence between *Neisseria* cells, which is probably responsible for the opaque phenotype observed in Opa<sup>+</sup> bacteria (172, 173). Opa proteins are also important in the context of infection, as they mediate interactions between *Neisseria* and host cells (174).

Opacity variation in *S. pneumoniae* occurs through a complex phase variation mechanism that involves DNA inversions in the colony opacity determinant (*cod*) locus (175). The *cod* locus encodes a type-1 restriction modification (RM) system containing three different alleles of the RM sequence specificity gene *hsdS*. Inversions within this region lead to the production of distinct *hsdS* alleles with different methylation specificities; expression of the specific allele *hsdS<sub>AI</sub>* leads to the opaque colony phenotype (175). However, the cellular component resulting in opacity is not definitively known. While opaque variants have been shown to produce more capsule than transparent variants, unencapsulated *S. pneumoniae* still undergoes opacity variation (157, 176, 177). It has been proposed that opacity variation is due to differences in the levels of wall teichoic acid, with other cell surface proteins also playing a role (177). Despite this uncertainty, it is known that opaque and transparent variants serve different roles during infection. Opaque variants exhibit greater virulence during systemic infection, but transparent variants show enhanced colonization of the nasopharynx (a pattern that has also been observed for opacity variants of *H. influenzae*) (157, 158, 176). In these cases, opacity variation is an adaptive strategy allowing bacteria to both colonize a host and subsequently cause disease.

In *A. baumannii*, opacity variation also plays an important role in infection. Opacity variation has been observed for many strains of *A. baumannii* (62, 178), but is best studied in strain AB5075 (61, 62, 110, 179). Opaque cells of AB5075 (designated VIR-O) are capable of causing disease in both mice and *Galleria* models, but translucent cells (designated AV-T) are avirulent (61, 62). Similarly to *S. pneumoniae*, VIR-O cells make more capsule than AV-T cells (62); however, unencapsulated AB5075 still undergoes opacity variation (26). Enhanced capsule production is thought to underlie the increased virulence of the VIR-O form by mediating resistance to host antimicrobials (61). The AV-T variant has been proposed to be adapted to life

outside the host, as this variant forms superior biofilms and exhibits enhanced growth under nutrient poor conditions (61). In addition to these phenotypes, AB5075 opacity variants also differ in terms of their cell morphology, motility, and gene expression (61, 62). VIR-O and AV-T cells interconvert in a density-dependent manner at a high frequency under laboratory conditions (62). The mechanisms mediating the interconversion in each direction are thought to be distinct, as some mutations affecting the switch in one direction do not affect the opposite switch (61, 110).

The mechanisms underlying opacity variation remain incompletely understood in *A. baumannii*. Three genetic loci have been reported to affect colony opacity variation in AB5075. The first is the OmpR/EnvZ two component system, which when mutated leads to increased VIR-O to AV-T switching and decreased virulence in a *Galleria* model (179). The second is the ArpAB efflux pump, which appears to positively regulate the VIR-O to AV-T switch. Mutations in *arpAB* lead to decreased VIR-O to AV-T switching (110). Finally, the TetR-type transcriptional regulator ABUW\_1645 has also been implicated in switching. *ABUW\_1645* is strongly upregulated in the AV-T variant (61). Mutation of this gene slightly increases the rate of AV-T to VIR-O switching, suggesting that this gene is involved in maintenance of the AV-T state (61). Interestingly, overexpression of *ABUW\_1645* in the VIR-O variant using a multi-copy plasmid leads to complete conversion of cells to the AV-T form, which in turn abolishes virulence (61). *ABUW\_1645* does not appear to regulate *ompR/envZ* or *arpAB* (61), and it is currently unclear how each of these three systems contributes to opacity variation in wild-type cells. More research is needed to determine the full mechanism of opacity variation and virulence switching in *A. baumannii*, as a better understanding of this mechanism would lead to

increased understanding of pathogenesis in this species, and could potentially lead to the development of anti-virulence therapeutics for this highly antibiotic resistant pathogen.

This work establishes a link between two types of phenotypic heterogeneity in AB5075. Chapter 2 demonstrates that aminoglycoside heteroresistance in AB5075 is due to amplification of the ANT gene *aadB*, which occurs via homologous recombination. Chapter 3 demonstrates that this same gene amplification also regulates the rate of VIR-O to AV-T switching, and impacts virulence of AB5075. Chapter 4 presents a summary of strategies that can be used to study opacity variation in *A. baumannii*. Finally, Chapter 5 discusses the implications of this work for future research and treatment of *A. baumannii* infections.

## References

1. Anonymous. 2013. Antibiotic Resistance Threats in the United States, 2013, *on* Centers for Disease Control and Prevention. <http://www.cdc.gov/drugresistance/pdf/ar-threats-2013-508.pdf>. Accessed 05/08/2016.
2. Peleg AY, Seifert H, Paterson DL. 2008. *Acinetobacter baumannii*: emergence of a successful pathogen. Clin Microbiol Rev 21:538-82.
3. Dexter C, Murray GL, Paulsen IT, Peleg AY. 2015. Community-acquired *Acinetobacter baumannii*: clinical characteristics, epidemiology and pathogenesis. Expert Rev Anti Infect Ther 13:567-73.
4. Davis KA, Moran KA, McAllister CK, Gray PJ. 2005. Multidrug-resistant *Acinetobacter* extremity infections in soldiers. Emerg Infect Dis 11:1218-24.
5. Petersen K, Riddle MS, Danko JR, Blazes DL, Hayden R, Tasker SA, Dunne JR. 2007. Trauma-related infections in battlefield casualties from Iraq. Ann Surg 245:803-11.
6. Hospenthal DR, Crouch HK, English JF, Leach F, Pool J, Conger NG, Whitman TJ, Wortmann GW, Robertson JL, Murray CK. 2011. Multidrug-resistant bacterial colonization of combat-injured personnel at admission to medical centers after evacuation from Afghanistan and Iraq. J Trauma 71:S52-7.
7. Johnson EN, Burns TC, Hayda RA, Hospenthal DR, Murray CK. 2007. Infectious complications of open type III tibial fractures among combat casualties. Clin Infect Dis 45:409-15.
8. Lee CR, Lee JH, Park M, Park KS, Bae IK, Kim YB, Cha CJ, Jeong BC, Lee SH. 2017. Biology of *Acinetobacter baumannii*: Pathogenesis, Antibiotic Resistance Mechanisms, and Prospective Treatment Options. Front Cell Infect Microbiol 7:55.

9. Lin MF, Lan CY. 2014. Antimicrobial resistance in *Acinetobacter baumannii*: From bench to bedside. *World J Clin Cases* 2:787-814.
10. Anonymous. 2017. WHO Priority Pathogens List for R&D of New Antibiotics, on World Health Organization. [http://who.int/medicines/publications/WHO-PPL-Short\\_Summary\\_25Feb-ET\\_NM\\_WHO.pdf](http://who.int/medicines/publications/WHO-PPL-Short_Summary_25Feb-ET_NM_WHO.pdf). Accessed Nov. 5.
11. Beijerinck MW. 1911. Pigmenten als oxydatieproducten gevormd door bacterien, vol 19, Versl. Koninklijke Akad. Wetensch. Amsterdam.
12. Baumann P, Doudoroff M, Stanier RY. 1968. A Study of the Moraxella Group II. Oxidative-negative Species (Genus *Acinetobacter*). *J Bacteriol* 95:1520-1541.
13. Brisou J, Prevot AR. 1954. [Studies on bacterial taxonomy. X. The revision of species under *Acromobacter* group]. *Ann Inst Pasteur (Paris)* 86:722-8.
14. Clemmer KM, Bonomo RA, Rather PN. 2011. Genetic analysis of surface motility in *Acinetobacter baumannii*. *Microbiology* 157:2534-44.
15. Barker J, Maxted H. 1975. Observations on the growth and movement of *Acinetobacter* on semi-solid media. *J Med Microbiol* 8:443-6.
16. McQueary CN, Kirkup BC, Si Y, Barlow M, Actis LA, Craft DW, Zurawski DV. 2012. Extracellular stress and lipopolysaccharide modulate *Acinetobacter baumannii* surface-associated motility. *J Microbiol* 50:434-43.
17. Bouvet PJM, Grimont PAD. 1986. Taxonomy of the Genus *Acinetobacter* with the Recognition of *Acinetobacter baumannii* sp. nov., *Acinetobacter haemolyticus* sp. nov., *Acinetobacter johnsonii* sp. nov., and *Acinetobacter junii* sp. nov. and Emended Descriptions of *Acinetobacter calcoaceticus* and *Acinetobacter lwoffii*. *Int J Syst Evol Microbiol* 36:228-240.

18. Bergogne-Berezin E, Towner KJ. 1996. *Acinetobacter* spp. as nosocomial pathogens: microbiological, clinical, and epidemiological features. Clin Microbiol Rev 9:148-65.
19. Jacobs AC, Thompson MG, Black CC, Kessler JL, Clark LP, McQueary CN, Gancz HY, Corey BW, Moon JK, Si Y, Owen MT, Hallock JD, Kwak YI, Summers A, Li CZ, Rasko DA, Penwell WF, Honnold CL, Wise MC, Waterman PE, Lesho EP, Stewart RL, Actis LA, Palys TJ, Craft DW, Zurawski DV. 2014. AB5075, a Highly Virulent Isolate of *Acinetobacter baumannii*, as a Model Strain for the Evaluation of Pathogenesis and Antimicrobial Treatments. mBio 5:e01076-14.
20. Gallagher LA, Ramage E, Weiss EJ, Radey M, Hayden HS, Held KG, Huse HK, Zurawski DV, Brittnacher MJ, Manoil C. 2015. Resources for Genetic and Genomic Analysis of Emerging Pathogen *Acinetobacter baumannii*. J Bacteriol 197:2027-35.
21. Harding CM, Hennon SW, Feldman MF. 2018. Uncovering the mechanisms of *Acinetobacter baumannii* virulence. Nat Rev Microbiol 16:91-102.
22. Wong D, Nielsen TB, Bonomo RA, Pantapalangkoor P, Luna B, Spellberg B. 2017. Clinical and Pathophysiological Overview of *Acinetobacter* Infections: a Century of Challenges. Clin Microbiol Rev 30:409-447.
23. Schweppe DK, Harding C, Chavez JD, Wu X, Ramage E, Singh PK, Manoil C, Bruce JE. 2015. Host-Microbe Protein Interactions during Bacterial Infection. Chem Biol 22:1521-1530.
24. Russo TA, Luke NR, Beanan JM, Olson R, Sauberan SL, MacDonald U, Schultz LW, Umland TC, Campagnari AA. 2010. The K1 Capsular Polysaccharide of *Acinetobacter baumannii* Strain 307-0294 Is a Major Virulence Factor. Infect Immun 78:3993-4000.

25. Lees-Miller RG, Iwashkiw JA, Scott NE, Seper A, Vinogradov E, Schild S, Feldman MF. 2013. A common pathway for O-linked protein-glycosylation and synthesis of capsule in *Acinetobacter baumannii*. *Mol Microbiol* 89:816-830.
26. Tipton KA, Chin CY, Farokhyfar M, Weiss DS, Rather PN. 2018. Role of Capsule in Resistance to Disinfectants, Host Antimicrobials, and Desiccation in *Acinetobacter baumannii*. *Antimicrob Agents Chemother* 62.
27. Wang N, Ozer EA, Mandel MJ, Hauser AR. 2014. Genome-wide identification of *Acinetobacter baumannii* genes necessary for persistence in the lung. *mBio* 5:e01163-14.
28. Geisinger E, Isberg RR. 2015. Antibiotic modulation of capsular exopolysaccharide and virulence in *Acinetobacter baumannii*. *PLoS Pathog* 11:e1004691.
29. Sanchez-Larrayoz AF, Elhosseiny NM, Chevrette MG, Fu Y, Giunta P, Spallanzani RG, Ravi K, Pier GB, Lory S, Maira-Litran T. 2017. Complexity of Complement Resistance Factors Expressed by *Acinetobacter baumannii* Needed for Survival in Human Serum. *J Immunol* 199:2803-2814.
30. Liu Y, Mi Z, Mi L, Huang Y, Li P, Liu H, Yuan X, Niu W, Jiang N, Bai C, Gao Z. 2019. Identification and characterization of capsule depolymerase Dpo48 from *Acinetobacter baumannii* phage IME200. *PeerJ* 7:e6173.
31. Luke NR, Sauberan SL, Russo TA, Beanan JM, Olson R, Loehfelm TW, Cox AD, St Michael F, Vinogradov EV, Campagnari AA. 2010. Identification and characterization of a glycosyltransferase involved in *Acinetobacter baumannii* lipopolysaccharide core biosynthesis. *Infect Immun* 78:2017-23.
32. Lin L, Tan B, Pantapalangkoor P, Ho T, Baquir B, Tomaras A, Montgomery JI, Reilly U, Barbacci EG, Hujer K, Bonomo RA, Fernandez L, Hancock RE, Adams MD, French

- SW, Buslon VS, Spellberg B. 2012. Inhibition of LpxC protects mice from resistant *Acinetobacter baumannii* by modulating inflammation and enhancing phagocytosis. *mBio* 3.
33. Choi CH, Hyun SH, Lee JY, Lee JS, Lee YS, Kim SA, Chae JP, Yoo SM, Lee JC. 2008. *Acinetobacter baumannii* outer membrane protein A targets the nucleus and induces cytotoxicity. *Cell Microbiol* 10:309-19.
34. Choi CH, Lee EY, Lee YC, Park TI, Kim HJ, Hyun SH, Kim SA, Lee SK, Lee JC. 2005. Outer membrane protein 38 of *Acinetobacter baumannii* localizes to the mitochondria and induces apoptosis of epithelial cells. *Cell Microbiol* 7:1127-38.
35. Moon DC, Choi CH, Lee JH, Choi CW, Kim HY, Park JS, Kim SI, Lee JC. 2012. *Acinetobacter baumannii* outer membrane protein A modulates the biogenesis of outer membrane vesicles. *J Microbiol* 50:155-60.
36. Kwon SO, Gho YS, Lee JC, Kim SI. 2009. Proteome analysis of outer membrane vesicles from a clinical *Acinetobacter baumannii* isolate. *FEMS Microbiol Lett* 297:150-6.
37. Rumbo C, Tomas M, Fernandez Moreira E, Soares NC, Carvajal M, Santillana E, Beceiro A, Romero A, Bou G. 2014. The *Acinetobacter baumannii* Omp33-36 porin is a virulence factor that induces apoptosis and modulates autophagy in human cells. *Infect Immun* 82:4666-80.
38. Tomaras AP, Dorsey CW, Edelmann RE, Actis LA. 2003. Attachment to and biofilm formation on abiotic surfaces by *Acinetobacter baumannii*: involvement of a novel chaperone-usher pili assembly system. *Microbiology* 149:3473-84.

39. Morris FC, Dexter C, Kostoulias X, Uddin MI, Peleg AY. 2019. The Mechanisms of Disease Caused by *Acinetobacter baumannii*. *Front Microbiol* 10:1601.
40. Harding CM, Kinsella RL, Palmer LD, Skaar EP, Feldman MF. 2016. Medically Relevant *Acinetobacter* Species Require a Type II Secretion System and Specific Membrane-Associated Chaperones for the Export of Multiple Substrates and Full Virulence. *PLoS Pathog* 12:e1005391.
41. Johnson TL, Waack U, Smith S, Mobley H, Sandkvist M. 2015. *Acinetobacter baumannii* Is Dependent on the Type II Secretion System and Its Substrate LipA for Lipid Utilization and *In Vivo* Fitness. *J Bacteriol* 198:711-9.
42. Perez A, Merino M, Rumbo-Feal S, Alvarez-Fraga L, Vallejo JA, Beceiro A, Ohneck EJ, Mateos J, Fernandez-Puente P, Actis LA, Poza M, Bou G. 2017. The FhaB/FhaC two-partner secretion system is involved in adhesion of *Acinetobacter baumannii* AbH12O-A2 strain. *Virulence* 8:959-974.
43. Bentancor LV, Camacho-Peiro A, Bozkurt-Guzel C, Pier GB, Maira-Litran T. 2012. Identification of Ata, a multifunctional trimeric autotransporter of *Acinetobacter baumannii*. *J Bacteriol* 194:3950-60.
44. Juttukonda LJ, Chazin WJ, Skaar EP. 2016. *Acinetobacter baumannii* Coordinates Urea Metabolism with Metal Import To Resist Host-Mediated Metal Limitation. *mBio* 7.
45. Alvarez-Fraga L, Vazquez-Ucha JC, Martinez-Guitian M, Vallejo JA, Bou G, Beceiro A, Poza M. 2018. Pneumonia infection in mice reveals the involvement of the *feoA* gene in the pathogenesis of *Acinetobacter baumannii*. *Virulence*  
doi:10.1080/21505594.2017.1420451:0.

46. Runci F, Gentile V, Frangipani E, Rampioni G, Leoni L, Lucidi M, Visaggio D, Harris G, Chen W, Stahl J, Averhoff B, Visca P. 2019. The contribution of active iron-uptake to *Acinetobacter baumannii* pathogenicity. *Infect Immun* doi:10.1128/iai.00755-18.
47. Subashchandrabose S, Smith S, DeOrnellas V, Crepin S, Kole M, Zahdeh C, Mobley HLT. 2016. *Acinetobacter baumannii* Genes Required for Bacterial Survival during Bloodstream Infection. *mSphere* 1:e00013-15.
48. Gaddy JA, Arivett BA, McConnell MJ, López-Rojas R, Pachón J, Actis LA. 2012. Role of Acinetobactin-Mediated Iron Acquisition Functions in the Interaction of *Acinetobacter baumannii* Strain ATCC 19606<sup>T</sup> with Human Lung Epithelial Cells, *Galleria mellonella* Caterpillars, and Mice. *Infect Immun* 80:1015-1024.
49. Nairn BL, Lonergan ZR, Wang J, Braymer JJ, Zhang Y, Calcutt MW, Lisher JP, Gilston BA, Chazin WJ, de Crecy-Lagard V, Giedroc DP, Skaar EP. 2016. The Response of *Acinetobacter baumannii* to Zinc Starvation. *Cell Host Microbe* 19:826-36.
50. Mortensen BL, Rathi S, Chazin WJ, Skaar EP. 2014. *Acinetobacter baumannii* response to host-mediated zinc limitation requires the transcriptional regulator Zur. *J Bacteriol* 196:2616-26.
51. Hood MI, Mortensen BL, Moore JL, Zhang Y, Kehl-Fie TE, Sugitani N, Chazin WJ, Caprioli RM, Skaar EP. 2012. Identification of an *Acinetobacter baumannii* zinc acquisition system that facilitates resistance to calprotectin-mediated zinc sequestration. *PLoS Pathog* 8:e1003068.
52. Gebhardt MJ, Gallagher LA, Jacobson RK, Usacheva EA, Peterson LR, Zurawski DV, Shuman HA. 2015. Joint Transcriptional Control of Virulence and Resistance to Antibiotic and Environmental Stress in *Acinetobacter baumannii*. *mBio* 6:e01660-15.

53. Fiester SE, Arivett BA, Schmidt RE, Beckett AC, Ticak T, Carrier MV, Ghosh R, Ohneck EJ, Metz ML, Sellin Jeffries MK, Actis LA. 2016. Iron-Regulated Phospholipase C Activity Contributes to the Cytolytic Activity and Virulence of *Acinetobacter baumannii*. PLoS One 11:e0167068.
54. Stahl J, Bergmann H, Gottig S, Ebersberger I, Averhoff B. 2015. *Acinetobacter baumannii* Virulence Is Mediated by the Concerted Action of Three Phospholipases D. PLoS One 10:e0138360.
55. Jacobs AC, Hood I, Boyd KL, Olson PD, Morrison JM, Carson S, Sayood K, Iwen PC, Skaar EP, Dunman PM. 2010. Inactivation of phospholipase D diminishes *Acinetobacter baumannii* pathogenesis. Infect Immun 78:1952-62.
56. Gebhardt MJ, Shuman HA. 2017. GigA and GigB are Master Regulators of Antibiotic Resistance, Stress Responses and Virulence in *Acinetobacter baumannii*. J Bacteriol doi:10.1128/jb.00066-17.
57. Aranda J, Bardina C, Beceiro A, Rumbo S, Cabral MP, Barbe J, Bou G. 2011. *Acinetobacter baumannii* RecA protein in repair of DNA damage, antimicrobial resistance, general stress response, and virulence. J Bacteriol 193:3740-7.
58. Cerqueira GM, Kostoulias X, Khoo C, Aibinu I, Qu Y, Traven A, Peleg AY. 2014. A global virulence regulator in *Acinetobacter baumannii* and its control of the phenylacetic acid catabolic pathway. J Infect Dis 210:46-55.
59. Bhuiyan MS, Ellett F, Murray GL, Kostoulias X, Cerqueira GM, Schulze KE, Mahamad Maifiah MH, Li J, Creek DJ, Lieschke GJ, Peleg AY. 2016. *Acinetobacter baumannii* phenylacetic acid metabolism influences infection outcome through a direct effect on neutrophil chemotaxis. Proc Natl Acad Sci U S A 113:9599-604.

60. Fernandez-Garcia L, Ambroa A, Blasco L, Bleriot I, Lopez M, Alvarez-Marin R, Fernandez-Cuenca F, Martinez-Martinez L, Vila J, Rodriguez-Bano J, Garnacho-Montero J, Cisneros JM, Pascual A, Pachon J, Bou G, Smani Y, Tomas M. 2018. Relationship Between the Quorum Network (Sensing/Quenching) and Clinical Features of Pneumonia and Bacteraemia Caused by *A. baumannii*. *Front Microbiol* 9:3105.
61. Chin CY, Tipton KA, Farokhyfar M, Burd EM, Weiss DS, Rather PN. 2018. A high-frequency phenotypic switch links bacterial virulence and environmental survival in *Acinetobacter baumannii*. *Nat Microbiol* 3:563-569.
62. Tipton KA, Dimitrova D, Rather PN. 2015. Phase-Variable Control of Multiple Phenotypes in *Acinetobacter baumannii* Strain AB5075. *J Bacteriol* 197:2593-9.
63. Sato K, Nakae T. 1991. Outer membrane permeability of *Acinetobacter calcoaceticus* and its implication in antibiotic resistance. *J Antimicrob Chemother* 28:35-45.
64. Sugawara E, Nikaido H. 2012. OmpA is the principal nonspecific slow porin of *Acinetobacter baumannii*. *J Bacteriol* 194:4089-96.
65. Heritier C, Poirel L, Fournier PE, Claverie JM, Raoult D, Nordmann P. 2005. Characterization of the naturally occurring oxacillinase of *Acinetobacter baumannii*. *Antimicrob Agents Chemother* 49:4174-9.
66. Bou G, Martinez-Beltran J. 2000. Cloning, nucleotide sequencing, and analysis of the gene encoding an AmpC beta-lactamase in *Acinetobacter baumannii*. *Antimicrob Agents Chemother* 44:428-32.
67. Marchand I, Damier-Piolle L, Courvalin P, Lambert T. 2004. Expression of the RND-type efflux pump AdeABC in *Acinetobacter baumannii* is regulated by the AdeRS two-component system. *Antimicrob Agents Chemother* 48:3298-304.

68. Damier-Piolle L, Magnet S, Bremont S, Lambert T, Courvalin P. 2008. AdeIJK, a resistance-nodulation-cell division pump effluxing multiple antibiotics in *Acinetobacter baumannii*. *Antimicrob Agents Chemother* 52:557-62.
69. Sun JR, Perng CL, Chan MC, Morita Y, Lin JC, Su CM, Wang WY, Chang TY, Chiueh TS. 2012. A truncated AdeS kinase protein generated by ISAbal insertion correlates with tigecycline resistance in *Acinetobacter baumannii*. *PLoS One* 7:e49534.
70. Heritier C, Poirel L, Nordmann P. 2006. Cephalosporinase over-expression resulting from insertion of ISAbal in *Acinetobacter baumannii*. *Clin Microbiol Infect* 12:123-30.
71. Corvec S, Caroff N, Espaze E, Giraudeau C, Drugeon H, Reynaud A. 2003. AmpC cephalosporinase hyperproduction in *Acinetobacter baumannii* clinical strains. *J Antimicrob Chemother* 52:629-35.
72. Ruzin A, Keeney D, Bradford PA. 2007. AdeABC multidrug efflux pump is associated with decreased susceptibility to tigecycline in *Acinetobacter calcoaceticus*-*Acinetobacter baumannii* complex. *J Antimicrob Chemother* 59:1001-4.
73. Qureshi ZA, Hittle LE, O'Hara JA, Rivera JI, Syed A, Shields RK, Pasculle AW, Ernst RK, Doi Y. 2015. Colistin-Resistant *Acinetobacter baumannii*: Beyond Carbapenem Resistance. *Clin Infect Dis* 60:1295-1303.
74. Adams MD, Nickel GC, Bajaksouzian S, Lavender H, Murthy AR, Jacobs MR, Bonomo RA. 2009. Resistance to colistin in *Acinetobacter baumannii* associated with mutations in the PmrAB two-component system. *Antimicrob Agents Chemother* 53:3628-34.
75. Vila J, Ruiz J, Goñi P, Jimenez de Anta T. 1997. Quinolone-resistance mutations in the topoisomerase IV *parC* gene of *Acinetobacter baumannii*. *J Antimicrob Chemother* 39:757-762.

76. Hujer KM, Hujer AM, Endimiani A, Thomson JM, Adams MD, Goglin K, Rather PN, Pennella T-TD, Massire C, Eshoo MW, Sampath R, Blyn LB, Ecker DJ, Bonomo RA. 2009. Rapid Determination of Quinolone Resistance in *Acinetobacter* spp. *J Clin Microbiol* 47:1436-1442.
77. Godeux AS, Lupo A, Haenni M, Guette-Marquet S, Wilharm G, Laaberki MH, Charpentier X. 2018. Fluorescence-based detection of natural transformation in drug resistant *Acinetobacter baumannii*. *J Bacteriol* doi:10.1128/jb.00181-18.
78. Harding CM, Tracy EN, Carruthers MD, Rather PN, Actis LA, Munson RS, Jr. 2013. *Acinetobacter baumannii* strain M2 produces type IV pili which play a role in natural transformation and twitching motility but not surface-associated motility. *mBio* 4.
79. Ramirez MS, Don M, Merkier AK, Bistue AJ, Zorreguieta A, Centron D, Tolmasky ME. 2010. Naturally competent *Acinetobacter baumannii* clinical isolate as a convenient model for genetic studies. *J Clin Microbiol* 48:1488-90.
80. Wachino JI, Jin W, Kimura K, Arakawa Y. 2019. Intercellular Transfer of Chromosomal Antimicrobial-resistance Genes between *Acinetobacter baumannii* Mediated by Prophages. *Antimicrob Agents Chemother* doi:10.1128/aac.00334-19.
81. Wilharm G, Piesker J, Laue M, Skiebe E. 2013. DNA uptake by the nosocomial pathogen *Acinetobacter baumannii* occurs during movement along wet surfaces. *J Bacteriol* 195:4146-53.
82. Pagano M, Martins AF, Barth AL. 2016. Mobile genetic elements related to carbapenem resistance in *Acinetobacter baumannii*. *Braz J Microbiol* 47:785-792.

83. Hamidian M, Nigro SJ, Hall RM. 2012. Variants of the gentamicin and tobramycin resistance plasmid pRAY are widely distributed in *Acinetobacter*. *J Antimicrob Chemother* 67:2833-6.
84. Fournier PE, Vallenet D, Barbe V, Audic S, Ogata H, Poirel L, Richet H, Robert C, Mangenot S, Abergel C, Nordmann P, Weissenbach J, Raoult D, Claverie JM. 2006. Comparative genomics of multidrug resistance in *Acinetobacter baumannii*. *PLoS Genet* 2:e7.
85. Šeputienė V, Povilonis J, Sužiedėlienė E. 2012. Novel Variants of AbaR Resistance Islands with a Common Backbone in *Acinetobacter baumannii* Isolates of European Clone II. *Antimicrob Agents Chemother* 56:1969-1973.
86. Rose A. 2010. TnAbaR1: a novel Tn7-related transposon in *Acinetobacter baumannii* that contributes to the accumulation and dissemination of large repertoires of resistance genes. *Biosci Horiz* 3:40-48.
87. Krizova L, Dijkshoorn L, Nemeč A. 2011. Diversity and Evolution of AbaR Genomic Resistance Islands in *Acinetobacter baumannii* Strains of European Clone I. *Antimicrob Agents Chemother* 55:3201-3206.
88. Karah N, Dwibedi CK, Sjöstrom K, Edquist P, Johansson A, Wai SN, Uhlin BE. 2016. Novel Aminoglycoside Resistance Transposons and Transposon-Derived Circular Forms Detected in Carbapenem-Resistant *Acinetobacter baumannii* Clinical Isolates. *Antimicrob Agents Chemother* 60:1801-18.
89. Nigro SJ, Hall RM. 2016. Structure and context of *Acinetobacter* transposons carrying the oxa23 carbapenemase gene. *J Antimicrob Chemother* 71:1135-1147.

90. Krahn T, Wibberg D, Maus I, Winkler A, Bontron S, Sczyrba A, Nordmann P, Puhler A, Poirel L, Schluter A. 2016. Intraspecies Transfer of the Chromosomal *Acinetobacter baumannii* bla(NDM-1) Carbapenemase Gene. *Antimicrob Agents Chemother* 60:3032-3040.
91. Schatz A, Bugle E, Waksman SA. 1944. Streptomycin, a Substance Exhibiting Antibiotic Activity Against Gram-Positive and Gram-Negative Bacteria. *Proc Soc Exp Biol Med* 55:66-69.
92. Becker B, Cooper MA. 2013. Aminoglycoside antibiotics in the 21st century. *ACS Chem Biol* 8:105-15.
93. Kaul M, Barbieri CM, Pilch DS. 2004. Fluorescence-based approach for detecting and characterizing antibiotic-induced conformational changes in ribosomal RNA: comparing aminoglycoside binding to prokaryotic and eukaryotic ribosomal RNA sequences. *J Am Chem Soc* 126:3447-53.
94. Ramirez MS, Tolmasky ME. 2010. Aminoglycoside modifying enzymes. *Drug Resist Updat* 13:151-71.
95. Doi Y, Arakawa Y. 2007. 16S ribosomal RNA methylation: emerging resistance mechanism against aminoglycosides. *Clin Infect Dis* 45:88-94.
96. Doi Y, Yokoyama K, Yamane K, Wachino J, Shibata N, Yagi T, Shibayama K, Kato H, Arakawa Y. 2004. Plasmid-mediated 16S rRNA methylase in *Serratia marcescens* conferring high-level resistance to aminoglycosides. *Antimicrob Agents Chemother* 48:491-6.

97. Yokoyama K, Doi Y, Yamane K, Kurokawa H, Shibata N, Shibayama K, Yagi T, Kato H, Arakawa Y. 2003. Acquisition of 16S rRNA methylase gene in *Pseudomonas aeruginosa*. *Lancet* 362:1888-93.
98. Wachino JI, Yamane K, Shibayama K, Kurokawa H, Shibata N, Suzuki S, Doi Y, Kimura K, Ike Y, Arakawa Y. 2006. Novel plasmid-mediated 16S rRNA methylase, RmtC, found in a *Proteus mirabilis* isolate demonstrating extraordinary high-level resistance against various aminoglycosides. *Antimicrob Agents Chemother* 50:178-184.
99. Galimand M, Courvalin P, Lambert T. 2003. Plasmid-mediated high-level resistance to aminoglycosides in *Enterobacteriaceae* due to 16S rRNA methylation. *Antimicrob Agents Chemother* 47:2565-71.
100. Krause KM, Serio AW, Kane TR, Connolly LE. 2016. Aminoglycosides: An Overview. *Cold Spring Harb Perspect Med* 6.
101. Magnet S, Courvalin P, Lambert T. 2001. Resistance-nodulation-cell division-type efflux pump involved in aminoglycoside resistance in *Acinetobacter baumannii* strain BM4454. *Antimicrob Agents Chemother* 45:3375-80.
102. Fernandez L, Hancock RE. 2012. Adaptive and mutational resistance: role of porins and efflux pumps in drug resistance. *Clin Microbiol Rev* 25:661-81.
103. Su XZ, Chen J, Mizushima T, Kuroda T, Tsuchiya T. 2005. AbeM, an H<sup>+</sup>-coupled *Acinetobacter baumannii* multidrug efflux pump belonging to the MATE family of transporters. *Antimicrob Agents Chemother* 49:4362-4.
104. Bryan LE, Van Den Elzen HM. 1977. Effects of membrane-energy mutations and cations on streptomycin and gentamicin accumulation by bacteria: a model for entry of

- streptomycin and gentamicin in susceptible and resistant bacteria. *Antimicrob Agents Chemother* 12:163-77.
105. Muir ME, Hanwell DR, Wallace BJ. 1981. Characterization of a respiratory mutant of *Escherichia coli* with reduced uptake of aminoglycoside antibiotics. *Biochim Biophys Acta* 638:234-41.
106. Kwon DH, Lu CD. 2006. Polyamines induce resistance to cationic peptide, aminoglycoside, and quinolone antibiotics in *Pseudomonas aeruginosa* PAO1. *Antimicrob Agents Chemother* 50:1615-22.
107. Kuo SC, Huang WC, Huang TW, Wang HY, Lai JF, Chen TL, Lauderdale TL. 2018. Molecular Epidemiology of Emerging blaOXA-23-Like- and blaOXA-24-Like-Carrying *Acinetobacter baumannii* in Taiwan. *Antimicrob Agents Chemother* 62.
108. Jiang M, Liu L, Ma Y, Zhang Z, Li N, Zhang F, Zhao S. 2016. Molecular Epidemiology of Multi-Drug Resistant *Acinetobacter baumannii* Isolated in Shandong, China. *Front Microbiol* 7:1687.
109. Yoon EJ, Chabane YN, Goussard S, Snesrud E, Courvalin P, De E, Grillot-Courvalin C. 2015. Contribution of resistance-nodulation-cell division efflux systems to antibiotic resistance and biofilm formation in *Acinetobacter baumannii*. *mBio* 6.
110. Tipton KA, Farokhyfar M, Rather PN. 2016. Multiple roles for a novel RND-type efflux system in *Acinetobacter baumannii* AB5075. *Microbiologyopen* doi:10.1002/mbo3.418.
111. Shaw KJ, Rather PN, Hare RS, Miller GH. 1993. Molecular genetics of aminoglycoside resistance genes and familial relationships of the aminoglycoside-modifying enzymes. *Microbiol Rev* 57:138-63.

112. Nemeč A, Dolzani L, Brisse S, van den Broek P, Dijkshoorn L. 2004. Diversity of aminoglycoside-resistance genes and their association with class 1 integrons among strains of pan-European *Acinetobacter baumannii* clones. *J Med Microbiol* 53:1233-40.
113. Liu CC, Tang CY, Chang KC, Kuo HY, Liou ML. 2014. A comparative study of class 1 integrons in *Acinetobacter baumannii*. *Gene* 544:75-82.
114. Messier N, Roy PH. 2001. Integron Integrases Possess a Unique Additional Domain Necessary for Activity. *J Bacteriol* 183:6699-6706.
115. Partridge SR, Recchia GD, Scaramuzzi C, Collis CM, Stokes HW, Hall RM. 2000. Definition of the *attI1* site of class 1 integrons. *Microbiology* 146 ( Pt 11):2855-64.
116. Hall RM, Brookes DE, Stokes HW. 1991. Site-specific insertion of genes into integrons: role of the 59-base element and determination of the recombination cross-over point. *Mol Microbiol* 5:1941-1959.
117. Deng Y, Bao X, Ji L, Chen L, Liu J, Miao J, Chen D, Bian H, Li Y, Yu G. 2015. Resistance integrons: class 1, 2 and 3 integrons. *Ann Clin Microbiol Antimicrob* 14:45.
118. Gillings MR. 2014. Integrons: past, present, and future. *Microbiol Mol Biol Rev* 78:257-77.
119. Stokes HW, Hall RM. 1989. A novel family of potentially mobile DNA elements encoding site-specific gene-integration functions: integrons. *Mol Microbiol* 3:1669-83.
120. Cagle CA, Shearer JE, Summers AO. 2011. Regulation of the integrase and cassette promoters of the class 1 integron by nucleoid-associated proteins. *Microbiology* 157:2841-53.
121. Hanau-Bercot B, Podglajen I, Casin I, Collatz E. 2002. An intrinsic control element for translational initiation in class 1 integrons. *Mol Microbiol* 44:119-30.

122. Levesque C, Brassard S, Lapointe J, Roy PH. 1994. Diversity and relative strength of tandem promoters for the antibiotic-resistance genes of several integrons. *Gene* 142:49-54.
123. Papagiannitsis CC, Tzouvelekis LS, Miriagou V. 2009. Relative strengths of the class 1 integron promoter hybrid 2 and the combinations of strong and hybrid 1 with an active p2 promoter. *Antimicrob Agents Chemother* 53:277-80.
124. Collis CM, Hall RM. 1995. Expression of antibiotic resistance genes in the integrated cassettes of integrons. *Antimicrob Agents Chemother* 39:155-162.
125. He W, Zhang X, Zhang J, Jia X, Zhang J, Sun W, Jiang H, Chen D, Murchie AI. 2013. Riboswitch control of induction of aminoglycoside resistance acetyl and adenylyltransferases. *RNA Biol* 10:1266-73.
126. Jia X, Zhang J, Sun W, He W, Jiang H, Chen D, Murchie AI. 2013. Riboswitch control of aminoglycoside antibiotic resistance. *Cell* 152:68-81.
127. Wang S, He W, Sun W, Zhang J, Chang Y, Chen D, Murchie AIH. 2019. Integron Derived Aminoglycoside-Sensing Riboswitches Control Aminoglycoside Acetyltransferase Resistance Gene Expression. *Antimicrob Agents Chemother* doi:10.1128/aac.00236-19.
128. Roth A, Breaker RR. 2013. Integron *attII* sites, not riboswitches, associate with antibiotic resistance genes. *Cell* 153:1417-8.
129. Hamidian M, Holt KE, Pickard D, Dougan G, Hall RM. 2014. A GC1 *Acinetobacter baumannii* isolate carrying AbaR3 and the aminoglycoside resistance transposon TnaphA6 in a conjugative plasmid. *J Antimicrob Chemother* 69:955-8.

130. Mabrouk A, Grosso F, Botelho J, Achour W, Ben Hassen A, Peixe L. 2017. GES-14-Producing *Acinetobacter baumannii* Isolates in a Neonatal Intensive Care Unit in Tunisia Are Associated with a Typical Middle East Clone and a Transferable Plasmid. *Antimicrob Agents Chemother* 61:e00142-17.
131. Bonnin RA, Nordmann P, Potron A, Lecuyer H, Zahar J-R, Poirel L. 2011. Carbapenem-Hydrolyzing GES-Type Extended-Spectrum  $\beta$ -Lactamase in *Acinetobacter baumannii*. *Antimicrob Agents Chemother* 55:349-354.
132. Andersson DI, Nicoloff H, Hjort K. 2019. Mechanisms and clinical relevance of bacterial heteroresistance. *Nat Rev Microbiol* doi:10.1038/s41579-019-0218-1.
133. Band VI, Crispell EK, Napier BA, Herrera CM, Tharp GK, Vavikolanu K, Pohl J, Read TD, Bosinger SE, Trent MS, Burd EM, Weiss DS. 2016. Antibiotic failure mediated by a resistant subpopulation in *Enterobacter cloacae*. *Nat Microbiol* 1:16053.
134. Band VI, Satola SW, Burd EM, Farley MM, Jacob JT, Weiss DS. 2018. Carbapenem-Resistant *Klebsiella pneumoniae* Exhibiting Clinically Undetected Colistin Heteroresistance Leads to Treatment Failure in a Murine Model of Infection. *mBio* 9.
135. Fusco DN, Alexander EL, Weisenberg SA, Mediavilla JR, Kreiswirth BN, Schuetz AN, Jenkins SG, Rhee KY. 2009. Clinical failure of vancomycin in a dialysis patient with methicillin-susceptible vancomycin-heteroresistant *S. aureus*. *Diagn Microbiol Infect Dis* 65:180-183.
136. Lin S-Y, Chen T-C, Chen F-J, Chen Y-H, Lin Y-I, Kristopher Siu L, Lu P-L. 2012. Molecular epidemiology and clinical characteristics of hetero-resistant vancomycin intermediate *Staphylococcus aureus* bacteremia in a Taiwan Medical Center. *J Microbiol Immunol Infect* 45:435-441.

137. Sola C, Lamberghini RO, Ciarlantini M, Egea AL, Gonzalez P, Diaz EG, Huerta V, Gonzalez J, Corso A, Vilaro M, Petiti JP, Torres A, Vindel A, Bocco JL. 2011. Heterogeneous vancomycin-intermediate susceptibility in a community-associated methicillin-resistant *Staphylococcus aureus* epidemic clone, in a case of Infective Endocarditis in Argentina. *Ann Clin Microbiol Antimicrob* 10:15.
138. Charles PGP, Ward PB, Johnson PDR, Howden BP, Grayson ML. 2004. Clinical Features Associated with Bacteremia Due to Heterogeneous Vancomycin-Intermediate *Staphylococcus aureus*. *Clin Infect Dis* 38:448-451.
139. Casapao AM, Davis SL, McRoberts JP, Lagnf AM, Patel S, Kullar R, Levine DP, Rybak MJ. 2014. Evaluation of vancomycin population susceptibility analysis profile as a predictor of outcomes for patients with infective endocarditis due to methicillin-resistant *Staphylococcus aureus*. *Antimicrob Agents Chemother* 58:4636-41.
140. Claeys KC, Lagnf AM, Hallesy JA, Compton MT, Gravelin AL, Davis SL, Rybak MJ. 2016. Pneumonia Caused by Methicillin-Resistant *Staphylococcus aureus*: Does Vancomycin Heteroresistance Matter? *Antimicrob Agents Chemother* 60:1708-1716.
141. Nicoloff H, Hjort K, Levin BR, Andersson DI. 2019. The high prevalence of antibiotic heteroresistance in pathogenic bacteria is mainly caused by gene amplification. *Nat Microbiol* 4:504-514.
142. Li J, Rayner CR, Nation RL, Owen RJ, Spelman D, Tan KE, Liolios L. 2006. Heteroresistance to colistin in multidrug-resistant *Acinetobacter baumannii*. *Antimicrob Agents Chemother* 50:2946-50.

143. Hawley JS, Murray CK, Jorgensen JH. 2008. Colistin heteroresistance in *Acinetobacter* and its association with previous colistin therapy. *Antimicrob Agents Chemother* 52:351-2.
144. Yau W, Owen RJ, Poudyal A, Bell JM, Turnidge JD, Yu HH, Nation RL, Li J. 2009. Colistin hetero-resistance in multidrug-resistant *Acinetobacter baumannii* clinical isolates from the Western Pacific region in the SENTRY antimicrobial surveillance programme. *J Infect* 58:138-44.
145. Srinivas P, Hunt LN, Pouch SM, Thomas K, Goff DA, Pancholi P, Balada-Llasat JM, Bauer KA. 2018. Detection of colistin heteroresistance in *Acinetobacter baumannii* from blood and respiratory isolates. *Diagn Microbiol Infect Dis*  
doi:10.1016/j.diagmicrobio.2018.01.028.
146. Barin J, Martins AF, Heineck BL, Barth AL, Zavascki AP. 2013. Hetero- and adaptive resistance to polymyxin B in OXA-23-producing carbapenem-resistant *Acinetobacter baumannii* isolates. *Ann Clin Microbiol Antimicrob* 12:15.
147. Fernandez Cuenca F, Sanchez Mdel C, Caballero-Moyano FJ, Vila J, Martinez-Martinez L, Bou G, Bano JR, Pascual A. 2012. Prevalence and analysis of microbiological factors associated with phenotypic heterogeneous resistance to carbapenems in *Acinetobacter baumannii*. *Int J Antimicrob Agents* 39:472-7.
148. Lee HY, Chen CL, Wang SB, Su LH, Chen SH, Liu SY, Wu TL, Lin TY, Chiu CH. 2011. Imipenem heteroresistance induced by imipenem in multidrug-resistant *Acinetobacter baumannii*: mechanism and clinical implications. *Int J Antimicrob Agents* 37:302-8.

149. Li P, Huang Y, Yu L, Liu Y, Niu W, Zou D, Liu H, Zheng J, Yin X, Yuan J, Yuan X, Bai C. 2017. Isolation and Whole-genome Sequence Analysis of the Imipenem Heteroresistant *Acinetobacter baumannii* Clinical Isolate HRAB-85. *Int J Infect Dis* 62:94-101.
150. Anderson SE, Sherman EX, Weiss DS, Rather PN. 2018. Aminoglycoside Heteroresistance in *Acinetobacter baumannii* AB5075. *mSphere* 3.
151. McGann P, Courvalin P, Snesrud E, Clifford RJ, Yoon EJ, Onmus-Leone F, Ong AC, Kwak YI, Grillot-Courvalin C, Lesho E, Waterman PE. 2014. Amplification of Aminoglycoside Resistance Gene *aphA1* in *Acinetobacter baumannii* Results in Tobramycin Therapy Failure. *mBio* 5.
152. Hjort K, Nicoloff H, Andersson DI. 2016. Unstable tandem gene amplification generates heteroresistance (variation in resistance within a population) to colistin in *Salmonella enterica*. *Mol Microbiol* 102:274-289.
153. El Meouche I, Siu Y, Dunlop MJ. 2016. Stochastic expression of a multiple antibiotic resistance activator confers transient resistance in single cells. *Sci Rep* 6:19538.
154. Sanchez-Romero MA, Casadesus J. 2014. Contribution of phenotypic heterogeneity to adaptive antibiotic resistance. *Proc Natl Acad Sci U S A* 111:355-60.
155. Stephens DS, McGee ZA. 1983. Association of virulence of *Neisseria meningitidis* with transparent colony type and low-molecular-weight outer membrane proteins. *J Infect Dis* 147:282-92.
156. Swanson J. 1978. Studies on gonococcus infection. XIV. Cell wall protein differences among color/opacity colony variants of *Neisseria gonorrhoeae*. *Infect Immun* 21:292-302.

157. Weiser JN, Austrian R, Sreenivasan PK, Masure HR. 1994. Phase variation in pneumococcal opacity: relationship between colonial morphology and nasopharyngeal colonization. *Infect Immun* 62:2582-9.
158. Weiser JN. 1993. Relationship between colony morphology and the life cycle of *Haemophilus influenzae*: the contribution of lipopolysaccharide phase variation to pathogenesis. *J Infect Dis* 168:672-80.
159. Liss A, Heiland RA. 1983. Colonial opacity variation in *Mycoplasma pulmonis*. *Infect Immun* 41:1245-51.
160. Rosengarten R, Wise KS. 1990. Phenotypic switching in mycoplasmas: phase variation of diverse surface lipoproteins. *Science* 247:315-8.
161. Bertin C, Pau-Roblot C, Courtois J, Manso-Silvan L, Thiaucourt F, Tardy F, Le Grand D, Poumarat F, Gaurivaud P. 2013. Characterization of free exopolysaccharides secreted by *Mycoplasma mycoides* subsp. *mycoides*. *PLoS One* 8:e68373.
162. van den Broek D, Chin AWTF, Eijkemans K, Mulders IH, Bloemberg GV, Lugtenberg BJ. 2003. Biocontrol traits of *Pseudomonas* spp. are regulated by phase variation. *Mol Plant Microbe Interact* 16:1003-12.
163. Achouak W, Conrod S, Cohen V, Heulin T. 2004. Phenotypic variation of *Pseudomonas brassicacearum* as a plant root-colonization strategy. *Mol Plant Microbe Interact* 17:872-9.
164. Yoshida S, Ogawa M, Mizuguchi Y. 1985. Relation of capsular materials and colony opacity to virulence of *Vibrio vulnificus*. *Infect Immun* 47:446-51.

165. Finkelstein RA, Boesman-Finkelstein M, Sengupta DK, Page WJ, Stanley CM, Phillips TE. 1997. Colonial opacity variations among the choleraenic vibrios. *Microbiology* 143 ( Pt 1):23-34.
166. McCarter LL. 1998. OpaR, a homolog of *Vibrio harveyi* LuxR, controls opacity of *Vibrio parahaemolyticus*. *J Bacteriol* 180:3166-73.
167. Stern A, Brown M, Nickel P, Meyer TF. 1986. Opacity genes in *Neisseria gonorrhoeae*: control of phase and antigenic variation. *Cell* 47:61-71.
168. Bhat KS, Gibbs CP, Barrera O, Morrison SG, Jahnig F, Stern A, Kupsch EM, Meyer TF, Swanson J. 1991. The opacity proteins of *Neisseria gonorrhoeae* strain MS11 are encoded by a family of 11 complete genes. *Mol Microbiol* 5:1889-901.
169. Rotman E, Seifert HS. 2014. The genetics of *Neisseria* species. *Annu Rev Genet* 48:405-31.
170. Hobbs MM, Seiler A, Achtman M, Cannon JG. 1994. Microevolution within a clonal population of pathogenic bacteria: recombination, gene duplication and horizontal genetic exchange in the *opa* gene family of *Neisseria meningitidis*. *Mol Microbiol* 12:171-80.
171. Stern A, Meyer TF. 1987. Common mechanism controlling phase and antigenic variation in pathogenic neisseriae. *Mol Microbiol* 1:5-12.
172. Swanson J. 1978. Studies on gonococcus infection. XII. Colony color and opacity variants of gonococci. *Infect Immun* 19:320-31.
173. LeVan A, Zimmerman LI, Mahle AC, Swanson KV, DeShong P, Park J, Edwards VL, Song W, Stein DC. 2012. Construction and characterization of a derivative of *Neisseria gonorrhoeae* strain MS11 devoid of all *opa* genes. *J Bacteriol* 194:6468-78.

174. Sadarangani M, Pollard AJ, Gray-Owen SD. 2011. Opa proteins and CEACAMs: pathways of immune engagement for pathogenic *Neisseria*. *FEMS Microbiol Rev* 35:498-514.
175. Li J, Li JW, Feng Z, Wang J, An H, Liu Y, Wang Y, Wang K, Zhang X, Miao Z, Liang W, Sebra R, Wang G, Wang WC, Zhang JR. 2016. Epigenetic Switch Driven by DNA Inversions Dictates Phase Variation in *Streptococcus pneumoniae*. *PLoS Pathog* 12:e1005762.
176. Kim JO, Weiser JN. 1998. Association of intrastrain phase variation in quantity of capsular polysaccharide and teichoic acid with the virulence of *Streptococcus pneumoniae*. *J Infect Dis* 177:368-77.
177. Li J, Zhang JR. 2019. Phase Variation of *Streptococcus pneumoniae*. *Microbiol Spectr* 7.
178. Ahmad I, Karah N, Nadeem A, Wai SN, Uhlin BE. 2019. Analysis of colony phase variation switch in *Acinetobacter baumannii* clinical isolates. *PLoS One* 14:e0210082.
179. Tipton KA, Rather PN. 2016. An ompR/envZ Two-Component System Ortholog Regulates Phase Variation, Osmotic Tolerance, Motility, and Virulence in *Acinetobacter baumannii* strain AB5075. *J Bacteriol* doi:10.1128/jb.00705-16.

**Chapter 2: Aminoglycoside Heteroresistance in *Acinetobacter baumannii* AB5075**

Sarah E. Anderson,<sup>a,b</sup> Edgar X. Sherman,<sup>a,b,c</sup> David S. Weiss,<sup>a,b,c,d,e</sup> Philip N. Rather<sup>a,b,e</sup>

<sup>a</sup>Department of Microbiology and Immunology, Emory University, Atlanta, Georgia, USA

<sup>b</sup>Emory Antibiotic Resistance Center, Emory University, Atlanta, Georgia, USA

<sup>c</sup>Emory Vaccine Center, Emory University, Atlanta, Georgia, USA

<sup>d</sup>Department of Medicine, Division of Infectious Diseases, Emory University School of  
Medicine, Atlanta, Georgia, USA

<sup>e</sup>Research Service, Atlanta VA Medical Center, Decatur, Georgia, USA

Published in:

mSphere, 2018

3:e00271-18

This manuscript was primarily written by S.E.A., with contributions to the methods and results from E.X.S and revisions by P.N.R. S.E.A. performed all experiments except for Fig. 2A-C and Supplemental Fig. S2, which were performed by E.X.S. P.N.R. isolated hetR variants.

## Abstract

Heteroresistance is a phenomenon where a subpopulation of cells exhibit higher levels of antibiotic resistance than the general population. Analysis of tobramycin resistance in *Acinetobacter baumannii* AB5075 using Etest strips demonstrated that colonies with increased resistance arose at high frequency within the zone of growth inhibition. The presence of a resistant subpopulation was confirmed by population analysis profiling (PAP). The tobramycin resistant subpopulation was cross-resistant to gentamicin, but not amikacin. The increased tobramycin resistance phenotype was highly unstable and cells reverted back to a less resistant population at frequencies of 60-90% after growth on non-selective media. Furthermore, the frequency of the resistant subpopulation was not increased by pre-incubation with subinhibitory concentrations of tobramycin. The tobramycin resistant subpopulation was shown to replicate during the course of antibiotic treatment, demonstrating that these were not persister cells. In *A. baumannii* AB5075, a large plasmid (p1AB5075), encodes *aadB*, a 2" nucleotidyltransferase that confers resistance to both tobramycin and gentamicin, but not amikacin. The *aadB* gene is part of an integron and is encoded adjacent to four additional resistance genes that are all flanked by copies of an integrase gene. In isolates with increased resistance, this region was highly amplified in a RecA-dependent manner. However, in a *recA* mutant, colonies with unstable tobramycin resistance arose by a mechanism that did not involve amplification of this region. These data indicate that tobramycin heteroresistance occurs by at least two mechanisms in *A. baumannii* and future studies to determine its effect on patient outcomes are warranted.

## Importance

*Acinetobacter baumannii* has become an important pathogen in hospitals worldwide, where the incidence of these infections has been increasing. *A. baumannii* infections have become exceedingly difficult to treat due to a rapid increase in the frequency of multidrug and pan-resistant isolates. This has prompted the World Health Organization to list *A. baumannii* as the top priority for the research and development of new antibiotics. This study reports for the first time a detailed analysis of aminoglycoside heteroresistance in *A. baumannii*. We define the mechanistic basis for heteroresistance, where the *aadB (ant2"')Ia* gene encoding an aminoglycoside adenylyltransferase becomes highly amplified in a RecA-dependent manner. Remarkably, this amplification of 20-40 copies occurs stochastically in 1/200 cells in the absence of antibiotic selection. In addition, we provide evidence for a second RecA-independent mechanism for aminoglycoside heteroresistance. This study reveals that aminoglycoside resistance in *A. baumannii* is far more complex than previously realized and has important implications for the use of aminoglycosides in treating *A. baumannii* infections.

## Introduction

Antibiotic heteroresistance occurs when subpopulations of an isogenic bacterial strain exhibit decreased susceptibility to a particular antibiotic (1). Although the clinical significance of heteroresistance has been the subject of debate, resistant subpopulations of otherwise susceptible strains have been demonstrated to mediate treatment failure in animal models (2), and have been associated with treatment failure in human patients (3-6). Heteroresistance has been reported to a wide variety of antibiotics, including  $\beta$ -lactams, glycopeptides, and antimicrobial peptides (1, 7-9). However, reports of aminoglycoside heteroresistance are uncommon. In 1947, it was reported that populations of type B *Haemophilus influenzae* contained rare cells with increased streptomycin resistance, although the mechanism responsible for the formation of these cells was not investigated (10). More recently, decreased expression of the porin gene *ompC* was associated with non-mutational kanamycin resistant subpopulations in *Salmonella enterica* (11). However, to our knowledge, heteroresistance to tobramycin or gentamicin has not been previously reported.

*Acinetobacter baumannii* is a Gram-negative, nosocomial, opportunistic pathogen (12-14). Widespread antibiotic resistance in this species recently led the World Health Organization to name carbapenem-resistant *A. baumannii* as its most critical priority pathogen for research and development of new interventions (15). Aminoglycoside resistance in *A. baumannii* has been associated with the acquisition, increased expression, and/or gene amplification of aminoglycoside modifying enzymes and efflux pumps (13, 16, 17). The multidrug resistant isolate AB5075 carries a number of antibiotic resistance genes, many of which are encoded on the large plasmid p1AB5075. This plasmid includes an integron-like structure encoding four aminoglycoside modifying enzymes, including the tobramycin resistance gene *aadB*, and a

chloramphenicol resistance transporter (18). The plasmid also encodes an additional tobramycin modifying enzyme, *aacA4* (18, 19). A recent study of loci required for tobramycin resistance in AB5075 showed that in addition to *aadB* and *aacA4*, thirty-four chromosomal genes also contribute to resistance to this drug (19).

AB5075 is resistant to tobramycin and gentamicin, meaning its MIC values for these drugs are above the CLSI breakpoints (19, 20). Here we report that AB5075 also exhibits tobramycin and gentamicin heteroresistance, as it produces subpopulations of cells that grow at concentrations of these drugs that are higher than the MIC for the general population. The subpopulations with increased resistance were shown to be unstable. We demonstrated that the integron-like structure of five adjacent antibiotic resistance genes, including *aadB*, becomes amplified to 20 to 40 copies in this resistant subpopulation. While this amplification was RecA-dependent, colonies with increased tobramycin resistance could also be selected in a *recA::Tc* mutant. These resistant isolates did not contain amplifications of the region containing *aadB*, indicating that tobramycin heteroresistance can occur by at least two distinct mechanisms.

## Results

**An AB5075 subpopulation exhibits increased tobramycin and gentamicin resistance.** When performing tobramycin Etest assays with the *A. baumannii* strain AB5075, we observed colonies arising at a high frequency within the zone of inhibition, consistent with a phenomenon termed heteroresistance (Fig. 1A). Heteroresistance was not observed during Etest assays with colistin, rifampin, or tetracycline (data not shown). In order to characterize the population with increased tobramycin resistance, colonies representative of this subpopulation were isolated by plating AB5075 on agar plates with varying inhibitory concentrations of tobramycin. In general, colonies representing the resistant subpopulation were heterogeneous in size on tobramycin plates, but exhibited normal size on media without drug. The colony size differences in the presence of tobramycin likely reflect differences in the levels of resistance. The frequency of resistant colonies decreased with increasing drug concentrations, so we chose a concentration 2X the baseline MIC to determine the frequency. In three independent experiments, colonies with increased resistance arose at an average frequency of  $0.52 \pm 0.24\%$ . Among the resistant subpopulation, both virulent opaque (VIR-O) and avirulent translucent (AV-T) colony variants were observed, as described previously (21, 22). Because VIR-O and AV-T variants were previously reported to exhibit subtle differences in tobramycin resistance (21, 23), both VIR-O and AV-T tobramycin resistant colonies were selected for further characterization. These resistant isolates were designated hetR-O2, hetR-O3, hetR-T1, and hetR-T4.

The subpopulation with increased tobramycin resistance was analyzed for cross-resistance to other antimicrobials. Etest assays were used to compare antimicrobial susceptibility of the tobramycin resistant isolates to wild-type VIR-O and AV-T variants with baseline levels of resistance. Etest assays for a variety of antimicrobials were conducted revealing that hetR-O2,

hetR-O3, hetR-T1, and hetR-T4 all exhibited cross-resistance to gentamicin, but not amikacin (Table 1). In addition, cross-resistance to non-aminoglycosides was not observed (Table 1).

**The tobramycin resistant subpopulation is not induced by tobramycin and is not composed of persister cells.**

Further phenotypic characterization of the tobramycin resistant subpopulation was performed. The ability of subinhibitory concentrations of tobramycin to induce the formation of the tobramycin resistant subpopulation was first investigated. Population analysis profile (PAP) results for treated and untreated cultures of AB5075 were identical (Fig. 2A), suggesting that the formation of the tobramycin resistant subpopulation was not increased by the presence of tobramycin. To confirm that the tobramycin resistant subpopulation is capable of growing in the presence of antibiotic, a killing assay with AB5075 was conducted. This assay clearly demonstrated that the tobramycin resistant subpopulation was capable of growing in high tobramycin concentrations, as the CFU counts increased during treatment (Fig. 2B). These data show that AB5075 forms a subpopulation with increased resistance to tobramycin that is distinct from persister cells, which are antibiotic tolerant at the expense of metabolic activity and active growth (24). Although exposure to a subinhibitory concentration of tobramycin does not increase the frequency of the resistant subpopulation, selection with a high-level of drug kills off the majority of susceptible cells, allowing the resistant subpopulation to dominate the culture.

**Increased tobramycin resistance is an unstable phenotype.** The stability of the increased tobramycin resistance phenotype was first tested in liquid culture. Cultures containing a mix of VIR-O and AV-T cells were grown, treated with tobramycin, and then subcultured without drug. Serial dilutions of cultures at each step indicated that following subculture without drug, the

population reverted from being almost entirely tobramycin resistant to containing only about 10% resistant cells (Fig. 2C). To determine whether VIR-O and AV-T representatives of the tobramycin resistant subpopulation behave similarly in terms of their resistance stability, the hetR-O2 and hetR-T1 stocks were examined for loss of resistance on agar plates. Colonies of hetR-O2 and hetR-T1 were passaged from plates containing tobramycin onto plates with and without drug. After 24 h and 48 h of growth, individual colonies were resuspended and serially diluted onto plates with and without tobramycin to determine the percent resistance within individual colonies (Fig. 2D, E). Interestingly, hetR-O2 and hetR-T1 exhibited differing levels of resistance stability. At 24 h, the percent resistance of hetR-T1 was similar for colonies grown with and without tobramycin, with about half of the cells from each condition exhibiting resistance. In contrast, hetR-O2 colonies grown without tobramycin for 24 h lost their increased resistance, whereas the majority of cells taken from colonies grown with tobramycin remained resistant (Fig. 2D). In colonies at 48 h, the frequency of resistant cells for both hetR-O2 and hetR-T1 continued to drop (Fig. 2E). Taken together, these results show that increased tobramycin resistance in AB5075 is an unstable phenotype, although the level of instability varies within the tobramycin resistant subpopulation.

**Tobramycin resistant subpopulations exhibit increased expression of *aadB*.** The mechanism of tobramycin heteroresistance in AB5075 was investigated by performing quantitative reverse transcriptase PCR (qRT-PCR) on hetR-O2 and hetR-T1, as well as the parental AB5075 VIR-O and AV-T variants not exposed to tobramycin. Two genes, *aadB* and *aacA4*, known to confer tobramycin resistance were selected for gene expression analysis (19). Differences in *aadB* or *aacA4* expression between the wild-type VIR-O and AV-T variants were not observed (Fig. 3A

and B). However, hetR-O2 and hetR-T1 exhibited 5- and 15-fold increased expression of *aadB*, respectively, compared to VIR-O (Fig. 3A). No differences in expression were observed for *aacA4* (Fig. 3B). These results are consistent with the aminoglycoside resistance profiles of hetR-O2 and hetR-T1, as *aadB* is associated with resistance to both tobramycin and gentamicin, but not amikacin (25).

### **Tobramycin resistant subpopulations contain a highly amplified region that includes *aadB*.**

To determine whether the pre-existing tobramycin resistant subpopulation in AB5075 could be due to gene amplification, we measured gene copy number of the region surrounding *aadB*. The *aadB* gene is found on the large plasmid p1AB5075 and is encoded adjacent to four other resistance genes that are all flanked by two copies of an integrase (*intI*) gene in the same orientation (Fig. 4). We hypothesized that if an amplification event were occurring, it would be within the interval flanked by the *intI* genes, possibly facilitated by recombination between the *intI* genes on adjacent plasmids during DNA replication. Gene copy number was measured by quantitative PCR (qPCR) using genomic DNA (gDNA) from the hetR-O2 and hetR-T1 isolates, as well as gDNA generated from VIR-O cells not exposed to tobramycin. The relative copy numbers of the *strB* and *aadB* genes (located immediately inside the interval flanked by *intI*) and the *ABUW\_4052* and *ABUW\_RS19335* genes (located immediately outside the *intI* region) were normalized to levels of *aacA4*, which is encoded outside this region and served as a control for changes in plasmid copy number. In both the hetR-O2 and hetR-T1 isolates, the *strB* and *aadB* genes were highly amplified, whereas the *ABUW\_4052* and *ABUW\_RS19335* genes were not amplified (Table 2). As presented previously in Fig 2, panels D and E, cells lost tobramycin resistance when grown in the absence of antibiotic. Consistent with this loss of resistance, the

levels of *aadB* amplification were reduced in colonies at 24 h in the absence of selection (Table 3). These results strongly suggest that tobramycin heteroresistance in AB5075 is due to the amplification of *aadB*.

To confirm the role of *aadB* in heteroresistance, we obtained three independent *aadB::T26* transposon insertion mutants from the University of Washington library. However, PCR analysis of the mutants revealed that all three had two copies of *aadB*, a wild-type copy and a T26 disrupted copy (data not shown). Similarly, in our wild-type VIR-O AB5075 parent strain, qPCR analysis indicated that there were two copies of *strB* and *aadB* relative to the *aacA4* gene (Table 2), which is in contrast to the published genome sequence where a single copy of each gene is present (18). Southern blot analysis confirmed that the region between the *intI* genes was duplicated in our AB5075 parental strain (data not shown). Due the duplication of *aadB* in our parental strain and the presence of a wild-type copy of *aadB* in the University of Washington library mutants, we have been unable to construct and test a defined *aadB* mutant.

### **Tobramycin heteroresistance can occur by RecA-dependent and independent mechanisms.**

To determine if the above amplification event between duplicated copies of the *intI* gene required homologous recombination, tobramycin heteroresistance was examined in a *recA::Tc* mutant. The *recA::Tc* mutant exhibited intrinsic levels of tobramycin resistance that were lower than the wild-type parent (Fig. 1B and Table 3). Although this strain still appeared heteroresistant, the frequency of tobramycin resistant colonies arising in the zone of clearing was lower than in wild-type cells (Fig. 1B). Introduction of the wild-type *recA* gene into the *recA::Tc* mutant partially restored heteroresistance (Fig. S1). Interestingly, when six tobramycin resistant isolates from the *recA::Tc* mutant were tested for amplification of *aadB*, the copy number was

similar to the *recA::Tc* parent strain (Table 4). This indicates that increased resistance arose in these isolates by a mechanism that did not involve *aadB* amplification. When three of these resistant isolates 1-2, 1-4, and 1-10 were cultured for approximately 30 generations in the absence of tobramycin, the frequency of cells retaining tobramycin resistance was 11%, 23%, and 35%, respectively, demonstrating that these isolates are not stable mutants. The resistant subpopulation in the *recA::Tc* mutant consisted of both VIR-O and AV-T cells (data not shown).

To confirm that the tobramycin resistant subpopulation in the *recA::Tc* mutant was capable of growing in the presence of antibiotic, a tobramycin killing assay was conducted (Fig. S2A, panel A). This indicated that the tobramycin resistant subpopulation was capable of growing in the presence of drug and was not composed of persister cells. In addition, PAP analysis demonstrated that pretreatment with tobramycin did not alter the frequency of cells that became resistant to tobramycin in the *recA::Tc* background (Fig. S2, panel B).

## Discussion

This study demonstrates that subpopulations of *A. baumannii* AB5075 exhibit heterogeneous levels of resistance to aminoglycosides. The subpopulation with increased tobramycin resistance can be visualized using both an Etest MIC assay and PAP analysis. Application of selective concentrations of tobramycin resulted in the outgrowth of the tobramycin resistant subpopulation, allowing it to dominate the surviving culture. However, once selective pressure was removed, the majority of the subpopulation returned to baseline levels of resistance. Independent isolates from the resistant subpopulation were found to exhibit increased expression and amplification of the 2''-aminoglycoside nucleotidyltransferase gene *aadB*. This gene is likely involved in heteroresistance as the substrate profile of this enzyme matches the resistance profile observed, i.e., resistance to tobramycin and gentamicin, but not amikacin.

The role of phenotypic heterogeneity in the formation of subpopulations that are able to survive antibiotic treatment is well appreciated. This has been best studied in the case of dormant persister cells and slow-growing small colony variants (SCVs), both of which exhibit increased tolerance to antibiotics, including aminoglycosides (26-29). Both persistence and SCV formation confer antibiotic tolerance at the expense of normal growth. In contrast, heteroresistance involves the formation of a subpopulation of cells with increased antibiotic resistance, which maintain the ability to actively grow during antibiotic exposure (1). Although heteroresistance has been reported in many species, including *A. baumannii* (30, 31), reports of aminoglycoside heteroresistance are exceedingly rare. This study is the first report of aminoglycoside heteroresistance in *A. baumannii*, and to our knowledge only the second definitive report of this phenomenon in any species. In *Salmonella enterica*, aminoglycoside heteroresistance has been

shown to occur when a subpopulation of cells expressed decreased levels of the porin gene *ompC*. This limits uptake of kanamycin into the cells, causing increased resistance (11).

This study demonstrates that tobramycin heteroresistance can arise by the extensive amplification (20-40 copies) of a region encoded on the large p1AB5075 plasmid that includes five resistance genes in tandem, including *aadB*, flanked by copies of an integrase (*intI*) gene. The mechanism by which the *aadB* containing region gets extensively amplified is unclear, but our work has established that RecA is required. Duplications can occur by non-equal recombination between directly repeated regions on adjacent replicons (32). Gene amplification of the aminoglycoside modifying enzyme *aphA1* has previously been reported to cause unstable tobramycin resistance in *A. baumannii* AB0057 and a clinical isolate (16). However, in that study, amplifications were dependent on prior exposure to tobramycin and were likely selected for by the antibiotic. Heteroresistance resulting from gene amplification of a chromosomal locus has also been reported in *Salmonella enterica*, where amplification of a region containing *pmrD* conferred colistin heteroresistance (33). Our data suggest that extensive amplifications pre-exist in 1/200 cells (i.e., the frequency of the resistant subpopulation) in the absence of any selective tobramycin pressure. As extensive gene amplifications typically require growth in the presence of selective pressures, this suggests that additional mechanisms, such as the rolling circle-dependent generation of tandem arrays, may contribute to amplification of this region in *A. baumannii* (32). In a *recA::Tc* mutant, cells with increased resistance still arose, but none of the isolates examined contained duplications of the *aadB* gene (Table 3). Therefore, heteroresistance can occur by at least one additional mechanism. A recent study by Gallagher et al., demonstrated at least 32 chromosomally encoded genes in AB5075 function to maintain intrinsic tobramycin resistance (19). In principle, amplification of any of these genes could potentially lead to

increased tobramycin resistance and may account for the resistant subpopulation that does not contain amplification of *aadB*. However, if this amplification is occurring, it does not appear to require RecA.

When the stability of the tobramycin resistant subpopulation was examined, contrasting results were found for the virulent opaque (VIR-O) and avirulent translucent (AV-T) isolates (Fig. 2D). As long as selection was maintained, the majority of hetR-O2 cells remained tobramycin resistant; however, resistance was lost in approximately 90% of the population in colonies grown without drug for 24 h. In contrast, cells of hetR-T1 lost their increased resistance at roughly the same rate regardless of whether selection was maintained, with approximately 50% of the population in a 24 h colony maintaining the increased resistance state. However, in both isolates the loss of heteroresistance at high rates is consistent with the unstable nature of extensive duplications (32). The increased stability of heteroresistance in hetR-T1 in the absence of selection may be due the larger number of tandem repeats that includes *aadB* (Table 2).

The clinical relevance of the aminoglycoside heteroresistance phenomenon described here remains to be determined. The plasmid-borne *aadB* gene is common in *A. baumannii* and strains carrying this gene should exhibit clinically relevant resistance to tobramycin and gentamicin (34-37). Further research is needed to determine whether *A. baumannii* strains identified as being aminoglycoside sensitive also exhibit heteroresistance, which could pose problems for appropriately treating these infections. It is possible that strains lacking *aadB* could still exhibit heteroresistance by an *aadB*-independent mechanism, similar to the *recA::Tc* mutant discussed in this work. The data presented here illustrate that the full picture of antibiotic resistance in *A. baumannii* is more complicated than has been traditionally recognized, with both

the acquisition of resistance determinants and phenotypic heterogeneity contributing to resistance.

## Materials and Methods

**Bacterial strains and growth conditions.** Strains of *A. baumannii* were maintained at -80°C in 15% glycerol. Pure stocks of opaque and translucent variants were prepared as previously described (23). Liquid cultures were prepared in sterile LB broth, supplemented as needed with tobramycin (Sigma-Aldrich, St. Louis, MO) at the concentrations indicated. Resistance stability experiments and experiments to select isolates with increased resistance were performed using 0.5x LB supplemented with 0.8% agar. All other experiments were performed using regular LB supplemented with 1.5% agar. Plates were supplemented with tobramycin as indicated.

A T26 insertion mutant in *recA* was obtained from the AB5075 transposon mutant library maintained at the University of Washington (18). A culture of this strain was grown overnight at 37°C with shaking and used to prepare genomic DNA (gDNA) as outlined below. A culture of VIR-O AB5075 was grown at 37°C with shaking to late log and used to prepare electrocompetent cells by washing three times with 10% glycerol. The *recA::T26* mutant DNA was electroporated into these cells and transformants were selected on LB supplemented with 10 µg/ml tetracycline. A single colony was isolated and designated strain *recA::Tc*. The presence of the *recA* mutation was confirmed by PCR.

Isolation of tobramycin resistant subpopulations was conducted by plating serial dilutions of an early-log phase culture of the wild-type or *recA::Tc* VIR-O variant on 0.5X LB and 0.5X LB containing tobramycin (Sigma-Aldrich, St. Louis, MO) at 2.5, 5, 10, 15, 20, 25, and 30 µg/ml. Colonies exhibiting increased resistance were apparent at 15 µg/ml tobramycin for wild-type and at 5 µg/ml for the *recA::Tc* mutant. Resistant colonies were restreaked on 0.5X LB with tobramycin and examined under a stereo microscope with oblique lighting to determine whether they were opaque or translucent variants.

**Oligonucleotides.** All oligonucleotides used in this study are listed in Supplemental Table 1

**Complementation of the *recA* mutant.** The wild-type *recA* gene was amplified by PCR using the primers oSA77 5'-GCTCATCGTTTCGTTTGAAC-3' and oSA78 5'- GAATAAAAACGTC GAGTTGTG-3' (Supplemental Table 1). This fragment was then cloned into the *Sma*I site of pQF1266Blue, a derivative of pQF50 (38) where a hygromycin resistance gene has been cloned into the *bla* gene encoding  $\beta$ -lactamase. In addition, this plasmid contains an origin of replication from pWH1266 (39) cloned into the *Nco*I site. The resulting plasmid was designated *precA*.

**MIC Assays.** MICs of different antibiotics were measured using Etest strips (bioMérieux, Marcy-l'Étoile, France). For the tobramycin MICs used to visualize heteroresistance, AB5075 wild-type or *recA::Tc* VIR-O cells were inoculated into LB broth and grown at 37° with shaking to a concentration of 1.1 to 1.3 x 10<sup>7</sup> CFU/ml. Lawns were inoculated by spreading 100  $\mu$ l of culture onto an LB plate, followed by application of the Etest strip. The plate was photographed following incubation for 16 h at 37°C.

For MIC experiments reported in Table 1, strains were inoculated into LB broth, grown overnight static at room temperature, grown at 37°C with shaking to an OD<sub>600</sub> of 0.1, and stored at 4°C for use later in the day. Etest strips were placed on LB plates and strains were inoculated next to each strip by spotting 10  $\mu$ l of culture next to the bottom of the strip, tilting the plate so that the culture spread up the side of the strip, and removing excess culture at the top of the strip by pipetting. Two strains were inoculated on each side of each strip to facilitate a direct comparison of susceptibility. MIC values were recorded after incubation for 5 h or 16 h at 37°C,

as noted. MIC experiments were performed two independent times to confirm the reproducibility of trends.

For the *recA::Tc* mutant, colonies that were growing in the zone of tobramycin inhibition were placed into a small vial of 20% glycerol and stored at -80°C. MIC experiments were performed by growing cells from the -80°C glycerol stock for several hours in LB and performing Etest assays as outlined above for the data presented in Table 1.

**Population analysis profile (PAP).** Population analysis profile (PAP) was performed by growing bacteria overnight to stationary phase and then plating serial dilutions on LB agar with or without various concentrations of tobramycin (Spectrum, New Brunswick, NJ). Plates were then incubated at 37°C and CFUs enumerated after 24 h. Percent tobramycin resistance was calculated as the number of bacterial colonies that grew on tobramycin plates divided by the number of bacteria that grew on LB alone without drug.

**Tobramycin killing assays.** Briefly, AB5075 was grown overnight to stationary phase in LB media and serially diluted to  $1 \times 10^6$  CFU/ml. Tobramycin (Spectrum) was added at a concentration of 64 µg/ml. 100 µl aliquots were taken at desired time points, serially diluted, and plated on LB media alone (to quantify total CFU) or LB plates containing 64 µg/ml tobramycin (to quantify resistant CFU).

**Stability measurements of the resistant subpopulation.** For experiments conducted with broth cultures, AB5075 was grown overnight to stationary phase in LB media. The bacteria were then serially diluted and plated on LB agar plates with and without 64 µg/ml tobramycin (Spectrum)

to enumerate total and resistant CFU for the pre-treatment group (day 1). A subculture (1:1000) was then grown overnight in LB supplemented with 64 µg/ml tobramycin, serially diluted, and plated on LB agar with or without 64 µg/ml tobramycin to enumerate total and resistant CFU for the treatment group (day 2). This process was repeated in LB broth without antibiotics (day 3) and dilutions were plated on agar plates with and without 64 µg/ml tobramycin to enumerate total and resistant CFU.

For experiments with hetR-O2 and hetR-T1 colonies, cells from the two subpopulations were struck from freezer stocks onto 0.5x LB supplemented with tobramycin 20 µg/ml (Sigma-Aldrich). Plates were incubated overnight at 37°C, and single colonies were resuspended in 1 ml LB and struck onto 0.5x LB agar with and without tobramycin 40 µg/ml. After 24 h or 48 h of incubation at 37°C, individual colonies were resuspended in 1 ml LB and serial dilutions were plated in duplicate on 0.5x LB with and without tobramycin 40 µg/ml. Plates were incubated for up to 48 h at 37°C, and colonies were enumerated to determine the percent tobramycin resistance by comparing the CFUs on plates with and without tobramycin.

**RNA isolation.** Cultures of different *A. baumannii* AB5075 subpopulations were grown in LB medium at 37°C with shaking to an OD<sub>600</sub> of 0.5. Cells were pelleted by centrifugation and RNA was isolated using the MasterPure RNA Purification Kit according to the manufacturer's protocol (Epicentre, Madison, WI). Contaminating DNA was degraded by two treatments with TURBO DNA-free according to the manufacturer's protocol (Invitrogen, Waltham, MA). DNA contamination was evaluated by PCR with purified RNA as template, and RNA concentration was measured with a NanoDrop ND-1000 spectrophotometer.

**Quantitative reverse transcriptase PCR.** Total RNA (1  $\mu$ g) was used to prepare cDNA using the iScript cDNA Synthesis kit (BioRad, Hercules, CA) with random primers and either iScript or SuperScript III (Invitrogen, Waltham, MA) reverse transcriptase. Reactions lacking reverse transcriptase were also performed as a control for the presence of contaminating DNA. Incubation conditions for cDNA synthesis were: 25°C for 5 min, 42°C for 45 min, and 85°C for 5 min. cDNA reactions and controls were then diluted 1:10 with sterile water and used as a template for reverse transcriptase quantitative PCR (qRT-PCR). Oligonucleotide primer pairs for qRT-PCR were designed to amplify approximately 150 bp fragments from each gene of interest and were generated using the Primer-BLAST program available at [www.ncbi.nlm.nih.gov/tools/primer-blast](http://www.ncbi.nlm.nih.gov/tools/primer-blast). qRT-PCR was performed using iQ SYBR Green Supermix (Bio-Rad, Hercules, CA) on a Bio-Rad CFX Connect cycler. Cycle parameters were as follows: 95°C for 3 min, followed by 40 cycles of 95°C for 10 s, 55°C for 10 s, and 72°C for 20 s. Melt curve data were then collected to confirm the specificity of the oligonucleotide primer pairs. Data were generated using cDNA prepared from three independent RNA isolations, and qRT-PCR reactions were performed in technical triplicate to ensure accuracy. Fold changes in gene expression relative to the control strain (VIR-O) and a control gene (*clpX*) were determined using the  $2^{-\Delta\Delta C_t}$  method (40).

**Genomic DNA isolation.** For experiments presented in Table 2, cultures of different AB5075 subpopulations were grown in LB medium with shaking at 37°C to an OD<sub>600</sub> of 0.5. For experiments presented in Table 3, colonies were grown for 24 h on 0.5x LB with or without tobramycin 40  $\mu$ g/ml; individual colonies were then resuspended in 1 ml of LB. In both cases, cells were pelleted by centrifugation and resuspended in TE. Cells were lysed by incubation

with 0.5% SDS and 400 µg/ml proteinase K for 1 h at 37°C. Following lysis, NaCl was added to a final concentration of 0.7 M, and DNA was extracted twice with equal volumes of phenol/chloroform/isoamyl alcohol. DNA was precipitated by mixing with 1.5 volumes of 95% ethanol until a precipitate formed. DNA pellets were collected by centrifugation, washed twice with 75% ethanol, dried, and resuspended in molecular grade water.

**Quantitative PCR (qPCR).** Concentrations of gDNA samples were determined using a NanoDrop ND-100 spectrophotometer. Samples were diluted to a concentration of 15 µg/ml and qPCR was performed as outlined above for cDNA samples. Standard curves using ten-fold serial dilutions of wild-type gDNA were used to ensure that primers exhibited similar efficiencies. Relative gene copy numbers normalized to *aacA4* were determined using the equation  $2^{-\Delta C_t}$  (40).

**Statistical analyses.** Statistical analyses were performed with Prism 7 (GraphPad Software, Inc. La Jolla, CA).

**Acknowledgements.** This study was supported by a VA Merit Award I01 BX001725 and a Research Career Scientist Award from the Department of Veterans Affairs to P.N.R. D.S.W. is supported by a Burroughs Wellcome Fund Investigator in the Pathogenesis of Infectious Disease award, VA Merit award I01 BX002788 and National Institutes of Health (NIH) grant AI098800. S.E.A. and E.X.S. were both supported by a T32 training grant AI106699 from the National Institutes of Health. The content is solely the responsibility of the authors and does not necessarily represent the official views of the NIH or the Department of Veterans Affairs. The authors have no conflicts of interest to disclose.

## References

1. El-Halfawy OM, Valvano MA. 2015. Antimicrobial heteroresistance: an emerging field in need of clarity. *Clin Microbiol Rev* 28:191-207.
2. Band VI, Crispell EK, Napier BA, Herrera CM, Tharp GK, Vavikolanu K, Pohl J, Read TD, Bosinger SE, Trent MS, Burd EM, Weiss DS. 2016. Antibiotic failure mediated by a resistant subpopulation in *Enterobacter cloacae*. *Nat Microbiol* 1:16053.
3. Fusco DN, Alexander EL, Weisenberg SA, Mediavilla JR, Kreiswirth BN, Schuetz AN, Jenkins SG, Rhee KY. 2009. Clinical failure of vancomycin in a dialysis patient with methicillin-susceptible vancomycin-heteroresistant *S. aureus*. *Diagn Microbiol Infect Dis* 65:180-183.
4. Lin S-Y, Chen T-C, Chen F-J, Chen Y-H, Lin Y-I, Kristopher Siu L, Lu P-L. 2012. Molecular epidemiology and clinical characteristics of hetero-resistant vancomycin intermediate *Staphylococcus aureus* bacteremia in a Taiwan Medical Center. *J Microbiol Immunol Infect* 45:435-441.
5. Sola C, Lamberghini RO, Ciarlantini M, Egea AL, Gonzalez P, Diaz EG, Huerta V, Gonzalez J, Corso A, Vilaro M, Petiti JP, Torres A, Vindel A, Bocco JL. 2011. Heterogeneous vancomycin-intermediate susceptibility in a community-associated methicillin-resistant *Staphylococcus aureus* epidemic clone, in a case of Infective Endocarditis in Argentina. *Ann Clin Microbiol Antimicrob* 10:15.
6. Charles PGP, Ward PB, Johnson PDR, Howden BP, Grayson ML. 2004. Clinical Features Associated with Bacteremia Due to Heterogeneous Vancomycin-Intermediate *Staphylococcus aureus*. *Clin Infect Dis* 38:448-451.

7. Napier BA, Band V, Burd EM, Weiss DS. 2014. Colistin heteroresistance in *Enterobacter cloacae* is associated with cross-resistance to the host antimicrobial lysozyme. *Antimicrob Agents Chemother* 58:5594-7.
8. Hiramatsu K, Aritaka N, Hanaki H, Kawasaki S, Hosoda Y, Hori S, Fukuchi Y, Kobayashi I. 1997. Dissemination in Japanese hospitals of strains of *Staphylococcus aureus* heterogeneously resistant to vancomycin. *Lancet* 350:1670-3.
9. Hung K-H, Wang M-C, Huang A-H, Yan J-J, Wu J-J. 2012. Heteroresistance to Cephalosporins and Penicillins in *Acinetobacter baumannii*. *J Clin Microbiol* 50:721-726.
10. Alexander HE, Leidy G. 1947. MODE OF ACTION OF STREPTOMYCIN ON TYPE b *HEMOPHILUS INFLUENZAE* : II. NATURE OF RESISTANT VARIANTS. *J Exp Med* 85:607-21.
11. Sanchez-Romero MA, Casadesus J. 2014. Contribution of phenotypic heterogeneity to adaptive antibiotic resistance. *Proc Natl Acad Sci U S A* 111:355-60.
12. Peleg AY, Seifert H, Paterson DL. 2008. *Acinetobacter baumannii*: emergence of a successful pathogen. *Clin Microbiol Rev* 21:538-82.
13. Lee CR, Lee JH, Park M, Park KS, Bae IK, Kim YB, Cha CJ, Jeong BC, Lee SH. 2017. Biology of *Acinetobacter baumannii*: Pathogenesis, Antibiotic Resistance Mechanisms, and Prospective Treatment Options. *Front Cell Infect Microbiol* 7:55.
14. Baumann P. 1968. Isolation of *Acinetobacter* from soil and water. *J Bacteriol* 96:39-42.
15. Anonymous. 2017. WHO Priority Pathogens List for R&D of New Antibiotics, on World Health Organization. [http://who.int/medicines/publications/WHO-PPL-Short\\_Summary\\_25Feb-ET\\_NM\\_WHO.pdf](http://who.int/medicines/publications/WHO-PPL-Short_Summary_25Feb-ET_NM_WHO.pdf). Accessed Nov. 5.

16. McGann P, Courvalin P, Snesrud E, Clifford RJ, Yoon EJ, Onmus-Leone F, Ong AC, Kwak YI, Grillot-Courvalin C, Lesho E, Waterman PE. 2014. Amplification of Aminoglycoside Resistance Gene *aphA1* in *Acinetobacter baumannii* Results in Tobramycin Therapy Failure. *Mbio* 5.
17. Yoon EJ, Balloy V, Fiette L, Chignard M, Courvalin P, Grillot-Courvalin C. 2016. Contribution of the Ade Resistance-Nodulation-Cell Division-Type Efflux Pumps to Fitness and Pathogenesis of *Acinetobacter baumannii*. *Mbio* 7.
18. Gallagher LA, Ramage E, Weiss EJ, Radey M, Hayden HS, Held KG, Huse HK, Zurawski DV, Brittnacher MJ, Manoil C. 2015. Resources for Genetic and Genomic Analysis of Emerging Pathogen *Acinetobacter baumannii*. *J Bacteriol* 197:2027-35.
19. Gallagher LA, Lee SA, Manoil C. 2017. Importance of Core Genome Functions for an Extreme Antibiotic Resistance Trait. *MBio* 8.
20. Jacobs AC, Thompson MG, Black CC, Kessler JL, Clark LP, McQueary CN, Gancz HY, Corey BW, Moon JK, Si Y, Owen MT, Hallock JD, Kwak YI, Summers A, Li CZ, Rasko DA, Penwell WF, Honnold CL, Wise MC, Waterman PE, Lesho EP, Stewart RL, Actis LA, Palys TJ, Craft DW, Zurawski DV. 2014. AB5075, a Highly Virulent Isolate of *Acinetobacter baumannii*, as a Model Strain for the Evaluation of Pathogenesis and Antimicrobial Treatments. *MBio* 5:e01076-14.
21. Tipton KA, Dimitrova D, Rather PN. 2015. Phase-Variable Control of Multiple Phenotypes in *Acinetobacter baumannii* Strain AB5075. *J Bacteriol* 197:2593-9.
22. Chin CY, Tipton KA, Farokhyfar M, Burd EM, Weiss DS, Rather PN. 2018. A high-frequency phenotypic switch links bacterial virulence and environmental survival in *Acinetobacter baumannii*. *Nat Microbiol* 3:563-569.

23. Tipton KA, Farokhyfar M, Rather PN. 2016. Multiple roles for a novel RND-type efflux system in *Acinetobacter baumannii* AB5075. *Microbiologyopen* doi:10.1002/mbo3.418.
24. Shah D, Zhang Z, Khodursky A, Kaldalu N, Kurg K, Lewis K. 2006. Persisters: a distinct physiological state of *E. coli*. *BMC Microbiol* 6:53.
25. Shaw KJ, Rather PN, Hare RS, Miller GH. 1993. Molecular genetics of aminoglycoside resistance genes and familial relationships of the aminoglycoside-modifying enzymes. *Microbiol Rev* 57:138-63.
26. Massey RC, Buckling A, Peacock SJ. 2001. Phenotypic switching of antibiotic resistance circumvents permanent costs in *Staphylococcus aureus*. *Current Biology* 11:1810-1814.
27. Edwards AM. 2012. Phenotype Switching Is a Natural Consequence of *Staphylococcus aureus* Replication. *J Bacteriol* 194:5404-5412.
28. Keren I, Shah D, Spoering A, Kaldalu N, Lewis K. 2004. Specialized persister cells and the mechanism of multidrug tolerance in *Escherichia coli*. *J Bacteriol* 186:8172-80.
29. Shan Y, Lazinski D, Rowe S, Camilli A, Lewis K. 2015. Genetic basis of persister tolerance to aminoglycosides in *Escherichia coli*. *MBio* 6.
30. Li P, Huang Y, Yu L, Liu Y, Niu W, Zou D, Liu H, Zheng J, Yin X, Yuan J, Yuan X, Bai C. 2017. Isolation and Whole-genome Sequence Analysis of the Imipenem Heteroresistant *Acinetobacter baumannii* Clinical Isolate HRAB-85. *Int J Infect Dis* 62:94-101.
31. Li J, Rayner CR, Nation RL, Owen RJ, Spelman D, Tan KE, Liolios L. 2006. Heteroresistance to colistin in multidrug-resistant *Acinetobacter baumannii*. *Antimicrob Agents Chemother* 50:2946-50.

32. Andersson DI, Hughes D. 2009. Gene amplification and adaptive evolution in bacteria. *Annu Rev Genet* 43:167-95.
33. Hjort K, Nicoloff H, Andersson DI. 2016. Unstable tandem gene amplification generates heteroresistance (variation in resistance within a population) to colistin in *Salmonella enterica*. *Mol Microbiol* 102:274-289.
34. Karah N, Dwibedi CK, Sjostrom K, Edquist P, Johansson A, Wai SN, Uhlin BE. 2016. Novel Aminoglycoside Resistance Transposons and Transposon-Derived Circular Forms Detected in Carbapenem-Resistant *Acinetobacter baumannii* Clinical Isolates. *Antimicrob Agents Chemother* 60:1801-18.
35. Aliakbarzade K, Farajnia S, Karimi Nik A, Zarei F, Tanomand A. 2014. Prevalence of Aminoglycoside Resistance Genes in *Acinetobacter baumannii* Isolates. *Jundishapur J Microbiol* 7:e11924.
36. Hamidian M, Nigro SJ, Hall RM. 2012. Variants of the gentamicin and tobramycin resistance plasmid pRAY are widely distributed in *Acinetobacter*. *J Antimicrob Chemother* 67:2833-6.
37. Nigro SJ, Hall RM. 2016. Loss and gain of aminoglycoside resistance in global clone 2 *Acinetobacter baumannii* in Australia via modification of genomic resistance islands and acquisition of plasmids. *J Antimicrob Chemother* 71:2432-40.
38. Farinha MA, Kropinski AM. 1990. Construction of broad-host-range plasmid vectors for easy visible selection and analysis of promoters. *J Bacteriol* 172:3496-9.
39. Hunger M, Schmucker R, Kishan V, Hillen W. 1990. Analysis and nucleotide sequence of an origin of DNA replication in *Acinetobacter calcoaceticus* and its use for *Escherichia coli* shuttle plasmids. *Gene* 87:45-51.

40. Schmittgen TD, Livak KJ. 2008. Analyzing real-time PCR data by the comparative C(T) method. *Nat Protoc* 3:1101-8.

**Table 1. The tobramycin resistant subpopulation exhibits increased cross-resistance to gentamicin, but not other antimicrobials.**

Strain	TOB <sup>a</sup>	CST <sup>a</sup>	RIF <sup>a</sup>	TET <sup>a</sup>	AMK <sup>b</sup>	CHL <sup>b</sup>	GEN <sup>b</sup>
VIR-O	48	1	4	3	192	256	96
hetR-O2	128	1	4	3	192	>256	192
VIR-O	64	1	4	3	96	96	32
hetR-O3	192	1	4	3	96	128	128
AV-T	48	1	4	2	128	256	96
hetR-T1	256	1	4	2	128	192	>256
AV-T	32	1	4	3	64	96	32
hetR-T4	384	1	4	3	64	96	128

MICs in µg/ml were determined using Etest strips. Direct comparisons between isolates were performed by inoculating two cultures at an optical density  $A_{600}$  of 0.1 along the same Etest strip; each direct comparison is separated by a black line. Two independent experiments were performed for each comparison to assess reproducibility; data from a single representative experiment are shown. <sup>a</sup>MICs were measured after 16 h of growth at 37°C. <sup>b</sup>MICs were measured after 5 h of growth at 37°C. Abbreviations: TOB, tobramycin; CST, colistin; RIF, rifampin; TET, tetracycline; AMK, amikacin; CHL, chloramphenicol; GEN, gentamicin.

**Table 2. HetR-O2 and hetR-T1 exhibit gene amplifications that include *aadB*.**

Strain	<i>ABUW_4052</i>	<i>strB</i>	<i>aadB</i>	<i>ABUW_RS19335</i>
VIR-O	1.31 ± 0.09	2.94 ± 0.07	2.45 ± 0.06	0.72 ± 0.01
hetR-O2	1.80 ± 0.53	20.26 ± 6.18*	17.23 ± 6.80*	0.83 ± 0.31
hetR-T1	1.44 ± 0.04	55.62 ± 9.27*	44.07 ± 8.26*	0.64 ± 0.03

Means and standard deviations of the relative copy number of genes surrounding *aadB* measured in three biological replicates are shown. Relative copy numbers were measured by qPCR using normalization to *aacA4*, a presumed single-copy gene located on the same plasmid. Copy numbers of *aadB* and *strB* were significantly increased in hetR-O2 and hetR-T1 relative to VIR-O not exposed to tobramycin (\*,  $p < 0.001$  relative to VIR-O by two-way ANOVA with Dunnett's post-test).

**Table 3. *aadB* copy number in the presence and absence of antibiotic selection.**

Strain	<i>aadB</i>	<i>ABUW_RS19335</i>
hetR-O2 + Tob	40.35 ± 0.62	0.72 ± 0.16
hetR-O2 – Tob	16.75 ± 0.16*	0.71 ± 0.03
hetR-T1 + Tob	55.12 ± 4.35	0.72 ± 0.05
hetR-T1 – Tob	40.38 ± 10.71	0.77 ± 0.08

The table depicts copy numbers of *aadB* and *ABUW\_RS19335* relative to *aacA4* in hetR-O2 and hetR-T1 colonies grown with or without tobramycin for 24 h. The means and standard deviations of two biological replicates are shown. Copy number of *aadB* was significantly decreased in hetR-O2 grown without tobramycin when compared to this strain grown in the presence of drug (\*,  $p < 0.05$  by paired two-tailed t-test).

**Table 4. Relative copy number of *aadB* in *recA::Tc* isolates with increased tobramycin resistance.**

Strain	<i>aadB</i>	MIC
<i>recA::Tc</i>	2.49 <sup>a</sup>	8
hetR- <i>recA</i> -1-1	3.34	16
hetR- <i>recA</i> -1-2	3.15	64
hetR- <i>recA</i> -1-3	2.85	16
hetR- <i>recA</i> -1-4	2.64	32
hetR- <i>recA</i> -1-5	2.63	16
hetR- <i>recA</i> -1-10	2.72	96

Relative copy number of *aadB* normalized to *aacA4* was measured using gDNA isolated from a *recA* transposon mutant and 6 independently isolated derivatives with increased tobramycin resistance. Data shown are from a single sample for each strain. None of the tobramycin resistant *recA::Tc* isolates exhibit increased copy number of *aadB*, suggesting that gene amplification of *aadB* in wild-type cells is RecA-dependent.

<sup>a</sup> The *recA::Tc* control sample was used as a control in three independent experiments; the value shown represents the average relative copy number across the three experiments.

## Figure Legends

### **Figure 1. AB5075 produces a subpopulation of cells with increased resistance to**

**tobramycin.** Virulent opaque (VIR-O) wild-type (A) or *recA::Tc* (B) cells of AB5075 were grown to  $1 \times 10^7$  CFU/ml and 100  $\mu$ l was plated on LB agar to obtain a lawn of growth. After plating, a tobramycin Etest strip was added and the plate was incubated for 16 h at 37°C.

### **Figure 2. Characterization of tobramycin heteroresistance in AB5075. A.**

Pre-incubation of AB5075 with a subinhibitory concentration of tobramycin had no effect on the population analysis profile (PAP) for this strain, indicating that increased resistance is not induced by exposure to this drug. **B.** Incubation of AB5075 in liquid culture with 64  $\mu$ g/ml of tobramycin resulted in killing of the majority of the population, while the CFU of the tobramycin resistant subpopulation continued to increase. This indicates that the tobramycin resistant subpopulation is distinct from persisters, which would be unable to replicate in the presence of drug. **C.** Increased tobramycin resistance is unstable in liquid cultures. Following exposure of AB5075 to 64  $\mu$ g/ml tobramycin, the majority of the surviving population exhibited increased tobramycin resistance. However, when tobramycin selection was removed, most of the cells in the population lost their increased resistance. **D.** Twenty-four hour stability of the tobramycin resistance phenotype in colonies was examined using stocks of hetR-O2 and hetR-T1. Colonies were plated from stock onto plates supplemented with tobramycin. Individual colonies were picked and passaged onto plates with 40  $\mu$ g/ml tobramycin or with no tobramycin. After 24 h of growth, individual colonies were resuspended and the percentages of resistant cells within each colony were determined. Data represent the means and standard error of means (SEMs) for four (hetR-T1) or three (hetR-O2) independent replicates. **E.** Forty-eight hour stability of the tobramycin

resistance phenotype was assessed for stocks of hetR-O2 and hetR-T1. The experiment was performed as in panel D, but with colonies incubated on plates with and without 40 µg/ml of tobramycin for 48 h. Data represent the means and SEMs for two independent replicates.

**Figure 3. Increased expression of *aadB* in cells with increased tobramycin resistance.**

Expression of aminoglycoside resistance genes *aadB* (A) and *aacA4* (B) were quantified by qRT-PCR. Data are presented as the averages and SEMs of three independent biological replicates (\*,  $p < 0.05$  \*\*\*\*,  $p < 0.0001$  relative to AB5075 VIR-O by one-way ANOVA with Dunnett's post-test).

**Figure 4. Amplified region in p1AB5075 that includes *aadB*.** The genes surrounding *aadB* on p1AB5075 are shown. Gene annotations are based on the most recent sequence annotation of p1AB5075 available on NCBI (accession NZ\_CP008707.1); some small annotated ORFs are not shown. Based on qPCR results, ORFs annotated in green were amplified in the tobramycin resistant subpopulation, whereas ORFs annotated in blue are not changed. The two integrase genes annotated in grey were not examined by qPCR.

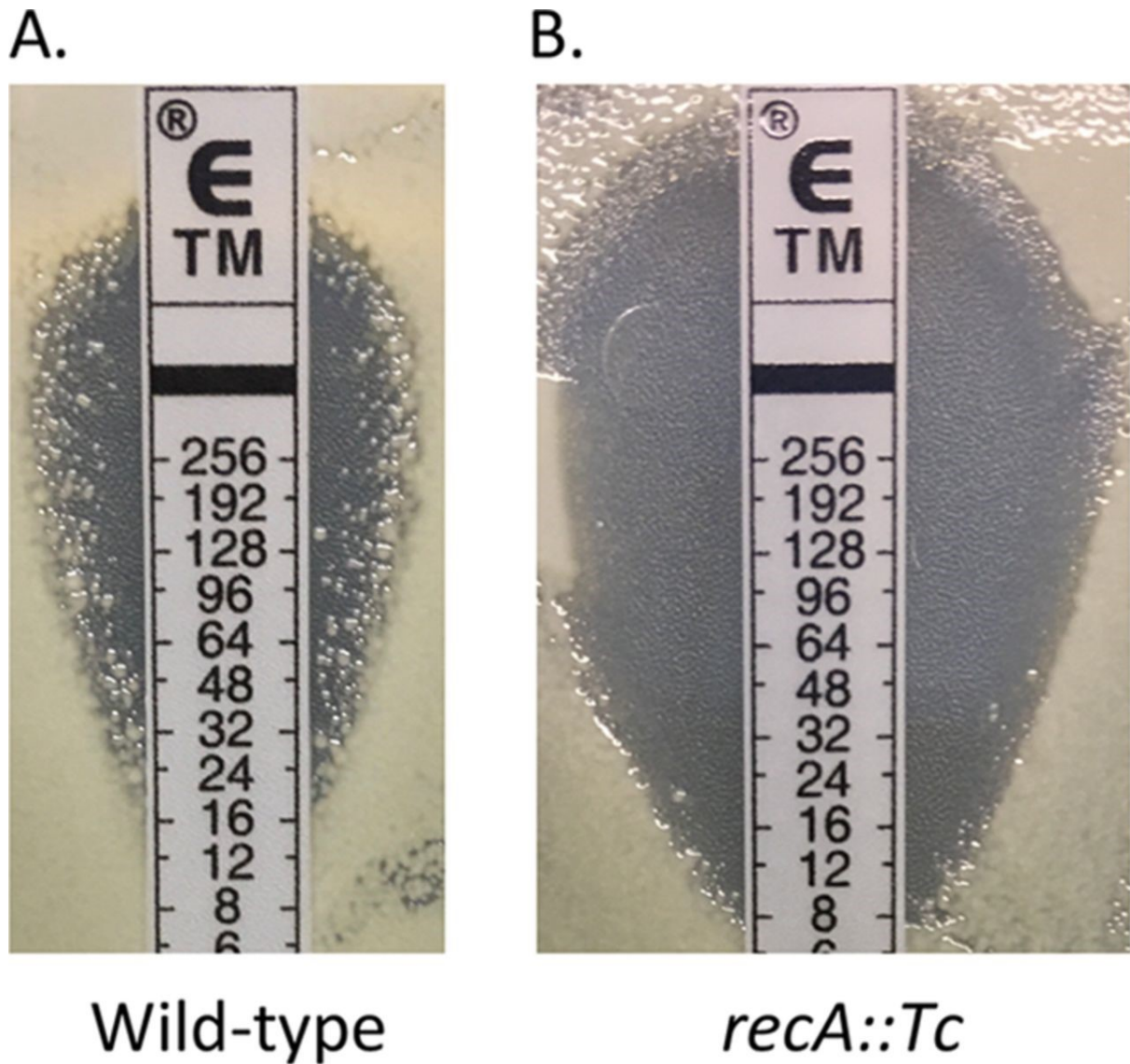
**Supplemental Fig. S1. Complementation of *recA* leads to increased heteroresistance in the *recA::Tc* mutant.** The *recA::Tc* strain was complemented by introducing the *recA* gene on a multicopy plasmid. Lawns were inoculated by spreading  $2 \times 10^6$  CFU of each strain on an LB plate. Lawns were overlaid with an Etest strip, incubated at 37°C for 16 h, and photographed.

**Supplemental Fig. S2. Characterization of tobramycin heteroresistance in a *recA* mutant. A.**

Incubation of the *recA::Tc* mutant in liquid culture with 16  $\mu\text{g/ml}$  of tobramycin resulted in growth of the resistant subpopulation over time. **B.** Population analysis profile (PAP) of the *recA::Tc* mutant with or without pre-incubation (3 hrs) in tobramycin.

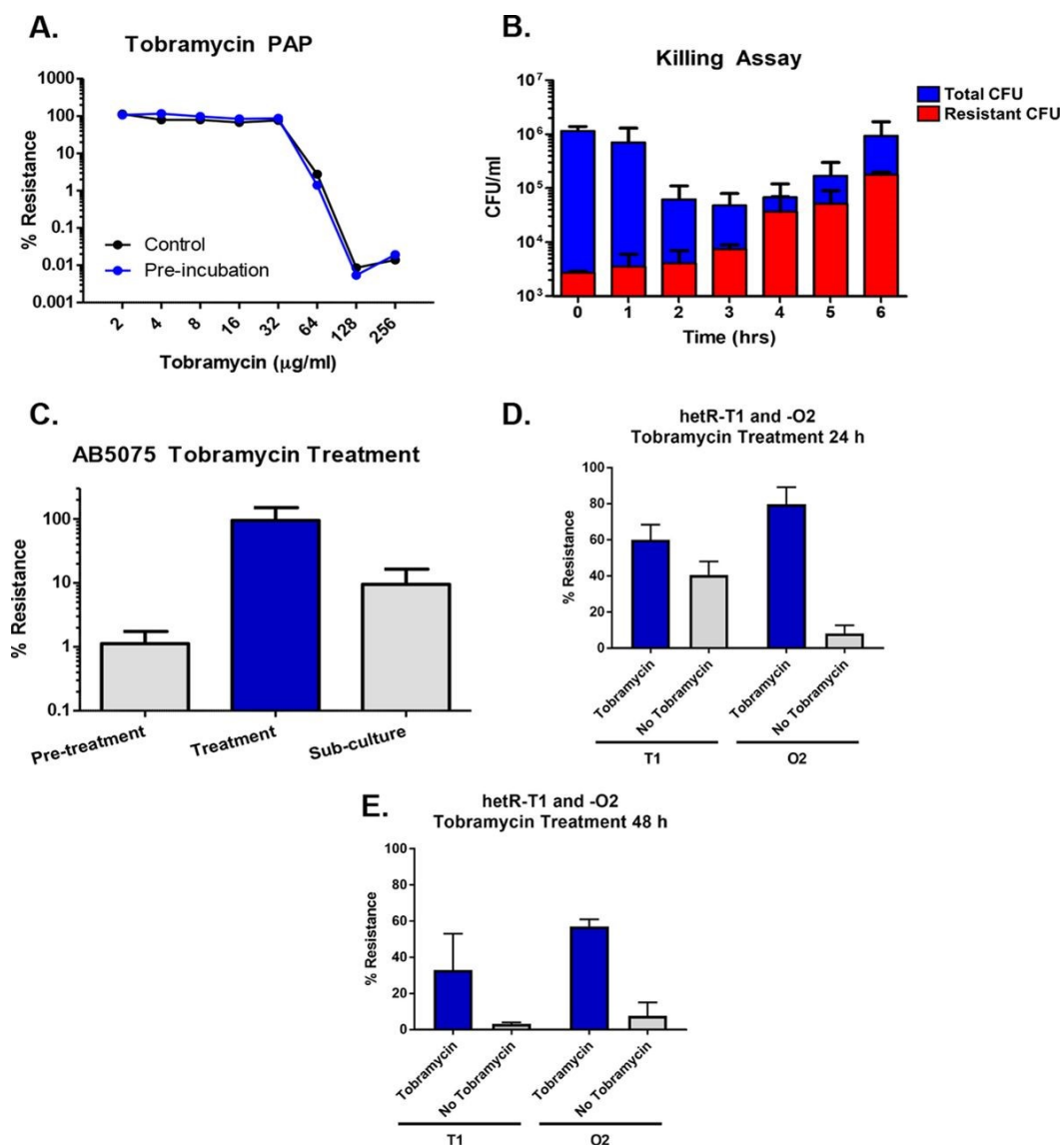
**Supplemental Table 1. Oligonucleotides used in this study.**

Figure 1



**Figure 1. AB5075 produces a subpopulation of cells with increased resistance to tobramycin.** Virulent opaque (VIR-O) wild-type (A) or *recA::Tc* (B) cells of AB5075 were grown to  $1 \times 10^7$  CFU/ml and 100  $\mu$ l was plated on LB agar to obtain a lawn of growth. After plating, a tobramycin Etest strip was added and the plate was incubated for 16 h at 37°C.

Figure 2



**Figure 2. Characterization of tobramycin heteroresistance in AB5075.** **A.** Pre-incubation of AB5075 with a subinhibitory concentration of tobramycin had no effect on the population analysis profile (PAP) for this strain, indicating that increased resistance is not induced by exposure to this drug. **B.** Incubation of AB5075 in liquid culture with 64  $\mu\text{g/ml}$  of tobramycin resulted in killing of the majority of the population, while the CFU of the tobramycin resistant subpopulation continued to increase. This indicates that the tobramycin resistant subpopulation is distinct from persisters, which would be unable to replicate in the presence of drug. **C.** Increased

tobramycin resistance is unstable in liquid cultures. Following exposure of AB5075 to 64  $\mu\text{g/ml}$  tobramycin, the majority of the surviving population exhibited increased tobramycin resistance. However, when tobramycin selection was removed, most of the cells in the population lost their increased resistance. **D.** Twenty-four hour stability of the tobramycin resistance phenotype in colonies was examined using stocks of hetR-O2 and hetR-T1. Colonies were plated from stock onto plates supplemented with tobramycin. Individual colonies were picked and passaged onto plates with 40  $\mu\text{g/ml}$  tobramycin or with no tobramycin. After 24 h of growth, individual colonies were resuspended and the percentages of resistant cells within each colony were determined. Data represent the means and standard error of means (SEMs) for four (hetR-T1) or three (hetR-O2) independent replicates. **E.** Forty-eight hour stability of the tobramycin resistance phenotype was assessed for stocks of hetR-O2 and hetR-T1. The experiment was performed as in panel D, but with colonies incubated on plates with and without 40  $\mu\text{g/ml}$  of tobramycin for 48 h. Data represent the means and SEMs for two independent replicates.

Figure 3

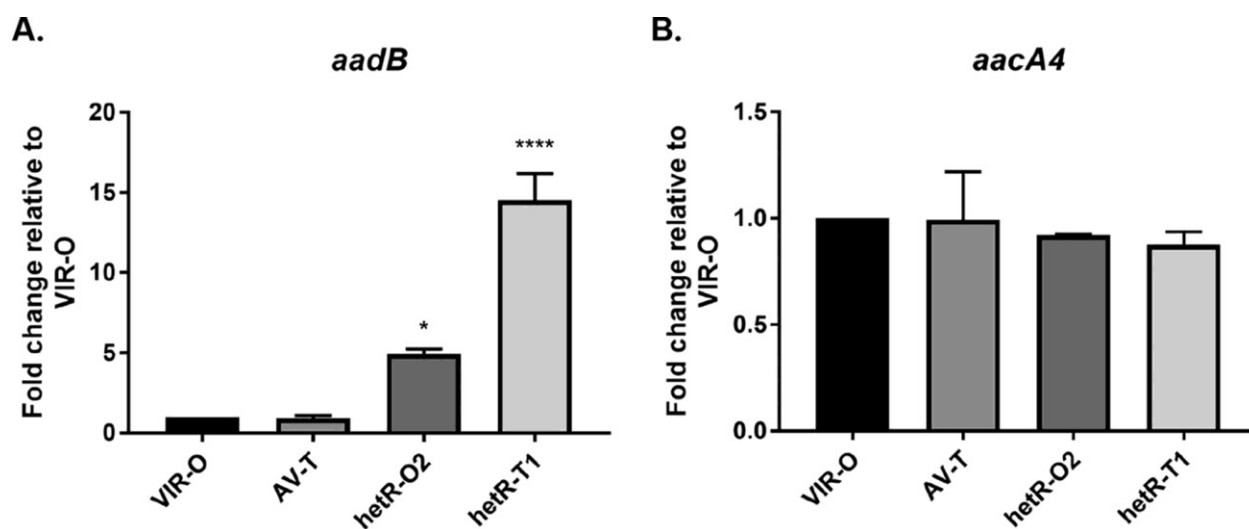


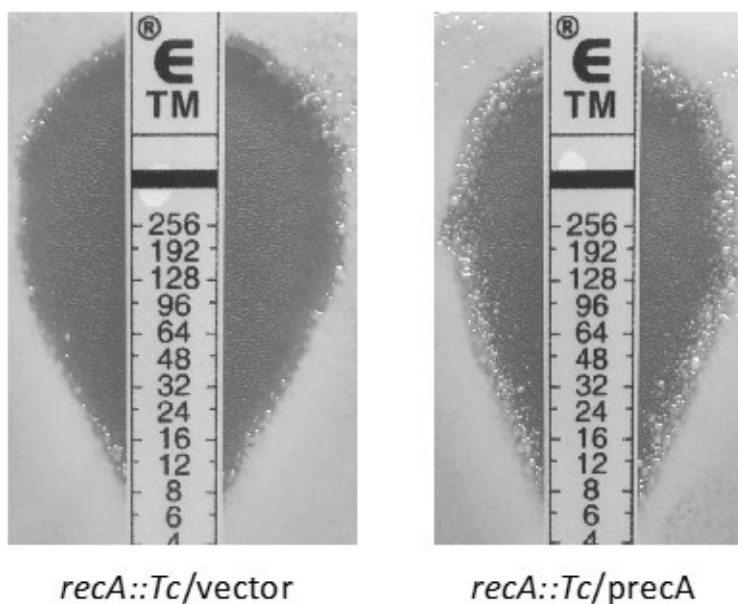
**Figure 3. Increased expression of *aadB* in cells with increased tobramycin resistance.**

Expression of aminoglycoside resistance genes *aadB* (A) and *aacA4* (B) were quantified by qRT-PCR. Data are presented as the averages and SEMs of three independent biological replicates (\*,  $p < 0.05$  \*\*\*\*,  $p < 0.0001$  relative to AB5075 VIR-O by one-way ANOVA with Dunnett's post-test).

**Figure 4**

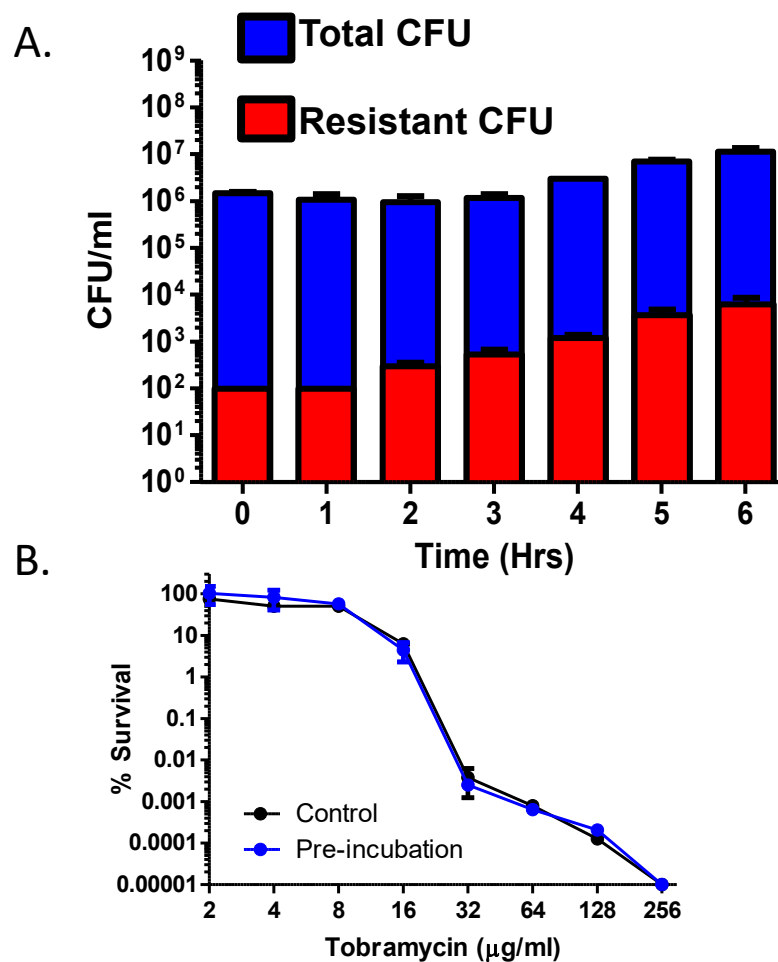
**Figure 4. Amplified region in p1AB5075 that includes *aadB*.** The genes surrounding *aadB* on p1AB5075 are shown. Gene annotations are based on the most recent sequence annotation of p1AB5075 available on NCBI (accession NZ\_CP008707.1); some small annotated ORFs are not shown. Based on qPCR results, ORFs annotated in green were amplified in the tobramycin resistant subpopulation, whereas ORFs annotated in blue are not changed. The two integrase genes annotated in grey were not examined by qPCR.

## Supplemental Figure S1



**Supplemental Fig. S1. Complementation of *recA* leads to increased heteroresistance in the *recA::Tc* mutant.** The *recA::Tc* strain was complemented by introducing the *recA* gene on a multicopy plasmid. Lawns were inoculated by spreading  $2 \times 10^6$  CFU of each strain on an LB plate. Lawns were overlaid with an Etest strip, incubated at 37°C for 16 h, and photographed.

Supplemental Figure S2



**Supplemental Fig. S2. Characterization of tobramycin heteroresistance in a *recA* mutant. A.** Incubation of the *recA::Tc* mutant in liquid culture with 16  $\mu\text{g/ml}$  of tobramycin resulted in growth of the resistant subpopulation over time. **B.** Population analysis profile (PAP) of the *recA::Tc* mutant with or without pre-incubation (3 hrs) in tobramycin.

**Supplemental Table 1. Oligonucleotides used in this study**

Primer	Sequence	Use
oSA61	ACTTGCCAAGCGTTTTAGCG	<i>aacA4</i> qPCR
oSA62	CTTGGTTCCCAAGCCTTTGC	<i>aacA4</i> qPCR
oSA69	TCCCCGATCTCCGCTAAGAA	<i>aadB</i> qPCR
oSA70	CAGATGAGCGAAATCTGCCG	<i>aadB</i> qPCR
oSA77	GTCATCGTTTCGTTTGAAC	<i>recA</i> complementation
oSA78	GAATAAAAACGTCGAGTTGTG	<i>recA</i> complementation
oSA84	AGCCACAGTACGTGCCATAG	<i>ABUW_4052</i> qPCR
oSA85	GGTGCAGCTTAGCGACAATG	<i>ABUW_4052</i> qPCR
oSA86	TAAGCGTCAGGCAGACAAG	<i>ABUW_RS19335</i> qPCR
oSA87	TTTTCCACTCTGCTGAAGG	<i>ABUW_RS19335</i> qPCR
oSA94	TCGGCAACGATGTGAGAGAG	<i>strB</i> qPCR
oSA95	ACTCCTGCAATCGTCAAGGG	<i>strB</i> qPCR

**Chapter 3: Copy Number of an Integron-Encoded Antibiotic Resistance Locus Regulates a  
Virulence and Opacity Switch in *Acinetobacter baumannii* AB5075**

Sarah E. Anderson,<sup>a,b</sup> Chui Yoke Chin,<sup>a,b,c</sup> David S. Weiss,<sup>a,b,c,d</sup> Philip N. Rather<sup>a,b,d</sup>

<sup>a</sup>Department of Microbiology and Immunology, Emory University, Atlanta, Georgia, USA

<sup>b</sup>Emory Antibiotic Resistance Center, Emory University, Atlanta, Georgia, USA

<sup>c</sup>Emory Vaccine Center, Emory University, Atlanta, Georgia, USA

<sup>d</sup>Research Service, Atlanta VA Medical Center, Decatur, Georgia, USA

Manuscript in preparation

S.E.A. wrote the manuscript, with the exception of the “Mice” and “Mouse pulmonary infection model” sections of the methods, which were written by C.Y.C. P.N.R. made revisions to the manuscript. S.E.A. performed all experiments with the exceptions of Fig. 7, which was performed by C.Y.C., and the sample preparation and data analysis for Fig 2A, which was performed by P.N.R.

## Abstract

*Acinetobacter baumannii* AB5075 undergoes a high-frequency switch between virulent opaque (VIR-O) and avirulent translucent (AV-T) colonies. Examination of wild-type VIR-O colonies revealed differential levels of switching to AV-T based on colony sectoring. Colonies exhibiting low or no sectoring at 24 h were designated as low-switching opaque (LSO) variants. LSO variants exhibited an approximately three-log decrease in switching relative to the predominant “normal” VIR-O variant. The LSO phenotype was relatively stable; however, 24 h LSO colonies were found to give rise to normal VIR-O colonies at a rate of 0.2%, while the reverse frequency of conversion was 4%. Whole-genome sequencing revealed a duplication in the normal VIR-O relative to the LSO on the plasmid p1AB5075. The duplication comprised part of a composite integron encoding resistance to aminoglycosides and chloramphenicol; copy number of this region was found to positively correlate with switching frequency in independent opaque isolates. Overexpression of a fragment of the duplicated region encoding the aminoglycoside adenylyltransferase gene *aadB* stimulated switching in the LSO background; however, production of AadB protein was found to be dispensable for this phenotype. Our data suggest that the element responsible for stimulating switching is likely a small RNA encoded within the 5' end and upstream of the *aadB* gene. Subsequent experiments were performed to fully characterize the phenotypic differences between LSO and normal VIR-O variants. Over 100 genes were found to be differentially expressed between the LSO and normal VIR-O. Surprisingly, the LSO variant was found to exhibit decreased virulence in a murine infection model, suggesting that these differences in gene expression affect *A. baumannii* virulence.

**Importance**

*Acinetobacter baumannii* remains a leading cause of hospital-acquired infections. Widespread multidrug resistance in this species has prompted the WHO to name carbapenem-resistant *A. baumannii* as its top priority for research and development of new antibiotics. Many strains of *A. baumannii* undergo a high-frequency virulence switch, which is an attractive target for novel therapeutics for this pathogen. However, the mechanisms controlling this switch are poorly understood. This study reports a novel mechanism controlling the frequency of switching in strain AB5075. The rate of switching from the virulent opaque (VIR-O) to the avirulent translucent (AV-T) variant is positively influenced by the copy number of an antibiotic resistance locus encoded on a plasmid-borne composite integron. Our data suggest that this locus encodes an sRNA that regulates opacity switching. Low-switching opaque (LSO) variants, which encode a single copy of this locus, also exhibit decreased virulence. This study increases our understanding of this critical phenotypic switch, while also identifying potential targets for virulence-based *A. baumannii* treatments.

## Introduction

*Acinetobacter baumannii* is a Gram-negative nosocomial pathogen. This bacterium causes a range of opportunistic infections, including pneumonia, urinary tract infections, meningitis, bloodstream infections, and wound infections (1). *A. baumannii* infections are frequently difficult to treat due to widespread antimicrobial resistance in this species, which has prompted the WHO to name carbapenem-resistant *A. baumannii* as its top priority for research and development of new antimicrobials (2). This highlights the need for the identification of new targets for virulence-focused therapeutics for *A. baumannii*. Although a number of virulence factors have been identified in *A. baumannii* (reviewed in (3)), a complete understanding of the regulation of virulence in this organism is lacking. Several studies have recently shown that many strains of *A. baumannii*, including the common laboratory isolate AB5075, are capable of undergoing a high frequency switch between virulent opaque (VIR-O) variants and avirulent translucent (AV-T) variants (4-8). Of these, only the VIR-O variant is capable of causing disease in mice and *Galleria mellonella* waxworms, and this variant is selected for *in vivo* (4, 6). Because the AV-T variant is avirulent, this virulence switch represents an attractive target for pathogenesis-focused therapeutics in *A. baumannii*, but currently the mechanisms underlying switching are incompletely understood.

Opacity variation in *A. baumannii* is known to be regulated by a number of genes. The OmpR/EnvZ two-component system negatively regulates VIR-O to AV-T switching (7), whereas this switch is positively regulated by the ArpAB efflux pump (6). The TetR-type transcriptional regulator ABUW\_1645 appears to be involved in maintenance of the AV-T state, as this gene is upregulated in the AV-T variant, converts cells to the AV-T form when overexpressed, and slightly increases the rate of AV-T to VIR-O switching when disrupted (4).

The interplay between these three systems is not understood, although ABUW\_1645 does not transcriptionally regulate *ompR/envZ* or *arpAB* (4). In this work we establish that VIR-O to AV-T switching in AB5075 is further positively controlled by copy number of an antibiotic resistance locus on the plasmid p1AB5075.

p1AB5075 is the largest plasmid carried by *A. baumannii* AB5075. It is nearly 84 kb in size and harbors Resistance Island 2 (RI-2) (9). RI-2 consists of two miniature inverted-repeat transposable elements (MITEs) flanking a composite integron (9). This composite integron is composed of two fused class 1 integrons, and therefore encodes two highly homologous copies of the integrase gene *intI* (one of which is actually a pseudogene) (9). The two *intI* alleles flank the resistance genes *aadB*, *cmlA*, *aadA1*, and *strAB* (9). These resistance genes are presumably expressed from the integron cassette promoter  $P_c$ , which is encoded upstream of *aadB* (10-13). Class 1 integron cassette promoter regions also encode binding sites for the DNA binding proteins FIS, LexA, IHF, and H-NS; a small open reading frame encoding ORF-11, a nonfunctional peptide whose translation enhances translation of cassette genes; and the integron *attI* site (10, 14, 15). These promoter characteristics appear to be conserved in RI-2. Previous research in our lab has shown that the genes between the two copies of *intI* undergo spontaneous, RecA-dependent, high-copy amplification, which results in increased resistance to tobramycin and gentamicin due to increased expression of the aminoglycoside adenylyltransferase gene *aadB* (16, 17).

In bacteria, sRNAs are generally 50-500 nt in length, and act as post-transcriptional regulators by base pairing to mRNA targets (18). sRNAs typically base pair with their targets over fairly short sequences, usually between 7-12 nt (19). For many sRNAs, this interaction is mediated by the chaperone protein Hfq (20); however, Hfq-independent sRNAs have also been

reported (21, 22), and other proteins such as ProQ and CsrA can also act as sRNA chaperones (23, 24). sRNAs can act as either positive or negative regulators of mRNA activity (18, 20, 25). These transcripts can be derived from intergenic regions or 5' or 3' UTRs of coding genes, and can be independently transcribed or generated by RNase cleavage of larger transcripts (18, 26-29).

In this paper we report that *A. baumannii* produces a third opacity variant along with AV-T and VIR-O. Designated the low-switching opaque (LSO) variant, this third subpopulation exhibits dramatically reduced levels of switching to AV-T relative to the normal VIR-O. Switching frequencies in the LSO and normal VIR-O variants are correlated with copy number of a region between the two copies of *intI* on RI-2. We demonstrate that the element controlling switching is encoded at the 5' end of the *aadB* gene within RI-2, and that this element is likely an sRNA. Finally, we also show that the LSO variant exhibits decreased virulence relative to the normal VIR-O, which may be due to decreased transcription of virulence factors in this variant.

## Results

**Wild-type AB5075 gives rise to multiple opaque subpopulations.** When plating stocks of virulent opaque (VIR-O) AB5075, we observed two distinct sectoring phenotypes. The majority of colonies within our wild-type VIR-O stocks appeared to switch to the avirulent translucent (AV-T) form at a high frequency, resulting in a highly sectored colony appearance by 24 h of growth (**Fig. 1A**). Because this phenotype was found in the majority of colonies, these colonies were designated as “normal” VIR-O. However, we occasionally observed colonies that did not sector by 24 h (**Fig. 1B**). Although we have found that high colony density can suppress sectoring in VIR-O colonies, these low-sectoring colonies could be found at low colony density, and their low-sectoring phenotype was stable upon restreaking. Therefore, we concluded that these colonies constituted a distinct subpopulation, which was designated low-switching opaque (LSO). Comparison of the switching frequencies between normal VIR-O and LSO colonies revealed a nearly three-log difference in switching (**Fig. 1C**). To determine whether the LSO subpopulation was formed due to random mutation, the rates of interconversion between normal VIR-O and LSO variants were measured in 24 h old colonies. Interestingly, the rate of conversion from normal VIR-O to LSO was 4% (**Fig. 1D**), which was higher than the 0.2% frequency found for the conversion from LSO to normal VIR-O (**Fig. 1E**). However, both frequencies were much higher than would be expected if the conversion were due to the generation of a random point mutation, suggesting that the LSO colonies are not spontaneous point mutants.

**The rate of switching in different opaque subpopulations is correlated with copy number of an antibiotic resistance locus.** To determine the genetic differences between the normal VIR-O

and LSO subpopulations, representatives from each were subjected to whole genome sequencing (WGS) with PacBio technology. WGS revealed an approximately 6 kb duplication in the normal VIR-O sample relative to the LSO. This duplication was localized to part of a composite integron (RI-2) encoded on the large plasmid p1AB5075 (9). The duplicated region consists of five genes flanked by two highly homologous copies of the integrase gene *intI*, which share 99% nucleic acid identity across 1062 bp (**Fig. 2A**). In the normal VIR-O variant, a tandem duplication of the entire locus has occurred, presumably through recombination between the two copies of *intI* (**Fig. 2A**). These results were confirmed through Southern blotting and qPCR (**Fig. 2B**, “Set A”). For the Southern blot, genomic DNA (gDNA) was digested with an enzyme that cuts outside of the duplication and the blot was treated with a probe specific for the duplicated region. Results were further confirmed by measuring copy number of *aadB*, the first gene within the duplication, by qPCR. Results for both of these assays matched those obtained through WGS, confirming that the VIR-O variant contains a duplication of this region. Aside from *intI*, all of the genes in the duplicated region mediate resistance to aminoglycosides or chloramphenicol. As expected, this duplication results in modest increases in resistance to some of these antimicrobials (**Table S1**). However, an obvious role for any of these genes in mediating differences in opacity switching was not immediately clear.

To determine whether copy number of this region is actually correlated with opacity switching frequency, we measured copy number of this region in a second set of related LSO and normal VIR-O variants. Starting with a normal VIR-O variant that was independent from that used for WGS, we isolated and stocked a rare LSO variant. This LSO stock was then used to isolate a second rare normal VIR-O stock (VIR-O2). These three related samples were designated “Set B” samples to distinguish them from the “Set A” samples used for WGS.

Southern blotting with the Set B LSO and original normal VIR-O variants gave band sizes identical to those seen for the Set A samples (**Fig. 2B**). Interestingly, Set B VIR-O2 yielded a larger band than the other two normal VIR-O samples, suggesting further amplification of this region. qPCR analysis confirmed the Southern results for the Set B normal VIR-O and LSO samples, and indicated that Set B VIR-O2 encodes four copies of the duplicated region (**Fig. 2B**). To determine whether VIR-O2 exhibits higher levels of switching due to this further increase in copy number, switching to AV-T of the Set B samples was quantified. Switching was measured after 16 h of growth, a time point before normal VIR-O colonies typically exhibit high levels of switching. VIR-O2 colonies exhibited an 86-fold increase in switching relative to the normal VIR-O, although the results were variable between samples and differences were not statistically significant (**Fig. 2C**). However, this trend towards increased switching with increased copy number suggests that amplification of this region does indeed affect switching rate.

Our lab previously reported that high-level, RecA-dependent amplifications of the same duplicated region are responsible for tobramycin heteroresistance in AB5075 (16). To determine whether colonies exhibiting high-level amplification of this region also exhibit hyperswitching to AV-T, we quantified switching in the previously characterized tobramycin resistant isolate hetR-O2, which encodes 17-20 copies of the duplicated region (16). After 16 h of growth, hetR-O2 exhibited a 15-fold increase in switching relative to the normal VIR-O (**Fig. 2D**). This result further suggests that the VIR-O to AV-T switching rate is controlled by something encoded within the duplicated region.

To more directly examine the influence of the duplicated region on VIR-O to AV-T switching, the LSO background was used to generate a strain that was cured of the p1AB5075 plasmid, designated LSO  $\Delta$ p1AB5075. LSO  $\Delta$ p1AB5075 exhibited similar levels of switching

to its parent variant (**Fig. 3A**), indicating that the duplicated region is not required for basal levels of VIR-O to AV-T switching. To test whether p1AB5075 plasmids encoding two copies of the duplicated region are sufficient to stimulate increased levels of switching, LSO  $\Delta$ p1AB5075 was transformed with gDNA isolated from either the LSO or normal VIR-O variant. Transformants that had taken up p1AB5075 were selected for using tobramycin. Transformants generated using LSO gDNA did not exhibit alterations in switching, as expected (**Fig. 3A**). Transformation with VIR-O gDNA yielded a mix of low-switching and normally switching colonies (**Fig. 3A**). However, when qPCR was used to measure *aadB* copy number in these transformants, it was determined that a low-switching transformant (transformant A) had taken up a plasmid containing one copy of the duplicated region, whereas a normally switching transformant (transformant B) had taken up a plasmid containing two copies (**Fig. 3B**). This experiment demonstrates that uptake of p1AB5075 encoding two copies of the duplicated region is sufficient to increase VIR-O to AV-T switching in AB5075.

**Overexpression of the *aadB* gene leads to increased opacity switching, but AadB protein is dispensable for this phenotype.** To identify the gene(s) responsible for stimulating switching within the duplicated region, portions of this region were overexpressed in the LSO variant and switching to AV-T was examined. The plasmid pWHaadB, consisting of the aminoglycoside resistance gene *aadB* cloned into plasmid pWH1266, was found to be sufficient to stimulate switching over 800-fold in the LSO background (**Fig. 4**). An overexpression construct was also generated containing all five resistance genes encoded in the duplicated region; this stimulated similar levels of switching as a construct encoding *aadB* alone, suggesting that all of the stimulatory activity in the duplicated region is derived from *aadB* (**Fig. S1**).

AadB mediates aminoglycoside resistance by adenylylating the antibiotic; this enzyme is not known to act on bacterial substrates. Therefore, it was unexpected that overproduction of this protein would have an effect on VIR-O to AV-T switching. To determine if the AadB protein was mediating the effect on switching, a nonsense mutation was introduced at the fifth amino acid of *aadB* (pWHaadBstop). This allele was still capable of stimulating switching over 800-fold when overexpressed in the LSO background (**Fig. S2**), demonstrating that AadB protein is not responsible for regulating the rate of VIR-O to AV-T switching.

**The element responsible for controlling switching rate is encoded upstream of *aadB*.** To determine where the element affecting switching was localized in the pWHaadB plasmid insert, we mutagenized this plasmid with the EZ-Tn5 <Kan-2> transposon. Mutant plasmids were transformed into the LSO variant and two screens were performed. Insertions that blocked the ability of the plasmid to cause switching were identified by screening for transformants that no longer exhibited the highly sectorial colony phenotype stimulated by pWHaadB. Insertions in *aadB* that did not abolish switching were also isolated by screening for plasmids that had lost the ability to confer tobramycin resistance in *Escherichia coli*, followed by a screen for plasmids that still stimulated switching in the LSO variant. When both groups of insertions were mapped onto the *aadB* region, all of the insertions blocking switching localized to the 5' end and upstream of *aadB*, while most of the insertions within the *aadB* open reading frame (ORF) did not affect switching (**Fig. 5A**). Insertions blocking switching were relatively evenly distributed between the 5' end of *aadB* and the  $P_c$  promoter, and did not localize to any previously annotated integrase promoter features (data not shown). Therefore, it appears that the element affecting switching is a novel sequence feature encoded towards the 5' end and upstream of *aadB*.

To confirm that the element responsible for stimulating switching is encoded upstream of *aadB*, truncated fragments of the *aadB* region were overexpressed in the LSO variant. As depicted in **Fig. 5A**, truncated insertions started at the 5' end of the insert in pWHaadB and extended differing lengths into the *aadB* gene. Plasmids pWHaadB-T (encoding the longest truncated insert), pWHaadB-TA, and pWHaadB-TB all appeared to stimulate switching in the LSO variant, although not to the same degree as the full-length pWHaadB plasmid (**Figs. 5B-D**). For unknown reasons, colonies overexpressing these plasmids exhibited high variability in their levels of switching, resulting in differences in switching between these transformants not being significantly higher than the empty vector controls. However, these plasmids were still classified as being biologically active, as transformants clearly exhibited more sectoring/switching than empty vector controls on average. The shortest truncated insert, pWHaadB-UP, did not stimulate sectoring, and appeared similar to the empty vector control in quantitative switching assays (**Fig. 5E**). The results of these truncation studies confirm those obtained through transposon mutagenesis of pWHaadB. The fragment encoded in pWHaadB-UP terminates upstream of some of the transposon insertions that blocked switching in pWHaadB, whereas the shortest truncated plasmid to still stimulate switching, pWHaadB-TB, includes the insertion sites for all transposons that blocked switching. Taken together, these results indicate that the element responsible for stimulating switching is encoded at the 5' end and upstream of *aadB*.

**Possible role for an sRNA in VIR-O to AV-T switching.** We hypothesized that the element affecting switching was likely an sRNA or a small peptide encoded upstream of *aadB*, but our data could also be explained by the presence of a protein binding site titrating a regulator required for controlling switching. To discriminate between these possibilities, site-directed

mutagenesis was used to introduce two base pair changes into the -35 of  $P_c$  (TTGACA → TTGAGT), in order to abolish transcription. This mutated allele was no longer able to stimulate switching when overexpressed in the LSO background (**Fig. 6A**), suggesting that transcription is required for the upstream element to regulate switching. This result indicates that the upstream element is likely an sRNA or a small peptide. While there are a number of small putative ORFs encoded within the upstream region of *aadB*, transposon insertions affecting switching stimulated by pWHaadB do not localize to any of these potential peptides, suggesting that none of them are responsible for controlling the switching rate (**Fig. S3**). This instead suggests that the element responsible for stimulating switching might be a functional sRNA.

To determine whether small transcript(s) are produced from the  $P_c$  promoter, Northern blotting was performed. Northern blots were conducted with probe oSA134 (**Table S2**), an ssDNA probe that only binds transcripts coming from the same strand as  $P_c$ . This probe hybridizes starting 40 nt downstream of the reported transcriptional start site for  $P_c$  (30). A Northern blot was performed using LSO  $\Delta$ p1AB5075 overexpressing pWHaadB, pWHaadB-TA, pWHaadB-TB, and pWHaadB-UP, along with an empty vector control (**Fig. 6B**). Strains containing the three longer plasmids all exhibited the same five major RNA products, which were roughly 300, 150, 110, 80, and 70 nt in size. All of these transcripts are too small to encode the full *aadB* gene (the *aadB* ORF is 534 bp). Interestingly, in the strain overexpressing pWHaadB-UP, the 300 nt RNA was largely absent. Since this plasmid is not capable of stimulating switching in the LSO background, this result suggests that the 300 nt RNA may be involved in stimulating switching.

To determine whether the multiple RNA species observed from  $P_c$  were produced through post-transcriptional processing, a Northern blot was performed using terminator

exonuclease (TEX). RNA generated from hetR-O2 was treated with TEX and used for a Northern blot with oSA134 along with an untreated control (**Fig. 6C**). HetR-O2 exhibited the same five major RNA bands as observed for the overexpression strains, confirming that these transcripts are also produced in wild-type cells. Upon treatment with TEX, the intensity of bands was diminished, and the 110 nt band appeared completely abolished. This suggests that at least the 110 nt transcript, and perhaps others, are generated by processing following transcription.

Bacterial sRNA-mRNA interactions are frequently mediated by the RNA chaperone Hfq. To determine whether Hfq is required for the stimulation of opacity switching, we measured switching to AV-T in a normal VIR-O *hfq::Tc* mutant (**Fig. 6D**). Switching frequencies were reduced over 120-fold, suggesting that Hfq is required for normal levels of VIR-O switching. To determine whether Hfq is acting through an sRNA encoded upstream of *aadB*, we overexpressed *aadB* in an LSO *hfq::Tc* mutant. Since both the pWHaadB plasmid and the *hfq::Tc* strain encode resistance to tetracycline, *aadB* was overexpressed in this strain using the hygromycin-resistant plasmid pQF1266.Blue (paadB). Switching of the LSO *hfq::Tc* paadB strain was reduced 17-fold compared to LSO paadB (**Fig. 6E**). However, switching was still elevated in this strain over 600-fold compared to the mutant empty vector control, demonstrating that *aadB* overexpression still has an effect in the absence of *hfq*. This suggests that either the upstream *aadB* region and Hfq affect switching via independent pathways, or that high-level overexpression of the upstream *aadB* region is sufficient to overcome the requirement for a chaperone.

**LSO and normal VIR-O subpopulations exhibit differences in virulence and global gene expression.** We hypothesized that because the normal VIR-O variant is more virulent than the AV-T variant, and because the LSO variant switches to AV-T at a lower frequency, that the LSO

variant would exhibit increased virulence relative to the normal VIR-O. To evaluate this possibility, mice were intranasally inoculated with either the normal VIR-O or LSO variant, and CFUs were enumerated in the lungs, spleen, and liver at 24 hours post-infection (hpi) (**Fig. 7**). Surprisingly, the LSO variant exhibited at least a 3-log decrease in the geometric mean of CFUs in all three organs, demonstrating that this variant is less virulent than the normal VIR-O.

To obtain a more global view of the differences between normal VIR-O and LSO variants, and to determine why the LSO variant might be less virulent, RNA-sequencing (RNA-seq) was performed on each subpopulation in triplicate. Results of the RNA-seq are detailed in **Supplemental Data File S1**. Using a fold-change cut-off of 1.5 ( $\log_2$ fold 0.7) and a p-value cut-off of 0.05, we identified 55 upregulated genes and 87 downregulated genes in the LSO variant. As expected, the genes encoded within the duplicated region were all downregulated in the LSO variant. Interestingly, several genes involved in pathways that have previously been implicated in *A. baumannii* virulence were found to be downregulated in the LSO variant, including the phospholipase C gene *plcI* (31), genes involved in cysteine metabolism/sulfur assimilation (*cysW*, *cysT*, *cysN*) (32), and genes involved in the phenylacetic acid catabolic pathway (*paaK*, *paaJ*, *paaI2*) (33, 34). The LSO variant also showed decreased expression of genes from the *csu* operon, which is involved in the production of pili important for surface adherence and biofilm formation (33, 35, 36). These differences in gene expression may underlie the decreased virulence observed in the LSO strain.

## Discussion

This study establishes that *A. baumannii* AB5075 produces at least two subpopulations of opaque variants, designated normal VIR-O and LSO. The two subpopulations differ not only in their rates of switching to AV-T, but also in their gene expression and virulence. The switching frequencies of these opaque variants are positively correlated with copy number of a locus encoded in RI-2 on plasmid p1AB5075, with normal VIR-O variants exhibiting two or more copies of this locus. High-level amplification of this locus also occurs, and leads to hyperswitching to AV-T and increased resistance to tobramycin (16). The element controlling switching is encoded towards the 5' end and upstream of the *aadB* gene in RI-2, and our evidence suggests that this element is an sRNA. Switching stimulated by overexpression of *aadB* requires transcription from the integron cassette promoter  $P_c$ , but does not appear to require any of the small ORFs encoded upstream of *aadB*. Northern blotting revealed multiple small transcripts produced downstream of  $P_c$ , providing further evidence to suggest that an sRNA encoded in this region is responsible for controlling switching. Although this sRNA does not appear to require Hfq to stimulate switching when overexpressed, disruption of *hfq* does lead to decreased switching to AV-T.

While our results strongly suggest that an sRNA produced from the 5' end of the *aadB* transcript is responsible for stimulating switching, more work is needed to fully validate this hypothesis. Both the sequence of the sRNA and the mechanism by which it is produced remain to be determined. Our Northern blotting results suggest that the sRNA may be around 300 nt in length, as an RNA of this length was found to be produced from overexpression plasmids that stimulated switching, but was dramatically reduced in a plasmid with no activity (**Fig. 6B**). This size also matches the results obtained from overexpressing truncated plasmids, as the shortest

active plasmid pWHaadB-TB encodes an insert that terminates 303 bp downstream of the annotated  $P_c$  transcriptional start site (30). Production of the 300 nt band was not blocked by treatment with TEX, indicating that any processing of this RNA must happen at the 3' end. TEX treatment did eliminate a band of ~110 nt from the Northern blot, demonstrating that at least some transcripts from this region are targeted for post-transcriptional processing. While it is likely from these results that the 300 nt sRNA is generated from the annotated  $P_c$  start site and is produced either through transcriptional termination or processing at the 3' end, these hypotheses remain to be verified. The target of the sRNA also has not been identified. Our data indicate that the target is not encoded on p1AB5075, as LSO  $\Delta$ p1AB5075 transformed with pWHaadB still exhibits increased switching (data not shown). Identification of the target(s) of this sRNA will be extremely valuable for understanding the regulation of switching in *A. baumannii*.

The putative sRNA described here exhibits a number of unusual genetic and regulatory features. First, it is interesting that the putative sRNA is encoded on a plasmid. Although this is unusual, there is precedence for horizontally-acquired sRNAs being produced in other bacterial species. For example, *Salmonella enterica* serovar Typhimurium has been shown to produce sRNAs from horizontally-acquired genetic elements (37, 38). One of these, *tnpA*, is produced from the 5' UTR of a transposase gene, and functions to regulate expression of virulence genes by directly binding to mRNA of the pathogenicity regulator *invF* (38). A plasmid-derived sRNA has also been shown to regulate genetic competence in *Legionella pneumophila* (39). sRNAs associated with mobile elements have also been identified in *Staphylococcus aureus* (40), *Xanthomonas campestris* (41), and *Coxiella burnetii* (42). Taken together, these studies and ours suggest that horizontally transferred elements may be an underappreciated source of sRNAs.

Furthermore, it is also unusual that two or more copies of the putative sRNA gene are required to stimulate observable levels of opacity switching. **Fig. 3** demonstrates that the sRNA is not required for baseline levels of switching, as strain LSO  $\Delta$ p1AB5075, which does not encode the sRNA, exhibits the same level of opacity switching as the wild-type LSO. Changes in switching to AV-T are only observed when copy number of the sRNA is increased, either through spontaneous amplification (**Figs. 2, 3**), or through overexpression on a multicopy plasmid (**Fig. 4**). This suggests that the sRNA must be expressed past a certain threshold before switching can be activated. This could potentially occur if the mRNA target(s) of this sRNA are produced in great excess to the sRNA; perhaps when the sRNA is present in single copy it is produced to insufficient levels to significantly affect target translation.

It is also interesting that the truncated plasmids pWHaadB-T, pWHaadB-TA, and pWHaadB-TB all caused much more variable switching phenotypes than the full-length plasmid pWHaadB. Although LSO colonies overexpressing the truncated plasmids exhibited increased average switching compared to an empty vector control, the differences were not found to be statistically significant due to the wide variability. The reason for this variability is unclear, but could be due to variable levels of sRNA production from these plasmids. Even if the entire sequence for the sRNA is encoded on each of these truncated inserts, it is possible that truncation of the inserts could affect the efficiency of post-transcriptional processing or transcriptional termination, which could potentially result in variable levels of transcripts between cells. If the sRNA only causes an observable phenotype when expressed past a certain threshold, then slight variations in sRNA levels between colonies could result in dramatic differences in switching phenotypes. However, more work is needed to confirm this hypothesis.

This work is not the first report of a regulatory RNA element being encoded in the promoter region of class 1 integrons. The promoter regions of aminoglycoside-resistance integrons have also been reported to encode aminoglycoside-responsive riboswitches, although the presence of these elements is controversial (43-45). In 2013, Jia *et al* characterized a putative 76 nt riboswitch that exhibits 97% sequence identity across 61 bp to the 5' UTR of *aadB* (43). Although our data suggest that the sRNA described here is much longer than 76 nt, it is interesting that the RI-2 promoter region may encode both a riboswitch and an sRNA. A riboswitch was recently reported to affect stability of an upstream sRNA encoded in *Vibrio cholerae* (46). In *Listeria monocytogenes* a riboswitch has also been shown as to act as an sRNA *in trans* (27), and a riboswitch-containing sRNA has also been identified in *Enterococcus faecalis* (47). More work will be needed to determine the interplay in regulation between the putative integron riboswitch and the sRNA described here.

It is unclear whether the mechanism controlling switching frequency described here is widespread in *A. baumannii*. RI-2 has only been identified in two other *A. baumannii* strains besides AB5075 (48, 49). However, it is possible that the putative sRNA described here could still be encoded in strains that lack RI-2. As the putative sRNA appears to be encoded mostly within the integron promoter region, it is probable that other integrons, even those not encoding *aadB*, could still encode this element. Indeed a BLAST search with the first 300 nt of the predicted *aadB* transcript yields hits to over one hundred *A. baumannii* genomes, with coverage ranging from 73-100%. Integrons encoding aminoglycoside modifying enzymes are also widely reported in the *A. baumannii* literature (50-55). Together, this evidence suggests that the putative sRNA is likely to be widespread in this species. However, the data presented here demonstrate that the presence of this sRNA is not enough to stimulate switching, as duplications

of the sRNA region are also required. In AB5075 the duplication likely occurs through homologous recombination between flanking *intI* alleles; however, in other strains amplifications of the sRNA could also occur by other mechanisms, including transposition or increases in plasmid copy number. Indeed, amplification of a different aminoglycoside-resistance encoding integron has been reported in a clinical isolate of *A. baumannii*, even though this strain lacks the flanking *intI* alleles (56). Therefore, even if RI-2 is not widespread, this general mechanism regulating switching may be found in other strains. Any *A. baumannii* strains that do not encode the putative sRNA (or are incapable of varying the sRNA copy number) would be expected to behave as LSO variants. However these strains could still have the ability to acquire this sRNA, since RI-2 is carried on a transmissible plasmid (9, 48, 57). As normal VIR-O variants encoding duplications within RI-2 exhibit increased virulence, dissemination of this plasmid could be of significant public health concern.

It is surprising that LSO variants exhibit decreased levels of virulence compared to normal VIR-O variants. Previous studies comparing virulence of normal VIR-O and AV-T isolates suggested that differences in virulence between the two variants are due to levels of capsule, which is a virulence factor that contributes to *A. baumannii* resistance to host lysozyme (4, 58). The increased capsule levels partly underlie the appearance of opaque *A. baumannii* colonies, as AB5075 VIR-O mutants lacking capsule appear more translucent than wild-type (58). However, the low virulence observed for the LSO variant demonstrates that an opaque colony appearance does not necessarily translate to increased virulence. This suggests that other factors in addition to capsule also contribute to the increased virulence of the normal VIR-O variant. The results of RNA-seq comparing the normal VIR-O and LSO variants demonstrate that the LSO exhibits decreased expression of some known virulence factors, which could

explain the decreased virulence of this variant (**Supplemental Data File S1**). While one could also hypothesize that the decreased virulence of the LSO variant indicates a role for the AV-T form in infection, preliminary infection experiments with mixtures of LSO and AV-T variants indicate that this is not the case (data not shown).

Finally, the discovery of LSO variants has important implications for future studies using *A. baumannii* AB5075. As LSO, normal VIR-O, and AV-T variants all exhibit distinct phenotypes in terms of colony morphology, virulence, and global gene expression (4, 5), it is critical that future studies of AB5075 take opacity variants into account when comparing phenotypes between mutant and control strains. This study demonstrates that opaque isolates in particular should be assessed for their degree of sectoring to AV-T prior to further experimentation to avoid spurious results in virulence and other studies.

## Materials and Methods

**Bacterial strains and growth conditions.** Stocks of bacteria were maintained at -80°C in 15% glycerol. Pure stocks of *A. baumannii* VIR-O isolates were generated as described previously (59). Liquid cultures were prepared in sterile LB broth, supplemented with tetracycline (Sigma-Aldrich, St. Louis, MO), hygromycin (Invitrogen, Carlsbad, CA), tobramycin (Sigma-Aldrich), or kanamycin (Sigma-Aldrich) as appropriate. To prevent opacity switching, which occurs at high culture density, cultures were grown overnight at room temperature or 37°C without shaking, followed by growth at 37°C with shaking to the desired OD<sub>600</sub>. MIC and cloning experiments were performed on LB media supplemented with 1.5% agar. For switching assays and qualitative examination of switching, 0.5x LB supplemented with 0.8% agar was used. Plates were supplemented with tetracycline, hygromycin, tobramycin, or kanamycin as indicated.

Wild-type LSO variants were isolated by plating serial dilutions of pure wild-type VIR-O stocks on 0.5x LB, 0.8% agar. Rare colonies that were lacking AV-T sectors at 24 h were passaged onto 0.5x LB, 0.8% agar to confirm phenotypic stability; single colonies from restreaks were cultured and stocked as described above. The wild-type isolate designated set B VIR-O2 was derived by plating serial dilutions of an isolated LSO colony onto 0.5x LB, 0.8% agar. Colonies were screened for sectoring at approximately 24 h of growth; a sectoring colony was passaged onto 0.5x LB, 0.8% agar to confirm the phenotype. A single colony was then cultured and stocked as above.

An LSO variant cured of plasmid p1AB5075 was serendipitously generated in an attempt to knockout *aadB*. A strain containing a T26 insertion in *aadB* was obtained from the AB5075 transposon library established at the University of Washington (9). Genomic DNA (gDNA) was prepared from an overnight culture of this strain grown at 37°C with shaking as described below.

Diluted gDNA was used as a template for PCR using Phusion Hot Start II DNA polymerase (Thermo Scientific, Waltham, MA) with primers oSA65 and oSA66 (**Table S2**) to amplify the *aadB* gene and the transposon disruption. The resulting fragment was ligated into the *SmaI* site of the counter-selectable suicide plasmid pEX100 (60); the ligation was transformed into TransforMax EC100 electrocompetent *E. coli* (Lucigen, Middleton, WI) and transformants were selected by plating on 10 µg/ml tetracycline. The resulting plasmid was designated pEX100-aadBTnS. A concentrated preparation of pEX100-aadBTnS was made by purifying plasmid from 4 ml of *E. coli* culture using the Qiaprep Miniprep Kit (Qiagen, Germantown, MD), followed by concentration through ethanol precipitation. This concentrated DNA was electroporated into an LSO culture of AB5075 as described below. Transformants were selected using 5 µg/ml tetracycline. Colonies were then screened for sensitivity to 10% sucrose to identify transformants that had incorporated the suicide plasmid by homologous recombination. Cells that had undergone a second crossover to lose the plasmid backbone were selected for by culturing for several hours without antibiotic at 37°C with shaking, followed by plating serial dilutions on no salt LB with 10% sucrose. Double crossover colonies were then screened for tetracycline resistance to determine whether they had retained the T26 marker. The colony designated LSO Δp1AB5075 was determined to be tetracycline sensitive, and was originally assumed to have reverted to the wild-type genotype upon the second crossover. We determined that LSO Δp1AB5075 had actually lost the p1AB5075 plasmid by attempting to amplify fragments of DNA from this plasmid using primer sets oSA69/70, oSA67/68, oSA86/87, and oSA104/105. All of these PCRs were unsuccessful, while control PCRs using primers in the chromosomal *mutS* gene (oSA7 and oSA8) still amplified the expected band.

Strains in which p1AB5075 had been reintroduced into LSO  $\Delta$ p1AB5075 were generated by electroporation. gDNA was prepared from normal VIR-O and LSO cultures grown to an OD of 0.5, as described below. gDNA from each strain was transformed into LSO  $\Delta$ p1AB5075 by electroporation, as described below. Transformants that had recovered the p1AB5075 plasmid were selected for by plating on 0.5x LB, 0.8% agar supplemented with 2  $\mu$ g/ml tobramycin. Switching phenotypes were assessed qualitatively by observing transformants under a dissecting microscope with oblique illumination; colonies were passaged onto 0.5x LB, 0.8% agar with 2  $\mu$ g/ml tobramycin and then cultured in LB to generate stocks as described above.

Disruption mutations in *hfq* were generated in both the normal VIR-O and LSO backgrounds. A transposon insertion in *hfq* was originally generated as part of a screen for insertions that blocked switching stimulated by paadB. This T26 transposon library was generated as described by Gallagher (61). The insertion in *hfq* was mapped to nucleotide 1,604,426 of the AB5075-UW genome (GenBank CP008706.1). A stationary phase culture of a strain carrying this insertion was used to prepare gDNA as described below; gDNA was then electroporated into the LSO and normal VIR-O variants as outlined below. Transformants were selected for using plates containing 10  $\mu$ g/ml of tetracycline. Transformants were passaged onto 0.5x LB, 0.8% agar to qualitatively compare phenotypes between isolates; representative colonies were then stocked as described above. Insertions in stocked isolates were confirmed by PCR with Taq DNA polymerase (New England Biolabs, Ipswich, MA) using primers hfq-for and hfq-rev (**Table S2**).

**Electroporation of AB5075.** Electroporations were conducted with cultures of AB5075 isolates grown at 37°C with shaking to late log phase. Cells were pelleted by centrifugation and washed

three times with 10% glycerol to induce electrocompetence. Cells were mixed with either gDNA or plasmid DNA in 2 mm cuvettes and electroporated at 2.50 KV. Transformants were recovered in 1 ml LB for 30 min at 37°C without shaking, followed by 1 h at 37°C with shaking. Transformants were then selected for by plating on the appropriate antibiotic.

**Opacity switching assays.** Switching frequencies to AV-T were calculated as previously described (59). Switching assays were conducted on plates containing 20 ml of 0.5x LB, 0.8% agar supplemented with 100 µg/ml hygromycin or 5 µg/ml tetracycline, as appropriate to ensure maintenance of plasmids. Assays were performed using six 24 h old colonies from at least two independent experiments, unless otherwise noted.

**VIR-O and LSO interconversion assays.** To estimate the rate at which normal VIR-O and LSO variants interconvert, serial dilutions of LSO and normal VIR-O stocks were plated on 0.5x LB, 0.8% agar. After 24 h, individual colonies were resuspended and serially diluted on 0.5x LB, 0.8% agar to determine CFUs; colony suspensions were then stored at 4°C. Following enumeration of CFUs, colony suspensions were plated to obtain approximately 50 colonies per plate across several plates in order to screen several hundred colonies. After 48 h of growth, colonies were screened for sectoring using a dissecting microscope with oblique illumination. Colonies that appeared to exhibit the phenotype of the other variant were passaged onto 0.5x LB, 0.8% agar alongside a normal VIR-O positive control to confirm the phenotype. The frequency of conversion was calculated by dividing the number of confirmed colonies of the other phenotype by the total number of colonies screened.

**gDNA isolation.** Unless otherwise noted, cultures used for gDNA preparations were grown with shaking at 37°C to an OD<sub>600</sub> of 0.5. One ml of cells was pelleted through centrifugation; pellets were then resuspended in Tris-EDTA. Cells were lysed by incubation for 1 h at 37°C with 0.5% SDS and 400 µg/ml proteinase K. Sodium chloride was added to a final concentration of 0.7 M, and DNA was extracted twice using equal volumes of phenol/chloroform/isoamyl alcohol. DNA was isolated by mixing with an equal volume of 95% ethanol until a precipitate was visible. DNA pellets were collected by centrifugation, washed twice with 75% ethanol, dried, and resuspended in molecular grade water.

**Whole genome sequencing (WGS).** PacBio WGS was performed at the University of Maryland Genomics Resource Center.

**MIC assays.** MICs were determined using a modified Etest assay as previously described (16). Briefly, two strains at an OD<sub>600</sub> of 0.1 were inoculated onto either side of an Etest strip (bioMérieux, Marcy-l'Étoile, France) by pipetting 10 µl of culture next to the bottom of the strip, tilting the plate to spread the culture up the side of the strip, and pipetting away excess culture at the top of the strip. MICs were assessed after 6 or 16 h, as noted. Experiments were performed two independent times to confirm the reproducibility of trends.

**Southern blotting.** A DNA probe specific for *aadB* was generated by PCR using primers oSA65 and oSA66 (**Table S2**) and Phusion Hot Start II DNA polymerase, with LSO gDNA as a template. The resulting fragment was gel purified using the UltraClean DNA purification kit (Mo Bio Laboratories, Carlsbad, CA). The PCR product was then diluted in Tris-EDTA, boiled

for 10 min to denature the DNA, and incubated in an ice water bath for 5 min. The DNA was then labeled with digoxigenin (DIG) by incubating with DIG labeling mix, hexanucleotide mix, and klenow polymerase (Roche, Mannheim, Germany) at 37°C for at least 4 h. The labeled probe was diluted 1:500 in prehybridization solution, which consists of 5x SSC (1x SSC is 0.15 M NaCl plus 0.015 M sodium citrate), 0.1% N-lauroylsarcosine, 0.02% SDS, and 5 mg/ml blocking reagent (Roche), and stored at -20°C. A DNA probe specific for the Gene Ruler High Range DNA ladder (Thermo Scientific) was also generated by the above protocol, using ladder diluted 1:2500 in Tris-EDTA.

gDNA samples for Southern blotting were generated as described above. Concentrations of gDNA samples were determined using a NanoDrop ND-100 spectrophotometer; between 3.4 and 4.6 µg of each sample was digested with *ScaI* (New England Biolabs) for 6 h at 37°C. Samples were electrophoresed alongside the Gene Ruler High Range DNA ladder on a 0.5% Tris-acetate-EDTA (TAE)-agarose gel overnight at 25 V. Gels were post-stained with ethidium bromide (EtBr) and photographed. Gels were washed for 10 min in 0.2 N HCl, rinsed three times with distilled water, washed twice for 15 min with denaturation solution (0.5 M NaOH, 1.5 M NaCl), and washed for 30 min with neutralization solution (0.5 M Tris-HCl, 1.5 M NaCl, pH 7.5). Nucleic acids were transferred onto a 0.22 µm nylon membrane via capillary transfer using a TurboBlotter (Schleicher & Schuell, Keene, NH) overnight at room temperature. Transfer was performed using 20x SSC as a buffer. The membrane was then baked in a vacuum oven at 80°C, 13 in Hg for 2 h. The membrane was cut to separate lanes containing gDNA samples from lanes containing ladder; the two sections were treated separately for subsequent steps. Membranes were incubated in prehybridization solution for 2 h at 65°C. Membranes were then incubated with the appropriate probe (*aadB* probe for gDNA lanes, ladder probe for ladder lanes) overnight

at 65°C. Probes were boiled for 10 min prior to addition to the membrane. Membranes were washed twice for 15 min with 2x SSC, 0.1% SDS, then washed twice for 15 min with 0.1x SSC, 0.1% SDS at 65°C. Membranes were then incubated for 2 min in buffer 1, which is 0.1 M Tris (pH 7.5), 0.15 M NaCl. Membranes were then blocked for 1 h in buffer 2, which is buffer 1 with 10 mg/ml blocking reagent. Membranes were incubated for 30 min in buffer 1 containing a 1:5000 dilution of  $\alpha$ -DIG alkaline phosphatase (Roche). Membranes were then washed twice for 15 min in buffer 1, followed by a 2 min incubation in buffer 3 (0.1 M Tris, 0.1 M NaCl, pH 9.5). Finally, membranes were developed in color substrate solution, which was prepared by adding 105  $\mu$ l 5-bromo-4-chloro-3-indolyl-phosphate (BCIP) and 135  $\mu$ l 4-nitro blue tetrazolium chloride (NBT) to 30 ml of buffer 3. Once bands were clearly visible, development was stopped by washing membranes for 5 min in distilled water. Following development, the two sections of the membrane were realigned and photographed.

**Quantitative PCR (qPCR).** qPCR was performed using gDNA samples prepared as described above. qPCR primers were designed to amplify approximately 150 bp fragments from each gene of interest and were generated using Primer-BLAST ([www.ncbi.nlm.nih.gov/tools/primer-blast](http://www.ncbi.nlm.nih.gov/tools/primer-blast)). qPCR of *aadB* was performed using primers oSA69 and oSA70, while qPCR of the control gene *aacA4* was done using primers oSA61 and oSA62 (**Table S2**). qPCR was performed using iQ SYBR Green Supermix (Bio-Rad, Hercules, CA) and a Bio-Rad CFX Connect cycler. Cycle parameters were: 95°C for 3 min, followed by 40 cycles of 95°C for 10 s, 55°C for 10 s, and 72°C for 20 s. Melt curves were then collected to confirm primer specificity. Copy number was calculated relative to a control strain (LSO), and a control gene (*aacA4*) using the  $2^{-\Delta\Delta C_t}$  method (62).

**Overexpression of duplicated region fragments.** Fragments for overexpression were generated by PCR using Phusion Hot Start II Polymerase and gDNA generated from a stationary phase culture of AB5075 (pWHAadB, pWHAadB-T, pWHAadB-TA, pWHAadB-TB, pWHAadB-UP, paadB) or gDNA from a mid-log LSO culture (pDR) as a template. All fragments were generated using oSA66 as a forward primer; reverse primers are indicated in **Table S2**. Fragments were ligated into pWH1266 (63) cut with *ScaI* (pWHAadB, pWHAadB-T, pWHAadB-TA, pWHAadB-TB, pWHAadB-UP) or pQF1266.Blue (see below) cut with *SmaI* (paadB, pDR). Plasmids were isolated using TransforMax EC100 electrocompetent *E. coli* plated on either 10 µg/ml tetracycline (pWH1266 derivatives), or 100 µg/ml hygromycin (pQF1266.Blue derivatives). Inserts were confirmed by restriction digestion and Sanger sequencing; plasmids were chosen with the inserts in the same orientation relative to the plasmid backbone. For the pWH1266 derivatives, inserts were all oriented with  $P_c$  on the opposite strand from the *bla*<sub>TEM-1</sub> promoter. Plasmids were introduced into the LSO, LSO  $\Delta$ p1AB5075, and LSO *hfq::Tc* isolates, as indicated, by electroporation.

Plasmid pQF1266.Blue was constructed from pQF50 (64) by first inserting a hygromycin resistance gene from pMQ310 (65) into the *ScaI* site within the beta-lactamase gene. This resulted in plasmid pQF50.hyg. Next, a 1.4 kb fragment containing the origin of replication from pWH1266 was generated by PCR using the primers ATATCCATGGGATCGTGAAATATCTATGA and ATATCCATGGGGATTTTATTTTGC GTTACA, each containing a site for the restriction enzyme *NcoI*. The resulting PCR product was digested with *NcoI* and ligated to *NcoI* digested pQF50.hyg. Plasmids containing the 1266 ori region in each orientation resulted in either blue or

white colonies on plates containing X-gal, indicating a promoter was present in one orientation that drove beta-galactosidase expression. This plasmid was designated pQF1266.Blue.

**Site-directed mutagenesis.** Mutagenized plasmids pWHaadBstop and pWHaadB-Q35 were generated using a Quikchange II XL Site-Directed Mutagenesis Kit (Agilent Technologies, Santa Clara, CA). Primers used for mutagenesis are listed in **Table S2**. Briefly, pWHaadB was amplified using mutagenesis primers according to the manufacturer's instructions. The parental plasmids were digested with Dpn-1 and the remaining mutagenized plasmids were transformed into TransforMax EC100 electrocompetent *E. coli*. Transformants were selected for using 10 µg/ml tetracycline, and mutations were confirmed by Sanger sequencing. Mutagenized plasmids were then electroporated into the LSO variant as described above.

**Screen for transposon insertions in pWHaadB.** Plasmid pWHaadB was mutagenized using the EZ-Tn5 <Kan-2> transposon kit (Lucigen) according to the manufacturer's instructions. The mutagenized plasmid was transformed into TransforMax EC100 electrocompetent *E. coli* and transformants were selected for by plating on LB with 50 µg/ml of kanamycin. Transformants were then pooled and plasmids were purified. To obtain insertions that blocked switching stimulated by pWHaadB, pooled plasmids were transformed into the LSO as described above and transformants were selected by plating on 10 µg/ml tetracycline. Transformants were pooled and serial dilutions were plated on 0.5x LB, 0.8% agar to screen for sectoring. Colonies that exhibited decreased sectoring were passaged onto 0.5x LB, 0.8% agar alongside positive controls to confirm phenotypes. Colonies were then cultured, plasmids were purified, and transposon

insertions were mapped by Sanger sequencing using the primers Kan-2 FP-1 and RP-1 (Lucigen).

To screen for insertions in *aadB* that did not block switching stimulated by pWHaadB, *E. coli* transformants were individually patched onto LB containing 10 µg/ml tetracycline and LB containing 10 µg/ml tobramycin. Patches that failed to grow on tobramycin were cultured, then plasmids were individually purified and transformed into the LSO variant. Transformants were screened for their ability to switch; plasmids that still stimulated switching were sequenced with primer Kan-2 FP-1 to map the insertion.

**RNA Purification.** RNA was prepared from cultures grown in LB medium to an OD<sub>600</sub> of 0.5. Cultures were supplemented with 5 µg/ml tetracycline, as appropriate. For the hetR-O2 strain, cultures were first grown overnight at room temperature and then at 37°C with shaking to an OD<sub>600</sub> of 0.1 in 16 µg/ml tobramycin, pelleted by centrifugation and washed to remove the antibiotic, resuspended, and then grown with shaking to an OD<sub>600</sub> of 0.5. Samples were collected using RNAProtect Bacteria Reagent (Qiagen), according to the manufacturer's protocol. Cell pellets were flash frozen and stored at -80°C. RNA was isolated using the MasterPure RNA purification kit (Epicentre, Madison, WI) according to the manufacturer's instructions.

**Northern blotting.** Indicated RNA samples were pre-treated with terminator exonuclease (TEX) (Lucigen) in Terminator 10x Reaction Buffer A according to the manufacturer's protocol. Reactions were diluted in 2x RNA loading dye (Thermo Scientific) and processed as described below.

Concentrations of RNA samples were determined using a NanoDrop ND-100 spectrophotometer. Either 2.3  $\mu\text{g}$  (**Fig. 6C**) or 3.6  $\mu\text{g}$  (**Fig. 6B**) of RNA was diluted in an equal volume of 2x RNA loading dye with 2.5 mM EDTA and incubated at 65°C for 10 min. Samples were then electrophoresed on a pre-run 10% Mini-PROTEAN TBE-Urea gel (Bio-Rad) at 200 V. Samples were run alongside Low Range ssRNA Ladder (New England Biolabs), which was denatured by incubating at 90°C for 5 min followed by a 2 min incubation on ice prior to electrophoresis. Gels were post-stained with EtBr in 0.1% diethyl pyrocarbonate (DEPC)-treated distilled water for 30 min and photographed. Gels were washed again with 0.1% DEPC distilled water for 30 min. Nucleic acids were transferred onto a 0.22  $\mu\text{m}$  nylon membrane via capillary transfer overnight at room temperature, as described above for the Southern blot. Membranes were visualized with a UV lamp and ladder bands were marked with a ball point pen; membranes were then baked in a vacuum oven at 80°C, 13 in Hg for 2 h. Membranes were incubated with DIG Easy Hyb (Roche) for 2 h at 39°C. Membranes were then incubated overnight at 39°C with the probe oSA134. oSA134 is a single stranded oligonucleotide labeled at the 3' and 5' ends with DIG (**Table S2**). oSA134 was diluted to 100 ng/ml in 0.1% DEPC prehybridization solution (see Southern blot) and boiled for 10 min before use. Following probing, membranes were washed for 15 min in 0.1% DEPC, 2x SSC, 0.1% SDS, followed by two 15 min washes in 0.1% DEPC, 0.2x SSC, 0.1% SDS at 65°C. Membranes were washed for 1 min in maleate buffer (100 mM maleic acid, 150 mM NaCl, 0.1% DEPC, pH 7.5). Membranes were then incubated for 1 h in maleate buffer containing 2% blocking reagent (Roche). Membranes were incubated for 30 min in maleate buffer containing 2% blocking reagent and a 1:5000 dilution of  $\alpha$ -DIG alkaline phosphatase (Roche). Membranes were then washed twice for 15 min with

maleate buffer, followed by a 5 min incubation in 0.1% DEPC buffer 3 (see Southern blot). Finally, membranes were developed as described above for the Southern blots.

**Mice.** WT C57BL/6J female mice were purchased from Jackson Laboratories and used at age 8-10 weeks. Mice were housed under specific pathogen-free conditions at Yerkes National Primate Center, Emory University. Experimental studies were performed in accordance with the Institutional Animal Care and Use Committee guidelines.

**Mouse pulmonary infection models.** Approximately  $5 \times 10^7$  CFU (24 h time point) were administered per mouse for infections to quantify the bacterial load. Overnight standing bacteria at room temperature were sub-cultured in LB broth and grown at 37°C with shaking to an OD<sub>600</sub> ~0.15, washed, and re-suspended in PBS. Fifty µl of bacterial inocula were inoculated intranasally (i.n.) to each mouse. Mice were anesthetized with isoflurane immediately prior to intranasal inoculation. At 24hpi (hour post-infection), the mice were sacrificed and the lungs, spleen and liver were harvested, homogenized, and plated for CFU on 0.5x LB plates.

**RNA-sequencing (RNA-seq).** RNA-seq was performed at the Yerkes Genomics Core at Emory University. RNA-seq was performed in triplicate using samples generated from three independent cultures of the LSO and normal VIR-O variants. Upon sample collection, cultures were struck onto a 0.5x LB, 0.8% agar plate and checked for the presence of contaminating AV-T variants, only samples with greater than ~95% opaque variants were used for RNA-seq. RNA purification was performed as outlined above, after which samples were treated twice with Turbo-DNA free (Thermo Fisher), according to the manufacturer's instructions. To confirm that

samples were not contaminated with DNA following DNase treatment, PCR of RNA samples was performed using primers abaR-qPCR-for and abaR-qPCR-rev.

**Statistical analyses.** Statistical analyses were performed with Prism 5 and 7 (GraphPad Software, Inc. La Jolla, CA).

**Acknowledgements**

This work was supported by grants from the Merit Review Program I01BX001725 and a Research Career Scientist Award IK6BX004470, both from the Department of Veterans Affairs, to P.N.R. D.S.W. is supported by a Burroughs Wellcome Fund Investigator in the Pathogenesis of Infectious Disease award, VA Merit award I01 BX002788 and NIH grant AI141883. S.E.A. was supported by T32 training grant AI106699 from the NIH.

The content is solely the responsibility of the authors and does not necessarily represent the official views of the NIH or the Department of Veterans Affairs.

We have no conflicts of interest to disclose.

## References

1. Peleg AY, Seifert H, Paterson DL. 2008. *Acinetobacter baumannii*: emergence of a successful pathogen. Clin Microbiol Rev 21:538-82.
2. Anonymous. 2017. WHO Priority Pathogens List for R&D of New Antibiotics, on World Health Organization. [http://who.int/medicines/publications/WHO-PPL-Short\\_Summary\\_25Feb-ET\\_NM\\_WHO.pdf](http://who.int/medicines/publications/WHO-PPL-Short_Summary_25Feb-ET_NM_WHO.pdf). Accessed Nov. 5.
3. Wong D, Nielsen TB, Bonomo RA, Pantapalangkoor P, Luna B, Spellberg B. 2017. Clinical and Pathophysiological Overview of *Acinetobacter* Infections: a Century of Challenges. Clin Microbiol Rev 30:409-447.
4. Chin CY, Tipton KA, Farokhyfar M, Burd EM, Weiss DS, Rather PN. 2018. A high-frequency phenotypic switch links bacterial virulence and environmental survival in *Acinetobacter baumannii*. Nat Microbiol 3:563-569.
5. Tipton KA, Dimitrova D, Rather PN. 2015. Phase-Variable Control of Multiple Phenotypes in *Acinetobacter baumannii* Strain AB5075. J Bacteriol 197:2593-9.
6. Tipton KA, Farokhyfar M, Rather PN. 2016. Multiple roles for a novel RND-type efflux system in *Acinetobacter baumannii* AB5075. Microbiologyopen doi:10.1002/mbo3.418.
7. Tipton KA, Rather PN. 2016. An ompR/envZ Two-Component System Ortholog Regulates Phase Variation, Osmotic Tolerance, Motility, and Virulence in *Acinetobacter baumannii* strain AB5075. J Bacteriol doi:10.1128/jb.00705-16.
8. Ahmad I, Karah N, Nadeem A, Wai SN, Uhlin BE. 2019. Analysis of colony phase variation switch in *Acinetobacter baumannii* clinical isolates. PLoS One 14:e0210082.

9. Gallagher LA, Ramage E, Weiss EJ, Radey M, Hayden HS, Held KG, Huse HK, Zurawski DV, Brittnacher MJ, Manoil C. 2015. Resources for Genetic and Genomic Analysis of Emerging Pathogen *Acinetobacter baumannii*. *J Bacteriol* 197:2027-35.
10. Cagle CA, Shearer JE, Summers AO. 2011. Regulation of the integrase and cassette promoters of the class 1 integron by nucleoid-associated proteins. *Microbiology* 157:2841-53.
11. Levesque C, Brassard S, Lapointe J, Roy PH. 1994. Diversity and relative strength of tandem promoters for the antibiotic-resistance genes of several integrons. *Gene* 142:49-54.
12. Papagiannitsis CC, Tzouvelekis LS, Miriagou V. 2009. Relative strengths of the class 1 integron promoter hybrid 2 and the combinations of strong and hybrid 1 with an active p2 promoter. *Antimicrob Agents Chemother* 53:277-80.
13. Collis CM, Hall RM. 1995. Expression of antibiotic resistance genes in the integrated cassettes of integrons. *Antimicrob Agents Chemother* 39:155-162.
14. Hanau-Bercot B, Podglajen I, Casin I, Collatz E. 2002. An intrinsic control element for translational initiation in class 1 integrons. *Mol Microbiol* 44:119-30.
15. Partridge SR, Recchia GD, Scaramuzzi C, Collis CM, Stokes HW, Hall RM. 2000. Definition of the *attI1* site of class 1 integrons. *Microbiology* 146 ( Pt 11):2855-64.
16. Anderson SE, Sherman EX, Weiss DS, Rather PN. 2018. Aminoglycoside Heteroresistance in *Acinetobacter baumannii* AB5075. *mSphere* 3.
17. Shaw KJ, Rather PN, Hare RS, Miller GH. 1993. Molecular genetics of aminoglycoside resistance genes and familial relationships of the aminoglycoside-modifying enzymes. *Microbiol Rev* 57:138-63.

18. Carrier MC, Lalaouna D, Masse E. 2018. Broadening the Definition of Bacterial Small RNAs: Characteristics and Mechanisms of Action. *Annu Rev Microbiol* 72:141-161.
19. Kunne T, Swarts DC, Brouns SJ. 2014. Planting the seed: target recognition of short guide RNAs. *Trends Microbiol* 22:74-83.
20. Vogel J, Luisi BF. 2011. Hfq and its constellation of RNA. *Nat Rev Microbiol* 9:578-89.
21. Frohlich KS, Forstner KU, Gitai Z. 2018. Post-transcriptional gene regulation by an Hfq-independent small RNA in *Caulobacter crescentus*. *Nucleic Acids Res* 46:10969-10982.
22. Bohn C, Rigoulay C, Bouloc P. 2007. No detectable effect of RNA-binding protein Hfq absence in *Staphylococcus aureus*. *BMC Microbiol* 7:10.
23. Muller P, Gimpel M, Wildenhain T, Brantl S. 2019. A new role for CsrA: promotion of complex formation between an sRNA and its mRNA target in *Bacillus subtilis*. *RNA Biol* doi:10.1080/15476286.2019.1605811:1-16.
24. Smirnov A, Forstner KU, Holmqvist E, Otto A, Gunster R, Becher D, Reinhardt R, Vogel J. 2016. Grad-seq guides the discovery of ProQ as a major small RNA-binding protein. *Proc Natl Acad Sci U S A* 113:11591-11596.
25. Frohlich KS, Papenfort K, Fekete A, Vogel J. 2013. A small RNA activates CFA synthase by isoform-specific mRNA stabilization. *Embo j* 32:2963-79.
26. Kim S, Reyes D, Beaume M, Francois P, Cheung A. 2014. Contribution of *teg49* small RNA in the 5' upstream transcriptional region of *sarA* to virulence in *Staphylococcus aureus*. *Infect Immun* 82:4369-79.
27. Loh E, Dussurget O, Gripenland J, Vaitkevicius K, Tiensuu T, Mandin P, Repoila F, Buchrieser C, Cossart P, Johansson J. 2009. A trans-acting riboswitch controls expression of the virulence regulator PrfA in *Listeria monocytogenes*. *Cell* 139:770-9.

28. Chao Y, Papenfort K, Reinhardt R, Sharma CM, Vogel J. 2012. An atlas of Hfq-bound transcripts reveals 3' UTRs as a genomic reservoir of regulatory small RNAs. *Embo j* 31:4005-19.
29. Chao Y, Vogel J. 2016. A 3' UTR-Derived Small RNA Provides the Regulatory Noncoding Arm of the Inner Membrane Stress Response. *Mol Cell* 61:352-363.
30. Guerin E, Jove T, Tabesse A, Mazel D, Ploy MC. 2011. High-level gene cassette transcription prevents integrase expression in class 1 integrons. *J Bacteriol* 193:5675-82.
31. Fiester SE, Arivett BA, Schmidt RE, Beckett AC, Ticak T, Carrier MV, Ghosh R, Ohneck EJ, Metz ML, Sellin Jeffries MK, Actis LA. 2016. Iron-Regulated Phospholipase C Activity Contributes to the Cytolytic Activity and Virulence of *Acinetobacter baumannii*. *PLoS One* 11:e0167068.
32. Gebhardt MJ, Gallagher LA, Jacobson RK, Usacheva EA, Peterson LR, Zurawski DV, Shuman HA. 2015. Joint Transcriptional Control of Virulence and Resistance to Antibiotic and Environmental Stress in *Acinetobacter baumannii*. *mBio* 6:e01660-15.
33. Cerqueira GM, Kostoulias X, Khoo C, Aibinu I, Qu Y, Traven A, Peleg AY. 2014. A global virulence regulator in *Acinetobacter baumannii* and its control of the phenylacetic acid catabolic pathway. *J Infect Dis* 210:46-55.
34. Bhuiyan MS, Ellett F, Murray GL, Kostoulias X, Cerqueira GM, Schulze KE, Mahamad Maifiah MH, Li J, Creek DJ, Lieschke GJ, Peleg AY. 2016. *Acinetobacter baumannii* phenylacetic acid metabolism influences infection outcome through a direct effect on neutrophil chemotaxis. *Proc Natl Acad Sci U S A* 113:9599-604.

35. Tomaras AP, Dorsey CW, Edelmann RE, Actis LA. 2003. Attachment to and biofilm formation on abiotic surfaces by *Acinetobacter baumannii*: involvement of a novel chaperone-usher pili assembly system. *Microbiology* 149:3473-84.
36. Pakharukova N, Tuittila M, Paavilainen S, Malmi H, Parilova O, Teneberg S, Knight SD, Zavialov AV. 2018. Structural basis for *Acinetobacter baumannii* biofilm formation. *Proc Natl Acad Sci U S A* doi:10.1073/pnas.1800961115.
37. Padalon-Brauch G, Hershberg R, Elgrably-Weiss M, Baruch K, Rosenshine I, Margalit H, Altuvia S. 2008. Small RNAs encoded within genetic islands of *Salmonella typhimurium* show host-induced expression and role in virulence. *Nucleic Acids Res* 36:1913-1927.
38. Ellis MJ, Trussler RS, Charles O, Haniford DB. 2017. A transposon-derived small RNA regulates gene expression in *Salmonella* Typhimurium. *Nucleic Acids Res* 45:5470-5486.
39. Durieux I, Ginevra C, Attaiech L, Picq K, Juan PA, Jarraud S, Charpentier X. 2019. Diverse conjugative elements silence natural transformation in *Legionella* species. *Proc Natl Acad Sci U S A* doi:10.1073/pnas.1909374116.
40. Pichon C, Felden B. 2005. Small RNA genes expressed from *Staphylococcus aureus* genomic and pathogenicity islands with specific expression among pathogenic strains. *Proc Natl Acad Sci U S A* 102:14249-54.
41. Chen XL, Tang DJ, Jiang RP, He YQ, Jiang BL, Lu GT, Tang JL. 2011. sRNA-Xcc1, an integron-encoded transposon- and plasmid-transferred trans-acting sRNA, is under the positive control of the key virulence regulators HrpG and HrpX of *Xanthomonas campestris* pathovar *campestris*. *RNA Biol* 8:947-53.

42. Wachter S, Raghavan R, Wachter J, Minnick MF. 2018. Identification of novel MITEs (miniature inverted-repeat transposable elements) in *Coxiella burnetii*: implications for protein and small RNA evolution. BMC Genomics 19:247.
43. Jia X, Zhang J, Sun W, He W, Jiang H, Chen D, Murchie AI. 2013. Riboswitch control of aminoglycoside antibiotic resistance. Cell 152:68-81.
44. Roth A, Breaker RR. 2013. Integron *attII* sites, not riboswitches, associate with antibiotic resistance genes. Cell 153:1417-8.
45. Wang S, He W, Sun W, Zhang J, Chang Y, Chen D, Murchie AIH. 2019. Integron Derived Aminoglycoside-Sensing Riboswitches Control Aminoglycoside Acetyltransferase Resistance Gene Expression. Antimicrob Agents Chemother doi:10.1128/aac.00236-19.
46. Pursley BR, Fernandez NL, Severin GB, Waters CM. 2019. The Vc2 cyclic di-GMP dependent riboswitch of *Vibrio cholerae* regulates expression of an upstream putative small RNA by controlling RNA stability. J Bacteriol doi:10.1128/jb.00293-19.
47. DebRoy S, Gebbie M, Ramesh A, Goodson JR, Cruz MR, van Hoof A, Winkler WC, Garsin DA. 2014. Riboswitches. A riboswitch-containing sRNA controls gene expression by sequestration of a response regulator. Science 345:937-40.
48. Mabrouk A, Grosso F, Botelho J, Achour W, Ben Hassen A, Peixe L. 2017. GES-14-Producing *Acinetobacter baumannii* Isolates in a Neonatal Intensive Care Unit in Tunisia Are Associated with a Typical Middle East Clone and a Transferable Plasmid. Antimicrob Agents Chemother 61:e00142-17.

49. Bonnin RA, Nordmann P, Potron A, Lecuyer H, Zahar J-R, Poirel L. 2011. Carbapenem-Hydrolyzing GES-Type Extended-Spectrum  $\beta$ -Lactamase in *Acinetobacter baumannii*. *Antimicrob Agents Chemother* 55:349-354.
50. Nemec A, Dolzani L, Brisse S, van den Broek P, Dijkshoorn L. 2004. Diversity of aminoglycoside-resistance genes and their association with class 1 integrons among strains of pan-European *Acinetobacter baumannii* clones. *J Med Microbiol* 53:1233-40.
51. Liu CC, Tang CY, Chang KC, Kuo HY, Liou ML. 2014. A comparative study of class 1 integrons in *Acinetobacter baumannii*. *Gene* 544:75-82.
52. Lin MF, Liou ML, Tu CC, Yeh HW, Lan CY. 2013. Molecular epidemiology of integron-associated antimicrobial gene cassettes in the clinical isolates of *Acinetobacter baumannii* from northern Taiwan. *Ann Lab Med* 33:242-7.
53. Lin MF, Chang KC, Yang CY, Yang CM, Xiao CC, Kuo HY, Liou ML. 2010. Role of integrons in antimicrobial susceptibility patterns of *Acinetobacter baumannii*. *Jpn J Infect Dis* 63:440-3.
54. Azizi O, Shakibaie MR, Badmasti F, Modarresi F, Ramazanzadeh R, Mansouri S, Shahcheraghi F. 2016. Class 1 integrons in non-clonal multidrug-resistant *Acinetobacter baumannii* from Iran, description of the new *blaIMP-55* allele in In1243. *J Med Microbiol* 65:928-36.
55. Mirshekar M, Shahcheraghi F, Azizi O, Solgi H, Badmasti F. 2018. Diversity of Class 1 Integrons, and Disruption of *carO* and *dacD* by Insertion Sequences Among *Acinetobacter baumannii* Isolates in Tehran, Iran. *Microb Drug Resist* 24:359-366.
56. McGann P, Courvalin P, Snesrud E, Clifford RJ, Yoon EJ, Onmus-Leone F, Ong AC, Kwak YI, Grillot-Courvalin C, Lesho E, Waterman PE. 2014. Amplification of

- Aminoglycoside Resistance Gene *aphA1* in *Acinetobacter baumannii* Results in Tobramycin Therapy Failure. *mBio* 5.
57. Hamidian M, Holt KE, Pickard D, Dougan G, Hall RM. 2014. A GC1 *Acinetobacter baumannii* isolate carrying AbaR3 and the aminoglycoside resistance transposon TnaphA6 in a conjugative plasmid. *J Antimicrob Chemother* 69:955-8.
  58. Tipton KA, Chin CY, Farokhyfar M, Weiss DS, Rather PN. 2018. Role of Capsule in Resistance to Disinfectants, Host Antimicrobials, and Desiccation in *Acinetobacter baumannii*. *Antimicrob Agents Chemother* 62.
  59. Anderson SE, Rather PN. 2019. Distinguishing Colony Opacity Variants and Measuring Opacity Variation in *Acinetobacter baumannii*. *Methods Mol Biol* 1946:151-157.
  60. Schweizer HP, Hoang TT. 1995. An improved system for gene replacement and *xylE* fusion analysis in *Pseudomonas aeruginosa*. *Gene* 158:15-22.
  61. Gallagher LA. 2019. Methods for Tn-Seq Analysis in *Acinetobacter baumannii*. *Methods Mol Biol* 1946:115-134.
  62. Schmittgen TD, Livak KJ. 2008. Analyzing real-time PCR data by the comparative C(T) method. *Nat Protoc* 3:1101-8.
  63. Hunger M, Schmucker R, Kishan V, Hillen W. 1990. Analysis and nucleotide sequence of an origin of DNA replication in *Acinetobacter calcoaceticus* and its use for *Escherichia coli* shuttle plasmids. *Gene* 87:45-51.
  64. Farinha MA, Kropinski AM. 1990. Construction of broad-host-range plasmid vectors for easy visible selection and analysis of promoters. *J Bacteriol* 172:3496-9.

65. Kalivoda EJ, Horzempa J, Stella NA, Sadaf A, Kowalski RP, Nau GJ, Shanks RMQ. 2011. New vector tools with a hygromycin resistance marker for use with opportunistic pathogens. *Molecular biotechnology* 48:7-14.

## Figure Legends

### Figure 1. Wild-type AB5075 produces at least two subpopulations of opaque variants. **A.**

Colonies representative of the normal VIR-O subpopulation were photographed after 24 h of growth on 0.5x LB, 0.8% agar using a dissecting microscope. The blue sectors forming around the colony edges are comprised of AV-T cells. **B.** Colonies representative of the LSO population were photographed after 24 h of growth on 0.5x LB, 0.8% agar using a dissecting microscope. **C.** Switching to AV-T of normal VIR-O and LSO colonies was quantified after 24 h of growth. Data represent averages and standard deviations (SDs) for six colonies collected in two independent experiments (\*\*\*\*,  $p \leq 0.0001$ , unpaired two-tailed t-test). **D.** Serial dilutions of 24 h-old normal VIR-O colonies were plated and the number of resulting LSO colonies were counted to determine the frequency of conversion. **E.** Serial dilutions of 24 h-old LSO colonies were plated and the number of resulting normal VIR-O colonies were counted to determine the frequency of conversion. For **D** and **E** data represent averages and SDs for five colonies collected in three independent experiments.

### Figure 2. Copy number of an antibiotic resistance locus positively correlates with switching frequency to AV-T. **A.** PacBio whole genome sequencing of the normal VIR-O and LSO

isolates revealed a duplication in the normal VIR-O variant. This duplication comprises part of a composite integron encoded on the plasmid p1AB5075 and consists of five antibiotic resistance genes flanked by two highly homologous copies of *intI*. **B.** Southern blot and qPCR analysis of the duplicated region in two sets of LSO and normal VIR-O isolates (set A samples were previously used for PacBio sequencing). For the Southern blot, gDNA was digested with *ScaI*. A digoxigenin-labeled probe specific for *aadB* showed larger bands for samples classified as

VIR-O in both sets of isolates, as predicted by PacBio sequencing. The table indicates copy number of *aadB* in each sample as calculated by qPCR. Copy number was normalized to *aacA4*, a gene encoded on p1AB5075 outside of the duplicated region. Data represent averages and SDs from three independent samples. **C.** Switching frequencies to AV-T were measured for set B normal VIR-O and LSO colonies after 16 h of growth. **D.** The AB5075 isolate hetR-O2 was previously reported to harbor 17-20 copies of the duplicated region (16). Switching to AV-T of hetR-O2 and the normal VIR-O was measured for colonies after 16 h of growth, showing that hetR-O2 exhibits increased switching. These data further confirm the positive correlation between switching frequency and duplication copy number (\*,  $p \leq 0.05$ , unpaired two-tailed t-test). In **D** and **E** data represent the averages and SDs of six colonies collected in two independent experiments.

**Figure 3. p1AB5075 carrying two copies of the duplicated region is sufficient to cause increased switching to AV-T.** **A.** Strain LSO  $\Delta$ p1AB5075, which has been cured of the p1AB5075 plasmid, was retransformed with DNA derived from the LSO or normal VIR-O variant to restore p1AB5075, and switching to AV-T was measured for parent variant and transformant colonies after 24 h of growth. LSO  $\Delta$ p1AB5075 exhibits similar levels of switching to the LSO variant, as do transformants generated with DNA from the LSO (LSO  $\Delta$ p1AB5075 x LSO). Transformants generated with DNA from the normal VIR-O fell into two phenotypic categories. Some transformants (i.e. LSO  $\Delta$ p1AB5075 x VIR-O A) did not exhibit increased switching, while others (i.e. LSO  $\Delta$ p1AB5075 x VIR-O B) exhibited significantly increased switching relative to the parent strain. Data represent averages and SDs of six colonies collected in three independent experiments (\*\*\*,  $p \leq 0.001$ ; \*\*\*\*,  $p \leq 0.0001$  relative to LSO

$\Delta p1AB5075$  by one-way ANOVA with Dunnett's post-test). **B.** Copy number of the *aadB* gene was measured for variants shown in **A** by qPCR. Isolates that exhibited low levels of switching to the AV-T contain zero or one copy of *aadB*, whereas isolates that exhibited increased switching contain about two copies of *aadB*. Data represent averages and SDs from two independent experiments (ND, not detectable).

**Figure 4. Overexpression of the *aadB* region is sufficient to stimulate switching.** The *aadB* gene was cloned along with its native promoter into the vector pWH1266 (63) and transformed into the LSO variant. Switching to the AV-T was measured for colonies after 24 h of growth, showing that the *aadB* gene is sufficient to stimulate switching of the LSO. Data shown represent averages and SDs of at least five colonies collected in two independent experiments (\*\*\*\*,  $p \leq 0.0001$  by unpaired two-tailed t-test).

**Figure 5. The element responsible for stimulating switching is encoded towards the 5' end and upstream of *aadB*.** **A.** The insert in plasmid pWHAadB contains part of the 5' end of the *intI* ORF (grey rectangle), as well as the promoters for *intI* ( $P_{intI}$ , grey bent arrow) and *aadB* ( $P_c$ , green bent arrow). To determine which part of the insert was responsible for stimulating switching, pWHAadB was mutagenized with EZ-Tn5 <Kan-2>. Insertions that blocked the stimulation of switching are indicated by closed triangles, whereas insertions that did not affect sectoring are indicated by open triangles. Plasmids were then generated containing truncated inserts of different lengths to further test for the stimulation of switching in the LSO variant. The length of each plasmid insert is indicated by brackets. **B-E.** Plasmids pWHAadB-T (**B**), pWHAadB-TA (**C**), pWHAadB-TB (**D**), and pWHAadB-UP (**E**) were transformed into the LSO

variant and switching to AV-T was measured for 24 h old colonies. Data shown represent averages and SDs of six colonies collected from at least two independent experiments (\*\*\*\*,  $p \leq 0.0001$ , one-way ANOVA with Tukey's post-test).

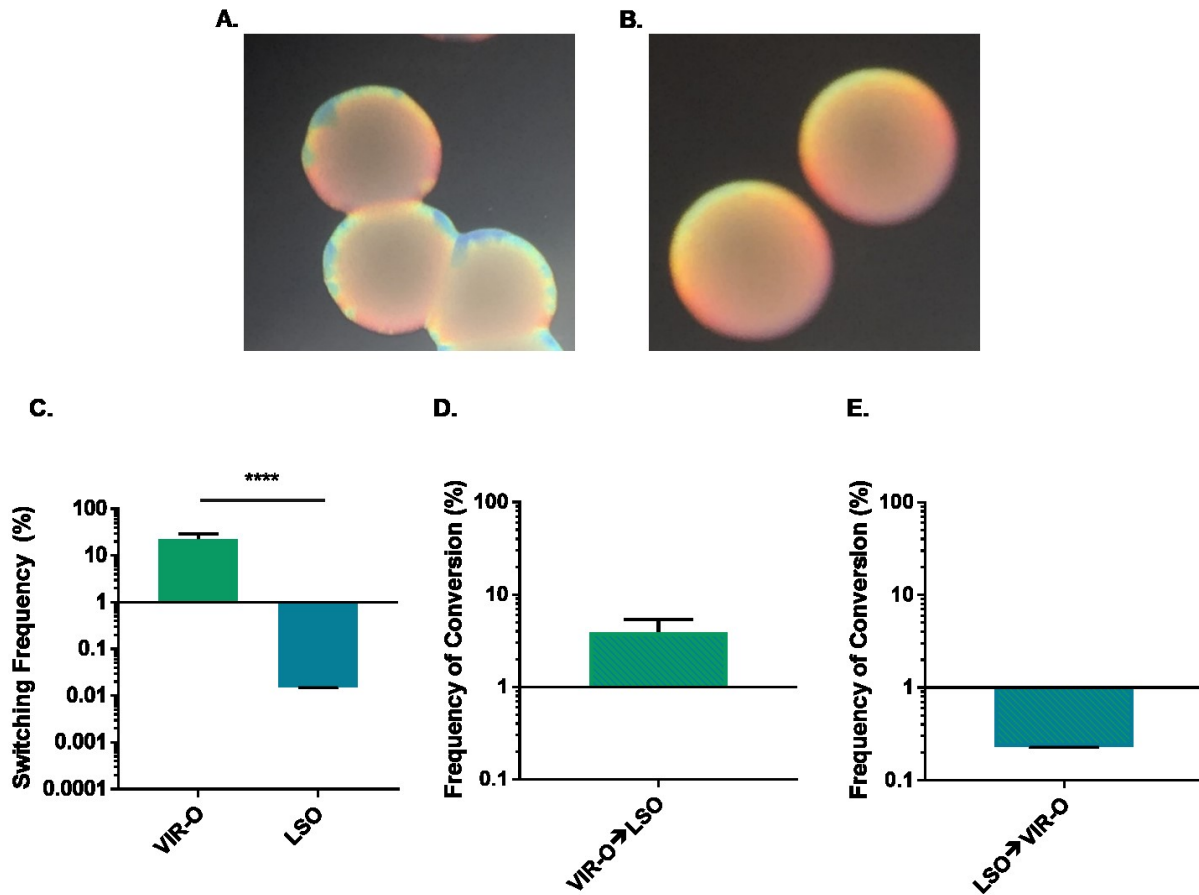
**Figure 6. Data suggest that the element controlling switching is a functional sRNA.** **A.** Two point mutations were introduced to disrupt the -35 of  $P_c$  in pWHaadB (TTGACA  $\rightarrow$  TTGAGT). The resulting plasmid (pWHaadB-Q35) no longer stimulated switching in 24 h old LSO colonies. Data represent averages and SDs for 6 colonies collected in two independent experiments (differences are not significant by unpaired two-tailed t-test). **B.** Northern blotting was performed to examine RNAs produced from overexpression plasmids transformed into LSO  $\Delta p1AB5075$ . Samples were probed with a 30 nt ssDNA probe that hybridizes 40 bp downstream of the reported transcriptional start site for  $P_c$  (30). Five major small RNAs seem to be produced from this region in samples pWHaadB, pWHaadB-TA, and pWHaadB-TB. A  $\sim 300$  nt RNA appears to be missing or reduced in sample pWHaadB-UP (white arrowhead). **C.** Northern blotting was performed to examine RNAs isolated from hetR-O2 in the presence and absence of terminator exonuclease (TEX). HetR-O2 yielded the same five small RNA species observed in **B.** TEX resulted in decreased intensity for all bands, and appeared to eliminate an RNA species of  $\sim 110$  nt (black arrowhead). **D.** An insertional mutation in *hfq* was engineered in the normal VIR-O background and switching to AV-T was quantified for 24 h old colonies. **E.** An insertional mutation in *hfq* was engineered in the LSO variant. Plasmid paadB was generated by cloning *aadB* under its native promoter into pQF1266.Blue. Switching for LSO *hfq::Tc* paadB was quantified after 24 h of growth alongside controls. For **D** and **E** data represent averages and

SDs from six colonies collected in two independent experiments (ns, not significant; \*\*\*\*,  $p \leq 0.0001$  by unpaired two-tailed t-test).

**Figure 7. The LSO variant exhibits decreased virulence in a mouse pneumonia infection**

**model.** Mice were inoculated intranasally with  $5 \times 10^7$  CFU VIR-O or LSO bacteria and CFU were enumerated at 24 hpi. The LSO variant showed decreased colonization of the lungs and dissemination to the spleen and liver compared to the normal VIR-O. Data represent the geometric mean of CFU counts from ten mice (\*\*\*,  $p \leq 0.001$  by two-tailed Mann-Whitney test).

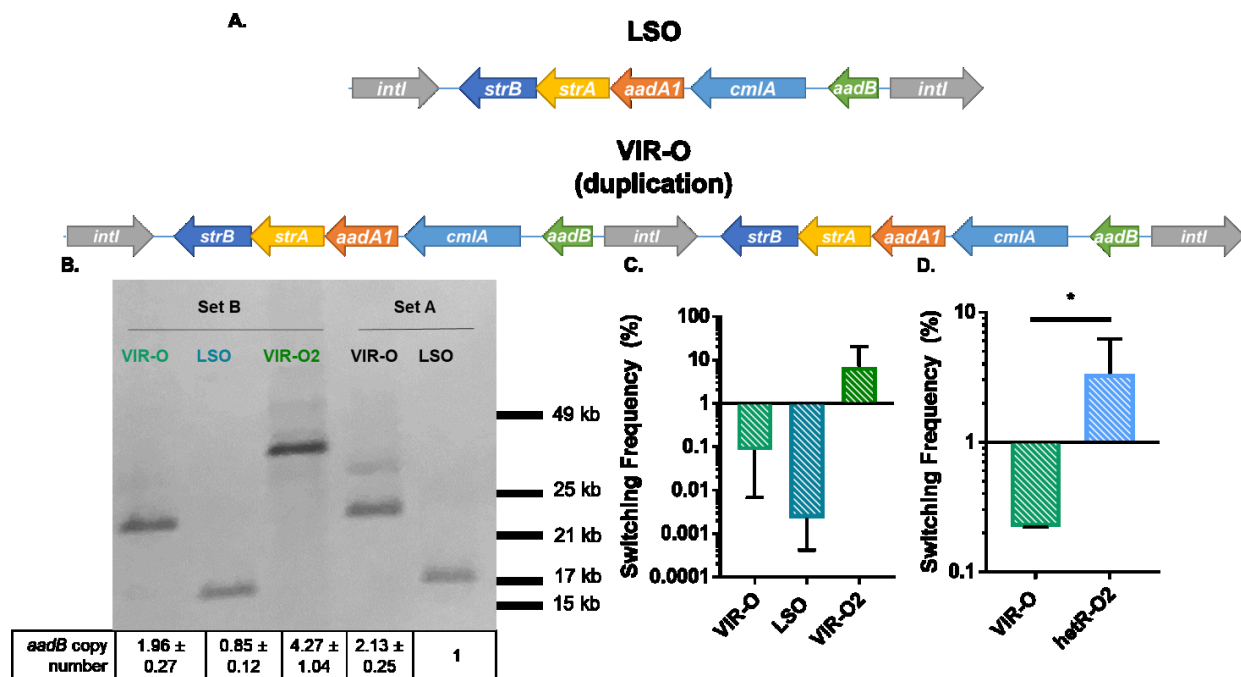
Figure 1



**Figure 1. Wild-type AB5075 produces at least two subpopulations of opaque variants. A.** Colonies representative of the normal VIR-O subpopulation were photographed after 24 h of growth on 0.5x LB, 0.8% agar using a dissecting microscope. The blue sectors forming around the colony edges are comprised of AV-T cells. **B.** Colonies representative of the LSO population were photographed after 24 h of growth on 0.5x LB, 0.8% agar using a dissecting microscope. **C.** Switching to AV-T of normal VIR-O and LSO colonies was quantified after 24 h of growth. Data represent averages and standard deviations (SDs) for six colonies collected in two independent experiments (\*\*\*\*,  $p \leq 0.0001$ , unpaired two-tailed t-test). **D.** Serial dilutions of 24

h-old normal VIR-O colonies were plated and the number of resulting LSO colonies were counted to determine the frequency of conversion. **E.** Serial dilutions of 24 h-old LSO colonies were plated and the number of resulting normal VIR-O colonies were counted to determine the frequency of conversion. For **D** and **E** data represent averages and SDs for five colonies collected in three independent experiments.

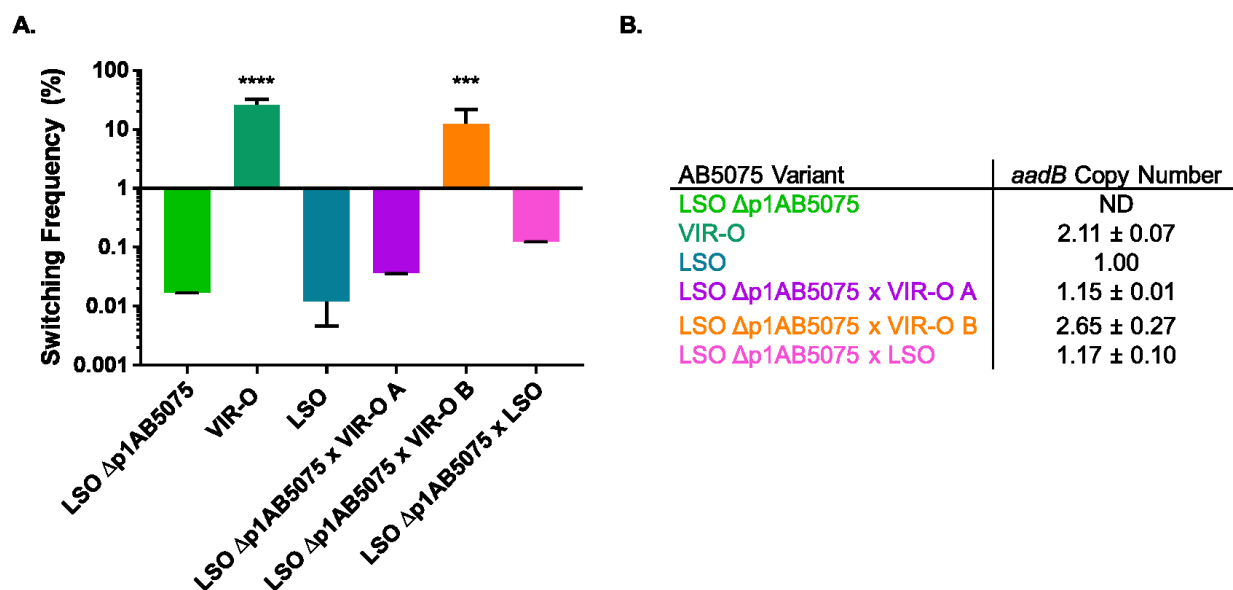
Figure 2



**Figure 2. Copy number of an antibiotic resistance locus positively correlates with switching frequency to AV-T.** **A.** PacBio whole genome sequencing of the normal VIR-O and LSO isolates revealed a duplication in the normal VIR-O variant. This duplication comprises part of a composite integron encoded on the plasmid p1AB5075 and consists of five antibiotic resistance genes flanked by two highly homologous copies of *intI*. **B.** Southern blot and qPCR analysis of the duplicated region in two sets of LSO and normal VIR-O isolates (set A samples were previously used for PacBio sequencing). For the Southern blot, gDNA was digested with *ScaI*. A digoxigenin-labeled probe specific for *aadB* showed larger bands for samples classified as VIR-O in both sets of isolates, as predicted by PacBio sequencing. The table indicates copy number of *aadB* in each sample as calculated by qPCR. Copy number was normalized to *aacA4*, a gene encoded on p1AB5075 outside of the duplicated region. Data represent averages and SDs from three independent samples. **C.** Switching frequencies to AV-T were measured for set B normal VIR-O and LSO colonies after 16 h of growth. **D.** The AB5075 isolate hetR-O2 was

previously reported to harbor 17-20 copies of the duplicated region (16). Switching to AV-T of hetR-O2 and the normal VIR-O was measured for colonies after 16 h of growth, showing that hetR-O2 exhibits increased switching. These data further confirm the positive correlation between switching frequency and duplication copy number (\*,  $p \leq 0.05$ , unpaired two-tailed t-test). In **D** and **E** data represent the averages and SDs of six colonies collected in two independent experiments.

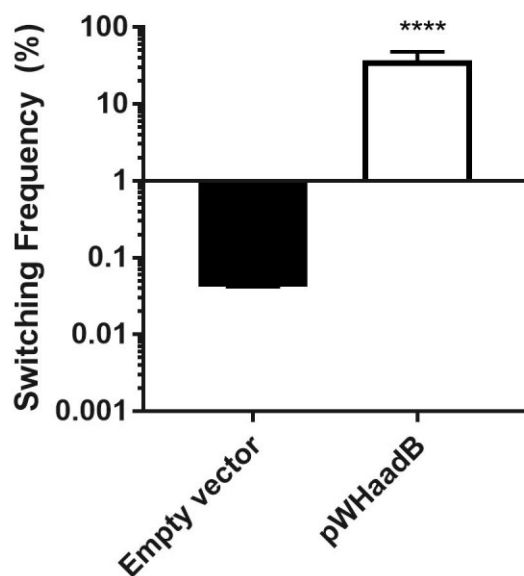
Figure 3



**Figure 3. p1AB5075 carrying two copies of the duplicated region is sufficient to cause increased switching to AV-T.** **A.** Strain LSO  $\Delta$ p1AB5075, which has been cured of the p1AB5075 plasmid, was retransformed with DNA derived from the LSO or normal VIR-O variant to restore p1AB5075, and switching to AV-T was measured for parent variant and transformant colonies after 24 h of growth. LSO  $\Delta$ p1AB5075 exhibits similar levels of switching to the LSO variant, as do transformants generated with DNA from the LSO (LSO  $\Delta$ p1AB5075 x LSO). Transformants generated with DNA from the normal VIR-O fell into two phenotypic categories. Some transformants (i.e. LSO  $\Delta$ p1AB5075 x VIR-O A) did not exhibit increased switching, while others (i.e. LSO  $\Delta$ p1AB5075 x VIR-O B) exhibited significantly increased switching relative to the parent strain. Data represent averages and SDs of six colonies collected in three independent experiments (\*\*\*,  $p \leq 0.001$ ; \*\*\*\*,  $p \leq 0.0001$  relative to LSO  $\Delta$ p1AB5075 by one-way ANOVA with Dunnett's post-test). **B.** Copy number of the *aadB* gene was measured for variants shown in A by qPCR. Isolates that exhibited low levels of switching to the AV-T contain zero or one copy of *aadB*, whereas isolates that exhibited increased

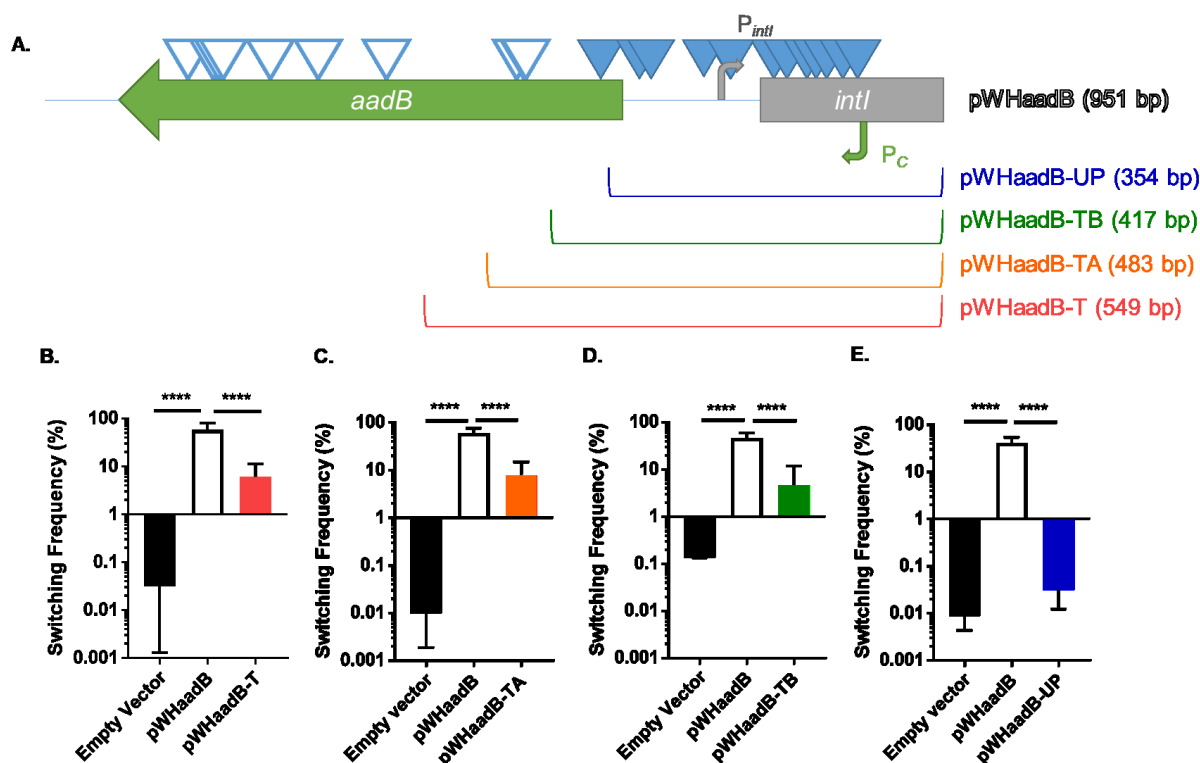
switching contain about two copies of *aadB*. Data represent averages and SDs from two independent experiments (ND, not detectable).

Figure 4



**Figure 4. Overexpression of the *aadB* region is sufficient to stimulate switching.** The *aadB* gene was cloned along with its native promoter into the vector pWH1266 (63) and transformed into the LSO variant. Switching to the AV-T was measured for colonies after 24 h of growth, showing that the *aadB* gene is sufficient to stimulate switching of the LSO. Data shown represent averages and SDs of at least five colonies collected in two independent experiments (\*\*\*\*,  $p \leq 0.0001$  by unpaired two-tailed t-test).

Figure 5



**Figure 5. The element responsible for stimulating switching is encoded towards the 5' end and upstream of *aadB*.** **A.** The insert in plasmid pWHaadB contains part of the 5' end of the *intI* ORF (grey rectangle), as well as the promoters for *intI* ( $P_{intI}$ , grey bent arrow) and *aadB* ( $P_c$ , green bent arrow). To determine which part of the insert was responsible for stimulating switching, pWHaadB was mutagenized with EZ-Tn5 <Kan-2>. Insertions that blocked the stimulation of switching are indicated by closed triangles, whereas insertions that did not affect sectoring are indicated by open triangles. Plasmids were then generated containing truncated inserts of different lengths to further test for the stimulation of switching in the LSO variant. The length of each plasmid insert is indicated by brackets. **B-E.** Plasmids pWHaadB-T (**B**), pWHaadB-TA (**C**), pWHaadB-TB (**D**), and pWHaadB-UP (**E**) were transformed into the LSO variant and switching to AV-T was measured for 24 h old colonies. Data shown represent

averages and SDs of six colonies collected from at least two independent experiments (\*\*\*\*,  $p \leq 0.0001$ , one-way ANOVA with Tukey's post-test).

Figure 6

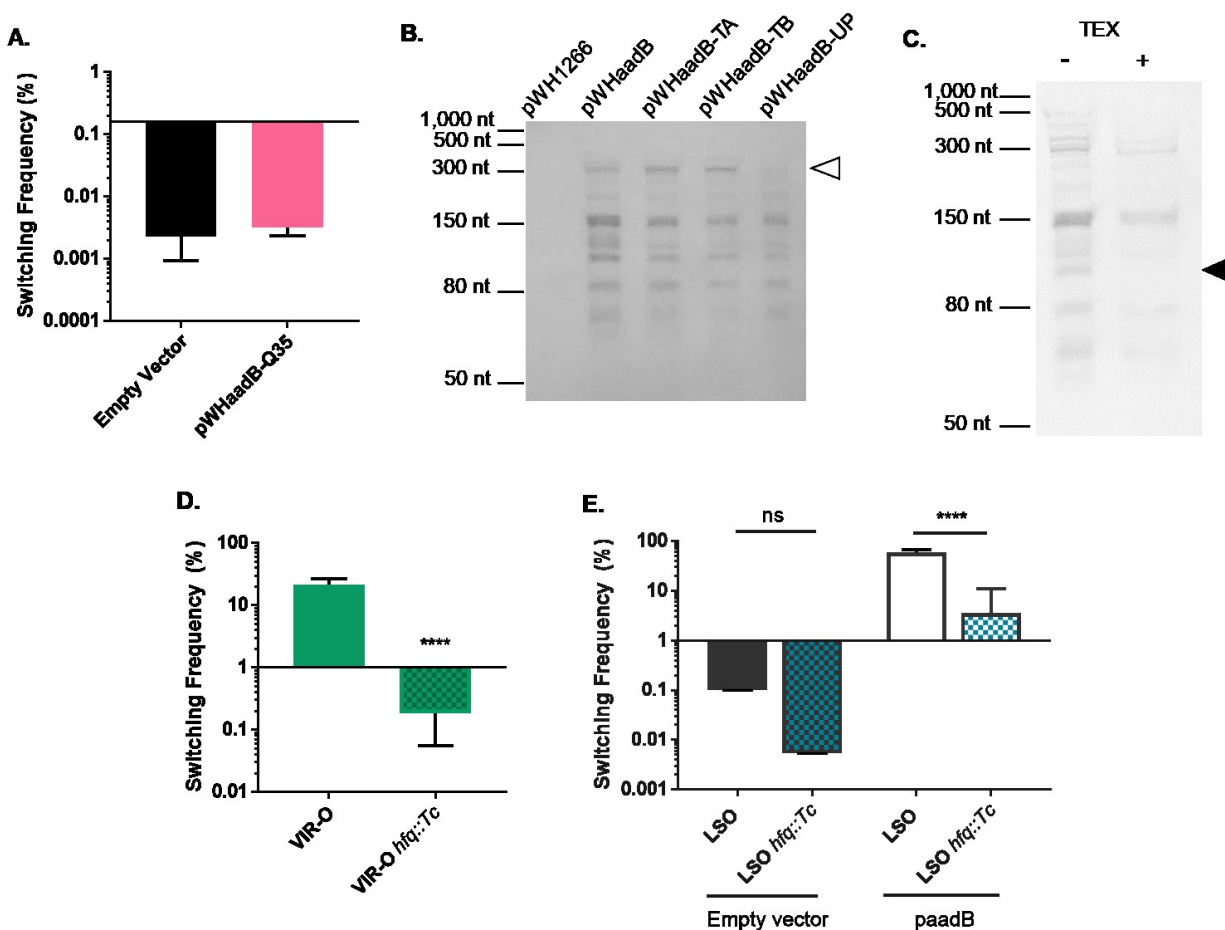


**Figure 6. Data suggest that the element controlling switching is a functional sRNA.** **A.** Two point mutations were introduced to disrupt the -35 of  $P_c$  in pWHaadB (TTGACA  $\rightarrow$  TTGAGT). The resulting plasmid (pWHaadB-Q35) no longer stimulated switching in 24 h old LSO colonies. Data represent averages and SDs for 6 colonies collected in two independent experiments (differences are not significant by unpaired two-tailed t-test). **B.** Northern blotting was performed to examine RNAs produced from overexpression plasmids transformed into LSO  $\Delta$ p1AB5075. Samples were probed with a 30 nt ssDNA probe that hybridizes 40 bp downstream

of the reported transcriptional start site for  $P_c$  (30). Five major small RNAs seem to be produced from this region in samples pWHaadB, pWHaadB-TA, and pWHaadB-TB. A ~300 nt RNA appears to be missing or reduced in sample pWHaadB-UP (white arrowhead). **C.** Northern blotting was performed to examine RNAs isolated from hetR-O2 in the presence and absence of terminator exonuclease (TEX). HetR-O2 yielded the same five small RNA species observed in **B.** TEX resulted in decreased intensity for all bands, and appeared to eliminate an RNA species of ~110 nt (black arrowhead). **D.** An insertional mutation in *hfq* was engineered in the normal VIR-O background and switching to AV-T was quantified for 24 h old colonies. **E.** An insertional mutation in *hfq* was engineered in the LSO variant. Plasmid paadB was generated by cloning *aadB* under its native promoter into pQF1266.Blue. Switching for LSO *hfq::Tc* paadB was quantified after 24 h of growth alongside controls. For **D** and **E** data represent averages and SDs from six colonies collected in two independent experiments (ns, not significant; \*\*\*\*,  $p \leq 0.0001$  by unpaired two-tailed t-test).

Figure 7

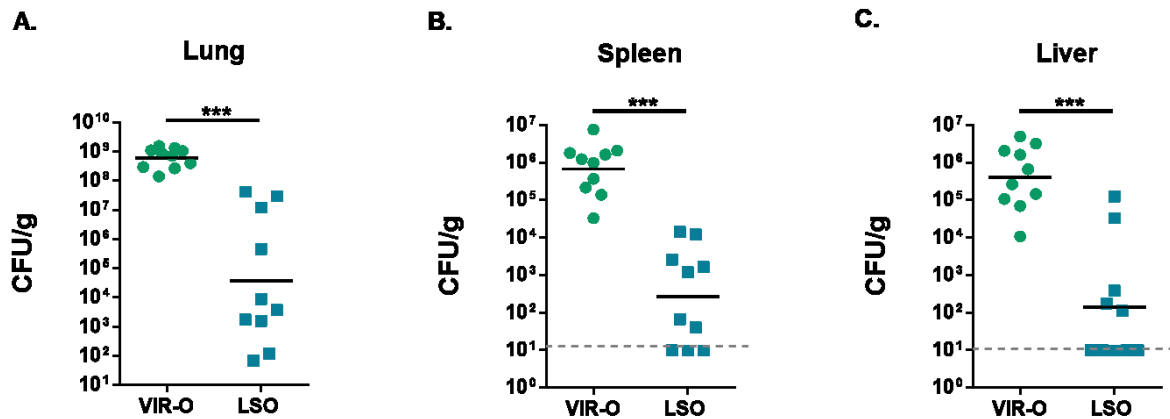


**Figure 7. The LSO variant exhibits decreased virulence in a mouse pneumonia infection model.** Mice were inoculated intranasally with  $5 \times 10^7$  CFU VIR-O or LSO bacteria and CFU were enumerated at 24 hpi. The LSO variant showed decreased colonization of the lungs and dissemination to the spleen and liver compared to the normal VIR-O. Data represent the geometric mean of CFU counts from ten mice (\*\*\*,  $p \leq 0.001$  by two-tailed Mann-Whitney test).

**Supplemental Table S1**

Variant	TOB <sup>a</sup>	GEN <sup>b</sup>	STR <sup>b</sup>
VIR-O	32	128	384
LSO	16	64	192

**Supplemental Table S1. The LSO variant exhibits decreases in antimicrobial resistance relative to the normal VIR-O.** Resistance was evaluated to the antibiotic targets of resistance genes encoded within the duplicated region on p1AB5075. Strains were directly compared by inoculating the two variants on either side of an Etest strip. Data shown are representative results from a single experiment; experiments were performed twice to assess the reproducibility of trends. <sup>a</sup>MICs were measured after 16 h of growth at 37°C. <sup>b</sup>MICs were measured after 6 h of growth at 37°C. The two variants did not exhibit a reproducible difference in resistance to chloramphenicol after 6 h of growth (data not shown). Abbreviations: TOB, tobramycin; GEN, gentamicin; STR, streptomycin.

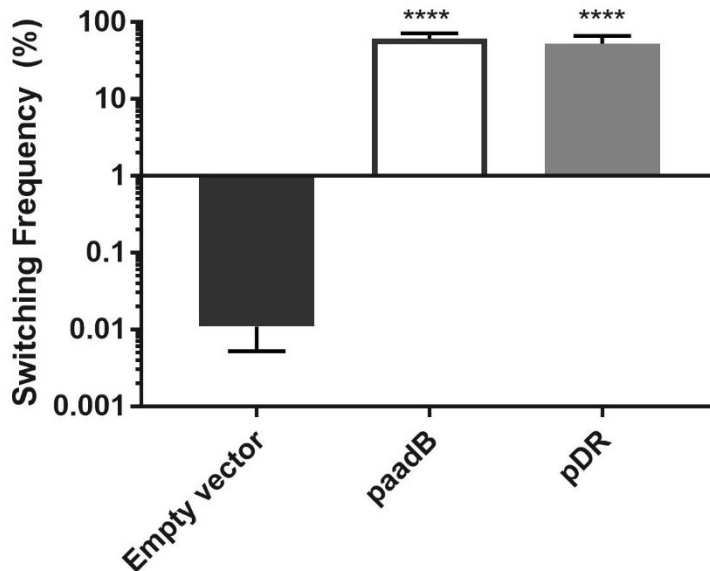
Supplemental Table S2

Oligo-nucleotide	Sequence	Use (Reference)
oSA7	ACTTTAACCGACGACGCACT	Chromosomal PCR
oSA8	TTTCACTTGGCATGAGGCGA	Chromosomal PCR
oSA61	ACTTGCCAAGCGTTTTAGCG	<i>aacA4</i> qPCR (16)
oSA62	CTTGGTTCCCAAGCCTTTGC	<i>aacA4</i> qPCR (16)
oSA65	AACTCAGCGAGGAGCCTTATTG	pWHaadB, paadB, Southern Blot
oSA66	AGAAATGCCTCGACTTCGCT	pWHaadB, paadB, pDR, pWHaadB-T, pWHaadB-A, pWHaadB-B, pWHaadB-UP, Southern Blot
oSA67	GACGCCCGTCTAACAATTTCG	p1AB5075 PCR
oSA68	CCCCTCGATGGAAGGGTTA	p1AB5075 PCR
oSA69	TCCCCGATCTCCGCTAAGAA	<i>aadB</i> qPCR (16)
oSA70	CAGATGAGCGAAATCTGCCG	<i>aadB</i> qPCR (16)
oSA79	TAGTGAGAGGTAGGGCAGCG	pDR
oSA86	TAAGCGTCAGGCAGACAAG	p1AB5075 PCR (16)
oSA87	TTTTCCA CTCTGCTGAAGG	p1AB5075 PCR (16)
oSA98	CTGCGTTGTGTCCATGC	pWHaadB-UP
oSA104	CACTCTGTCCATCGCTCCC	p1AB5075 PCR

oSA105	ATATCAGAGACGGCTTCACGC	p1AB5075 PCR
oSA134	[DIG]CCACTGCGCCGTTACCACCGCTGCGTTCGG[DIG]	Northern Blot
oSA162	CTCCATGACGCGCCCGCCGA	pWHaadB-T
oSA163	GTGTATCAATGTGACCTACGTTGTGTCCATGCGGC	pWHaadBstop
oSA164	GCCGCATGGACACAACGTAGGTCACATTGATACAC	pWHaadBstop
oSA165	CGTCAGATCAATATCATCGT	pWHaadB-TA
oSA166	ACCGATCCAGAGCGGCAG	pWHaadB-TB
oSA177	CGAACCGAACAGGCTTAACTCAACTGGGTTCGTGCC	pWHaadB-Q35
oSA178	GGCACGAACCCAGTTGAGTTAAGCCTGTTCGGTTCG	pWHaadB-Q35
abaR- qPCR-for	AAATGTCGGTTGGGCTCAGT	DNA contamination PCR
abaR- qPCR-rev	GCAATGCTGGAATGCACTGT	DNA contamination PCR
hfq-for	AAGCAAATTTGCACACTGTCTTTTT	<i>hfq</i> PCR
hfq-rev	ATTTTAAGAAACAGAGATGGACCGC	<i>hfq</i> PCR

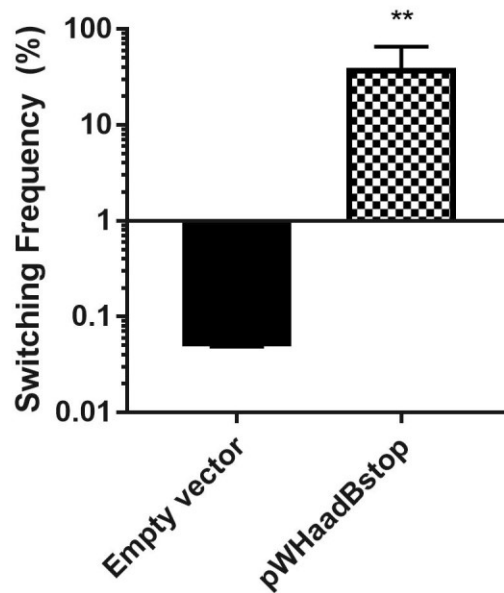
**Supplemental Table S2. Oligonucleotides used in this study.** Abbreviations: DIG, digoxigenin.

Supplemental Figure S1



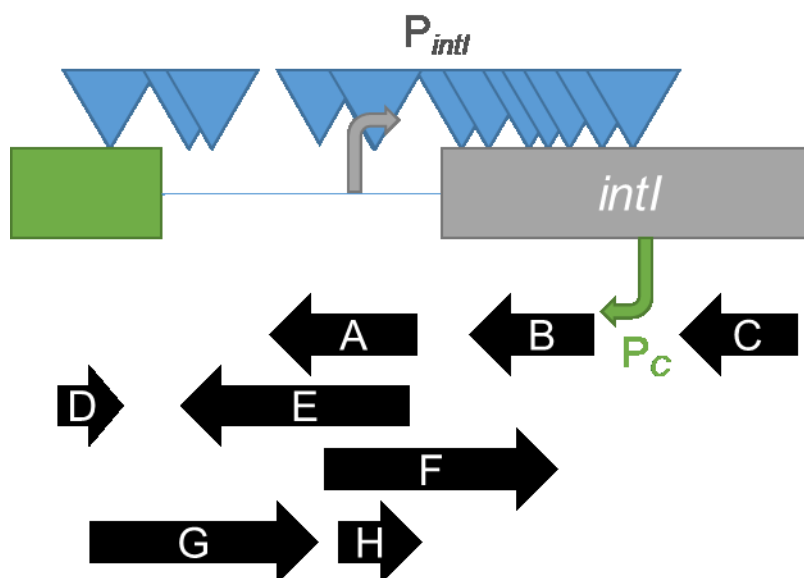
**Supplemental Figure S1. Overexpression of the entire duplicated region increases switching to the same level as overexpression of *aadB* alone.** The *aadB* gene (paadB) and the duplicated region stretching from *strB* to *aadB* (pDR) were cloned into vector pQF1266. Blue and overexpressed in the LSO variant. Switching to AV-T was measured for colonies after 24 h of growth, indicating that pDR and paadB both stimulate switching similarly compared to the empty vector control. Data shown represent averages and SDs of at least five colonies collected in two independent experiments (\*\*\*\*,  $p \leq 0.0001$ , one-way ANOVA with Tukey's post-test).

## Supplemental Figure S2



**Supplemental Figure S2. AadB protein production is not required for stimulation of switching by the *aadB* region.** A stop codon was introduced into the fifth amino acid of *aadB* on plasmid pWHaadB and the resulting plasmid (pWHaadBstop) was transformed into the LSO variant. Twenty-four h old colonies expressing pWHaadBstop still exhibited increased switching to AV-T relative to an empty vector control. Data shown represent averages and SDs of six colonies collected in two independent experiments (\*\*,  $p \leq 0.01$  by unpaired two-tailed t-test).

## Supplemental Figure S3



**Supplemental Figure S3. Transposon insertions blocking switching do not localize to any predicted ORFs encoded in the *aadB* upstream region.** The insert in pWHaadB-TB, the shortest plasmid insert that appears to stimulate switching, is shown. Sequence features are as indicated in **Fig. 5A**. Predicted ORFs in this region were identified using NCBI ORFfinder using both ATG and alternative start codons. ORFs are represented by black arrows; only ORFs completely contained within the pWHaadB-TB fragment are shown. The transposon insertions blocking switching do not align specifically with any of these ORFs, suggesting that none of these ORFs are responsible for the switching phenotype stimulated by this construct.

## Supplemental File S1

Genes upregulated in LSO (log<sub>2</sub>fold > 0.7, *p* < 0.05)

Accession Number	Gene Name	log <sub>2</sub> FoldChange (LSO/AB5075)	p value	Putative function
ABUW_1144		3.883689561	0.044048211	Val-tRNA
ABUW_3581	<i>htpG</i>	2.105399735	0.008396493	chaperone protein
ABUW_0307		1.915236361	2.27E-06	hypothetical protein (Fer2_BFD domain)
ABUW_2737	<i>clpB</i>	1.652028332	5.14E-07	ATP-dependent chaperone
ABUW_0917	<i>groS</i>	1.583078971	9.38E-06	chaperonin
ABUW_2801		1.493739341	8.03E-06	AsnC family transcriptional regulator
ABUW_2665		1.413859561	4.53E-06	hypothetical protein
ABUW_3878	<i>grpE</i>	1.408250183	5.83E-06	co-chaperone
ABUW_2783		1.361876886	0.000336722	hypothetical (DUF3237 superfamily)
ABUW_2434		1.307676955	0.024229001	hypothetical protein
ABUW_2666		1.296632111	0.000299439	hypothetical (DUF2158 superfamily)
ABUW_2785	<i>hcaG</i>	1.155392471	0.00451887	tannase and feruloyl esterase
ABUW_2865	<i>lon</i>	1.123482737	0.000746026	protease
ABUW_2478	<i>dcaA1</i>	1.079912155	0.014223704	acyl-coA dehydrogenase
ABUW_3578		1.058264225	0.000207722	DSBA oxidoreductase
ABUW_1119		0.967915879	0.000135275	peptidase S49
ABUW_0443	<i>prlC</i>	0.958449935	0.000371337	oligopeptidase a
ABUW_1536		0.939547941	0.005489398	hypothetical protein
ABUW_4064		0.923979497	0.002794675	hypothetical protein
ABUW_1630	<i>pepN</i>	0.922898648	0.001032854	peptidase M1, alanyl aminopeptidase
ABUW_1861		0.917164804	0.007233619	ring hydroxylating dioxygenase, Rieske
ABUW_2917	<i>yhgI</i>	0.91264496	0.012399318	IscR-regulated protein
ABUW_1983		0.894673322	0.000206021	hypothetical
ABUW_0037	<i>dnaJ</i>	0.888843932	0.003838192	DnaJ domain-containing protein
ABUW_1526		0.880092613	0.000615082	hypothetical protein
ABUW_2852		0.873073346	0.001039233	transcriptional regulator, MerR family
ABUW_1355		0.869824156	0.001267618	complement control module protein
ABUW_0687	<i>ecnB</i>	0.863674168	0.005679318	entericidin EcnAB
ABUW_2432		0.860870861	0.000183354	hypothetical protein
ABUW_0548		0.831468634	0.045774658	hypothetical protein

ABUW_2782	<i>hcaE</i>	0.81751426	0.000797589	porin
ABUW_1984		0.792391422	0.000862927	type 3 helix-turn-helix domain-containing protein (xenobiotic response element family of transcriptional regulators)
ABUW_3513	<i>hslO</i>	0.789111959	0.007720361	heat shock protein 33
ABUW_2655		0.784112062	0.000412555	hypothetical protein
ABUW_4098	<i>traL</i>	0.780416359	0.016974794	Type IV conjugative transfer system protein
ABUW_2429		0.779775241	0.005031434	proline dehydrogenase transcriptional activator
ABUW_3370	<i>grxC</i>	0.77056054	0.001820603	glutaredoxin 3
ABUW_2309		0.757327688	0.048049528	hypothetical protein
ABUW_0971		0.756687314	0.003855183	hypothetical protein
ABUW_1047	<i>uvrB</i>	0.755454707	0.012182054	excinuclease ABC, B subunit
ABUW_0100	<i>dtd</i>	0.751394293	0.00658284	D-tyrosyl-tRNA(Tyr) deacylase
ABUW_2589		0.751326885	0.022451392	transcriptional regulator, DUF24 family
ABUW_2178		0.750489483	0.002326278	rhizobactin siderophore biosynthesis protein RhdD
ABUW_1631		0.746629361	0.023314535	hypothetical protein (SCPU domain)
ABUW_2104	<i>aspA</i>	0.743897161	0.006120957	fumarate lyase
ABUW_2886		0.742587483	0.015669039	hypothetical protein
ABUW_4073		0.736337028	0.015821309	hypothetical protein (GrpE domain)
ABUW_1158		0.732372021	0.024679278	hypothetical protein (prevent-host-death family protein)
ABUW_3371	<i>secB</i>	0.732354272	0.001785961	protein export chaperone
ABUW_0547		0.728763453	0.00940539	hypothetical protein (TORPIM nucleotidyl transferase/hydrolase domain)
ABUW_0549		0.708883135	0.013125728	hypothetical protein (HTH XRE-family domain)
ABUW_1170	<i>basB</i>	0.707554463	0.019130201	non-ribosomal peptide synthetase
ABUW_3708		0.705279978	0.015828142	transglycosylase SLT domain protein
ABUW_3198		0.703915519	0.030622615	hypothetical protein (DUF1852 domain)
ABUW_1225		0.701295182	0.01702739	hypothetical protein (peptidase family C39 like domain)

**Genes downregulated in LSO ( $\log_2\text{fold} < -0.7, p < 0.05$ )**

Accession Number	Gene Name	log2FoldChange (LSO/VIR-O)	p value	Function
ABUW_1941		-2.410857213	0.042809	TauE-like transmembrane protein (pseudogene)
ABUW_0807		-2.262717305	0.035098	hypothetical protein
ABUW_2380	<i>tauC</i>	-2.14857002	3.01E-07	taurine transport permease protein
ABUW_1019	<i>cysT</i>	-2.075668615	1.63E-07	sulfate ABC transporter, permease protein
ABUW_2379	<i>tauD</i>	-2.065335794	7.91E-09	taurine dioxygenase
ABUW_2697		-1.94243806	6.05E-11	tRNA-Met
ABUW_1018	<i>cysW</i>	-1.804912542	2.52E-06	sulfate ABC transporter, permease protein
ABUW_2513	<i>csp2</i>	-1.794094515	3.23E-09	cold shock DNA -binding domain protein
ABUW_2696		-1.764016256	1.16E-12	hypothetical protein
ABUW_2381	<i>tauB</i>	-1.656808395	1.33E-05	taurine import ATP-binding protein
ABUW_0070	<i>fahA</i>	-1.651656492	1.60E-07	fumarylacetoacetase
ABUW_2053		-1.637522423	0.000104	pili assembly chaperone
ABUW_0273		-1.631122243	0.041557	tRNA-Glu
ABUW_2052		-1.62252175	1.24E-06	fimbrial subunit
ABUW_2690	<i>csp1</i>	-1.549672198	1.44E-05	cold-shock DNA binding domain protein
ABUW_2422		-1.532398037	0.001391	glnQ glutamate/aspartate ABC transporter
ABUW_0277		-1.515954517	0.000437	tRNA-Ala
ABUW_0069	<i>maiA</i>	-1.448206066	5.27E-05	maleylacetoacetate isomerase
ABUW_0276		-1.445801851	0.009224	tRNA-Glu
ABUW_1020		-1.435621602	0.000173	serine hydrolase
ABUW_0789		-1.432912113	0.013505	hypothetical protein
ABUW_2511		-1.419316855	0.039613	hypothetical protein
ABUW_4057	<i>aadA1</i>	-1.380911486	3.58E-08	aminoglycoside 3"-adenyltransferase
ABUW_4055	<i>strB</i>	-1.365818246	1.42E-06	streptomycin resistance protein b
ABUW_0382		-1.332808697	0.010376	hypothetical protein
ABUW_2421		-1.323175975	0.000424	ABC transporter periplasmic binding protein
ABUW_0068		-1.305223042	0.000667	glyoxalase/bleomycin resistance protein/dioxygenase
ABUW_4059	<i>cmlA</i>	-1.304119978	4.57E-08	chloramphenicol resistance protein/drug resistance transporter
ABUW_2531	<i>paaK</i>	-1.241266352	0.000193	phenylacetate coA ligase
ABUW_4056	<i>strA</i>	-1.232074135	4.23E-08	aminoglycoside phosphotransferase
ABUW_1488		-1.215089735	0.030976	CsuA spore coat protein U domain
ABUW_2813		-1.195910335	0.024101	hypothetical protein

ABUW_4042		-1.180571618	0.00043	hypothetical protein
ABUW_4061	<i>intl</i>	-1.145671553	0.008024	integrase
ABUW_2489		-1.14552372	0.008064	acyl carrier protein phosphodiesterase
ABUW_0696		-1.117759956	0.019324	tRNA-Val
ABUW_3125	<i>bfr2</i>	-1.102604965	0.002605	bacterioferritin
ABUW_0158		-1.099435359	0.000207	hypothetical protein (Gdt1 UPF0016 superfamily)
ABUW_2054		-1.0757285	0.000744	outer membrane fimbrial usher protein
ABUW_0298	<i>gltB</i>	-1.037740529	5.64E-06	glutamate synthase, large subunit
ABUW_1040		-1.015766707	0.001011	hypothetical protein
ABUW_4001	<i>repAci6</i>	-1.012722429	0.000415	replicase
ABUW_2607		-0.980473221	0.003829	hypothetical protein (MntH domain)
ABUW_2614		-0.976400146	0.002925	hypothetical protein
ABUW_2423		-0.975974658	0.032428	ArtM protein
ABUW_1329		-0.973453295	0.00657	tRNA-arg
ABUW_0381		-0.972744437	1.26E-05	DEAD/DEAH box helicase
ABUW_0201	<i>gabP</i>	-0.957253401	1.16E-05	GABA permease
ABUW_2420		-0.954608026	0.003809	ABC transporter, periplasmic binding protein
ABUW_2811		-0.945728137	0.003831	hypothetical protein
ABUW_2098	<i>atoE</i>	-0.932780062	0.002383	short-chain fatty acid transporter
ABUW_0473		-0.919930469	0.000601	hypothetical protein
ABUW_0313	<i>fimT</i>	-0.913669962	0.000919	pilin protein
ABUW_0772		-0.911065281	0.02577	hypothetical protein
ABUW_2337		-0.910301874	0.018072	luciferase-like monooxygenase
ABUW_5009		-0.90719022	0.000343	transposase component (pseudogene)
ABUW_3891		-0.904704564	0.003291	integral membrane protein TerC
ABUW_0239		-0.903450701	0.04753	hypothetical protein
ABUW_2387		-0.897606521	0.003177	hypothetical protein
ABUW_0831		-0.892114966	0.013452	ammonium transporter
ABUW_0304		-0.888270641	0.007054	type IV pilin structural subunit
ABUW_1996		-0.883603596	0.01264	hypothetical protein
ABUW_2532	<i>paaJ</i>	-0.882028269	0.018792	phenylacetate-CoA oxygenase, PaaJ subunit
ABUW_0777		-0.875848955	0.000727	phage head morphogenesis protein
ABUW_0792		-0.863820123	0.015397	hypothetical protein
ABUW_3429	<i>calB</i>	-0.852166686	0.012907	aldehyde dehydrogenase
ABUW_2533	<i>paaI2</i>	-0.839804777	0.005787	phenylacetate-CoA oxygenase, PaaI subunit
ABUW_2628	<i>pcaK2</i>	-0.82456546	0.031633	4-hydroxybenzoate transporter

ABUW_2097	<i>atoA</i>	-0.822911028	0.005989	3-oxoacid CoA-transferase, subunit B
ABUW_0306	<i>bfr1</i>	-0.820326294	0.021415	bacterioferritin
ABUW_0077	<i>hutU</i>	-0.81518017	0.037862	urocanate hydratase
ABUW_1682	<i>plc1</i>	-0.797194862	0.002637	phospholipase C, phosphocholine-specific
ABUW_1487		-0.793582724	0.016456	CsuA/B
ABUW_0203	<i>gabT</i>	-0.793477928	0.001126	4-aminobutyrate transaminase
ABUW_2630		-0.788277949	0.003768	lipid A biosynthesis lauroyl acyltransferase
ABUW_4071		-0.781652835	0.004533	hypothetical protein
ABUW_3843		-0.772726092	0.013775	putative oxidoreductase
ABUW_1299		-0.770155018	0.008493	major capsid protein
ABUW_0204	<i>gabDI</i>	-0.76735297	0.001772	succinate-semialdehyde dehydrogenase (NADP <sup>+</sup> )
ABUW_4070		-0.750759623	0.007696	hypothetical protein
ABUW_2516		-0.750358235	0.002794	hypothetical protein
ABUW_0314	<i>pilV</i>	-0.750262163	0.015493	type IV pilus modification protein PilV
ABUW_2113		-0.740040588	0.042183	succinate dehydrogenase
ABUW_4060	<i>aadB</i>	-0.736263616	0.030585	2'-aminoglycoside nucleotidyltransferase
ABUW_2096	<i>atoD</i>	-0.716922564	0.025248	3-oxoacid CoA-transferase, subunit A
ABUW_0299	<i>gltD</i>	-0.712151642	0.00089	glutamate synthase, small subunit
ABUW_2895	<i>cysN</i>	-0.701285864	0.005163	sulfate adenylyltransferase subunit 1

**Supplemental Data File S1. RNA-seq results comparing the normal VIR-O and LSO.**

Triplicate cultures of the normal VIR-O and LSO variants were grown to mid-log phase and subjected to RNA-seq. Data sets indicate genes that were significantly up- or downregulated at least 1.5-fold ( $\log_2$ fold of 0.7) in the LSO variant.

**Chapter 4: Distinguishing Colony Opacity Variants and Measuring Opacity Variation in**  
*Acinetobacter baumannii*

Sarah E. Anderson,<sup>a,b</sup> Philip N. Rather<sup>a,b,c</sup>

<sup>a</sup>Department of Microbiology and Immunology, Emory University, Atlanta, Georgia, USA

<sup>b</sup>Emory Antibiotic Resistance Center, Emory University, Atlanta, Georgia, USA

<sup>c</sup>Research Service, Atlanta VA Medical Center, Decatur, Georgia, USA

Published in:

*Acinetobacter baumannii* Methods and Protocols, 2019

Methods in Molecular Biology vol. 1946

pp. 151-158

S.E.A. wrote the manuscript with revisions from P.N.R. P.N.R. prepared the figures.

- i. Opacity Variation
- ii. Many strains of *Acinetobacter baumannii*, including the highly virulent strain AB5075, undergo a high-frequency switch that results in two cell types that are distinguished by their opaque or translucent colony opacities when viewed by oblique lighting. Opaque (VIR-O) and translucent (AV-T) colonies exhibit multiple phenotypic differences, including virulence. Here we describe how to distinguish between VIR-O and AV-T colony variants, and how to generate highly pure stocks of each variant. We also describe methods for measuring opacity switching frequencies of cells grown on agar plates and in liquid cultures.
- iii. *Acinetobacter baumannii*, opacity, phenotypic switch, opaque, translucent

## 1. Introduction

*Acinetobacter baumannii* strain AB5075, as well as many clinical isolates, undergoes a high-frequency switch that generates two cell types distinguished by their colony opacity. Opaque (VIR-O) and translucent (AV-T) colonies of *A. baumannii* appear identical under room lighting, but are easily distinguished using a dissecting microscope with oblique illumination [1]. VIR-O and AV-T variants of AB5075 exhibit a number of distinct phenotypic properties, including differing levels of motility, biofilm formation, and virulence [1,2]. While VIR-O variants are virulent in animal models, AV-T variants are unable to cause disease and are selected against *in vivo* [1,2] Opacity switching in AB5075 occurs at a high rate in both liquid cultures and on agar plates [1,2]. Although the mechanisms underlying opacity switching remain incompletely understood, it is thought that distinct mechanisms control VIR-O to AV-T and AV-T to VIR-O switches, as mutations affecting switching

frequencies in one direction often have no effect on frequencies in the other direction [3,4]. Because the VIR-O and AV-T cells exhibit differential phenotypes, it is important to control for opacity when comparing different strains of *A. baumannii* to ensure that differential phenotypes observed are actually due to the mutations being tested and not to differences in opacity between strains [5,6]. Herein we describe how to distinguish opacity variants in *A. baumannii* (Section 3.1), how to generate highly pure stocks of each variant (Section 3.2), and two easy methods for quantifying switching frequencies from colonies and liquid cultures (Sections 3.3 and 3.4, respectively).

## 2. Materials

1. 0.5x LB agar: 5 g NaCl, 5 g tryptone, 2.5 g yeast extract, 8 g agar in 1 L distilled water.
2. Dissecting microscope with oblique illumination (**Figure 1**).
3. LB broth: 10 g NaCl, 5 g tryptone, 5 g yeast extract in 1 L distilled water
4. LB agar: 10 g NaCl, 5 g tryptone, 5 g yeast extract, 15 g agar in 1 L distilled water

## 3. Methods

### 3.1. Distinguishing opaque and translucent colony types

1. Plate 10-fold serial dilutions of a glycerol stock, resuspended colony, or culture of *A. baumannii* onto 0.5x LB so that individual colonies can be distinguished (*see Note 1*).
2. Incubate plates overnight at 37°C.

3. Visualize plates on a dissecting microscope with oblique lighting (*see Note 2*).  
Colonies are easier to distinguish at lower magnification. The differences between opaque and translucent colony phenotypes are shown in **Figure 2**.

### 3.2. Generating pure stocks of opaque and translucent cells

1. Streak a stock of the strain of interest onto 0.5x LB.
2. Incubate plate overnight at 37°C.
3. Select a well-isolated colony of the desired opacity phenotype (visualized using a dissecting microscope) and passage onto a 1x LB plate (*see Note 3*).
4. Incubate the plate at 37°C for 6-8 h.
5. Using a dissecting microscope to visualize small colonies, pick 6-12 colonies and inoculate separately into LB broth (*see Note 4*).
6. Incubate cultures overnight at room temperature.
7. Cultures should be slightly turbid ( $OD_{600} < 0.1$ ), if not shake for a short period of time (*see Note 5*).
8. Using a sterile loop, streak cells from each tube onto a 0.5x LB plate to assess purity.  
Store broth cultures from step 5 above at 4°C overnight, or make glycerol stocks of all cultures and freeze at -80°C.
9. Incubate plates overnight at 37°C.
10. Using a dissecting microscope, visualize streaks of cultures to check for purity of the opacity phenotype. Only cultures that have an estimated purity of greater than 99% should be selected for further use. If broth cultures were stored overnight at 4°C, use sufficiently pure culture to make a glycerol stock and freeze at -80°C. If all cultures

were used to make glycerol stocks in step 8, dispose of stocks derived from cultures that are insufficiently pure.

### 3.3. Measuring switching frequencies of individual colonies

1. Plate 10-fold serial dilutions of pure VIR-O or AV-T glycerol stocks of the strains of interest onto 0.5x LB so that individual colonies can be isolated (*see Note 6*).
2. Incubate plates for the desired length of time at 37°C (*see Note 7*).
3. Isolate individual colonies by using a sterile toothpick to cut the agar around the colony so that a small section of agar containing the complete colony can be lifted from the plate. Transfer individual colonies to tubes containing 1 ml LB broth and vortex to resuspend cells. Typically six individual colonies should be tested for each strain (*see Note 8*).
4. Perform 10-fold serial dilutions with the isolated colonies down to a dilution of  $10^{-6}$ .
5. Plate 100  $\mu\text{l}$  of the  $10^{-3}$ ,  $10^{-4}$ , and  $10^{-6}$  serial dilutions for each colony onto 0.5x LB to obtain final dilutions of  $10^{-4}$ ,  $10^{-5}$ , and  $10^{-7}$ , respectively.
6. Incubate plates at 37° overnight.
7. Using the dissecting microscope with oblique lighting, determine the frequencies of opaque and translucent colonies from each strain.
8. If the switching frequency of the original colony taken in Step 3 was low, then the majority of the colonies from the serial dilutions will exhibit the same opacity phenotype as the original colony. The switching frequency can be determined by counting the total number of colonies of the opposite opacity phenotype on the  $10^{-4}$  or  $10^{-5}$  dilution plates. The total number of colonies of both phenotypes on the  $10^{-7}$  plate

should also be counted. The switching frequency would then be given by the following equation:

$$Frequency = \frac{(total\ colonies\ opposite\ phenotype)(plate\ dilution\ factor)}{(total\ colonies\ both\ phenotypes)(10^7)} * 100\%$$

9. If the switching frequency of the original colony taken in Step 3 was high (>10%), the switching frequency can more easily be determined by counting the number of opaque and translucent colonies on sectors of the  $10^{-5}$  plate. Sectors of the plate should be chosen that exhibit clearly defined colonies that can be easily counted. To ensure that colonies are not counted multiple times, crush colonies with a toothpick as they are being counted. At least 100 total colonies should be enumerated to ensure accuracy. Using this counting method the switching frequency would be:

$$Frequency = \frac{total\ colonies\ opposite\ phenotype}{total\ colonies\ both\ phenotypes} * 100\%$$

### 3.4. Measuring switching frequencies from liquid cultures

1. Inoculate cultures directly from highly pure frozen glycerol stocks into LB broth (*see Note 9*).
2. Incubate cultures overnight at room temperature (*see Note 10*).
3. Grow cultures at 37°C in a shaking incubator until they reach the desired OD (*see Note 11*).
4. Perform 10-fold serial dilutions of cultures. Typically a lowest dilution of  $10^{-6}$  is sufficient, depending upon the density of the culture.
5. Plate 100 µl of serial dilutions on 0.5x LB plates. Depending on the density of the original culture, final dilutions of  $10^{-4}$  through  $10^{-7}$  are typically sufficient.

6. Incubate 0.5x LB plates overnight at 37°C.
7. Enumerate colonies and determine switching frequencies as in Steps 7-9 of Section 3.3.

#### 4. Notes

1. Colony density has a profound effect on the ability to distinguish VIR-O and AV-T colonies. For unknown reasons, VIR-O and AV-T colonies are almost impossible to distinguish at low colony density. The easiest way to ensure that colonies can be easily distinguished is to plate serial dilutions yielding a range of colony densities. Similarly, it is also very hard to distinguish VIR-O and AV-T colonies grown on 1x LB plates, so it is important that 0.5x LB is used.
2. Even with oblique illumination, it can initially be difficult for the untrained eye to distinguish opaque and translucent colonies. However, adjusting the angle of the light source can often dramatically improve visualization of the two colony types. It is also important to have VIR-O and AV-T stocks as a reference
3. For unknown reasons, colonies often switch less readily on 1x LB than on 0.5x LB plates. Therefore, when trying to generate pure VIR-O or AV-T stocks, it is better to use 1x LB so that colonies will not switch while growing.
4. It is important to use very young and small colonies to inoculate when generating stocks, as switching occurs in a density-dependent manner [1]. Picking multiple colonies increases the chances that at least one culture will be mostly pure and of the desired opacity phenotype (6-8 h colonies are too small to distinguish colony opacity).

5. Because switching occurs at higher cell densities, it is important not to grow cultures past early-log phase, i.e., barely turbid to the visible eye.
6. For unknown reasons, plate thickness and moisture content can affect switching frequencies. Therefore, it is important to use plates that are roughly the same thickness and dryness across experiments to ensure reproducibility of results. We typically perform switching assays with plates made using 20 ml of 0.5x agar. Best results are also obtained if all plates used in a single experiment were generated from the same batch of media.
7. We typically perform switching assays after 24 or 48 h, but other incubation times may be used. It is important to keep the length of incubation consistent between experiments, as cell density and the age of the colony can affect switching.
8. For unknown reasons, colony density can affect the degree of switching, particularly for VIR-O colonies. Colonies at high density often switch less, and are more difficult to cut out of plates. Therefore, it is typically preferable to pick colonies off of very low density plates for switching assays. Plating serial dilutions in Step 1 allows a range of colony densities to be obtained such that colonies from similar densities can be used across all strains.
9. It is important to culture cells directly from pure stocks rather than streaking stocks on to plates and inoculating from isolated colonies. Switching will occur once colonies are grown up on plates, so the inoculum from a plate will no longer be pure. Since no stock is 100% pure, it is generally advisable to qualitatively compare that the purity of stocks to be compared are similar, so that observed differences in switching are not actually due to differences in the purity of the inoculum.

10. Minimal switching should occur during incubation at room temperature overnight.

To ensure that cultures are similarly pure before growing at 37°C, a loopful of each culture can be struck onto a 0.5x LB plate to qualitative compare purity. If there are concerns about cultures switching differently during the room temperature incubation, switching frequencies can also be quantified from overnight cultures. Switching following incubation at 37°C could then be compared to the level of overnight switching for each sample using a fold-change.

11. The OD<sub>600</sub> of the overnight cultures at room temp should be roughly similar so that the cultures spend comparable amounts of time shaking before the desired OD is reached. Typically cultures should be grown at 37°C shaking to an OD<sub>600</sub> between 1.1-1.8 to ensure that appreciable switching will have occurred. It is important that all cultures should be taken at a similar OD, and that cultures should not be grown past the desired OD and then back-diluted, as this will affect the switching frequency.

This work is supported by the following awards to P.N.R., VA Merit Award I01 BX001725, Research Career Scientist Award IK6BX004470, both the Department of Veterans Affairs, and R01AI072219 from the National Institutes of Health. S.E.A. is supported by a T32 training grant AI106699 from the National Institutes of Health.

## 5. References

1. Tipton KA, Dimitrova D, Rather PN (2015) Phase-Variable Control of Multiple Phenotypes in *Acinetobacter baumannii* Strain AB5075. *Journal of bacteriology* 197 (15):2593-2599.  
doi:10.1128/jb.00188-15
2. Chin CY, Tipton KA, Farokhyfar M, Burd EM, Weiss DS, Rather PN (2018) A high-frequency phenotypic switch links bacterial virulence and environmental survival in *Acinetobacter baumannii*. *Nature microbiology* 3 (5):563-569. doi:10.1038/s41564-018-0151-5
3. Tipton KA, Farokhyfar M, Rather PN (2016) Multiple roles for a novel RND-type efflux system in *Acinetobacter baumannii* AB5075. *MicrobiologyOpen*. doi:10.1002/mbo3.418
4. Tipton KA, Rather PN (2016) An *ompR/envZ* Two-Component System Ortholog Regulates Phase Variation, Osmotic Tolerance, Motility, and Virulence in *Acinetobacter baumannii* strain AB5075. *Journal of bacteriology*. doi:10.1128/jb.00705-16
5. Harding CM, Tracy EN, Carruthers MD, Rather PN, Actis LA, Munson RS, Jr. (2013) *Acinetobacter baumannii* strain M2 produces type IV pili which play a role in natural transformation and twitching motility but not surface-associated motility. *mBio* 4 (4).  
doi:10.1128/mBio.00360-13
6. Clemmer KM, Bonomo RA, Rather PN (2011) Genetic analysis of surface motility in *Acinetobacter baumannii*. *Microbiology (Reading, England)* 157 (Pt 9):2534-2544.  
doi:10.1099/mic.0.049791-0

## 6. **Figure legends**

**Figure 1. Examples of stereo microscopes with oblique illumination that can be used to visualize colony opacity.** Two separate microscopes that are used in our lab to visualize differences in colony opacity. It is essential to have a light source with an angle that can be adjusted to visualize the colony opacity phenotypes.

**Figure 2. Examples of translucent (AV-T), opaque (VIR-O), and switching VIR-O colonies.** A 24 hour 0.5X LB agar plate with a mixture of VIR-O, AV-T and VIR-O colonies that are switching to AV-T variants is shown.

**Figure 1**

**Figure 1. Examples of stereo microscopes with oblique illumination that can be used to visualize colony opacity.** Two separate microscopes that are used in our lab to visualize differences in colony opacity. It is essential to have a light source with an angle that can be adjusted to visualize the colony opacity phenotypes.

Figure 2

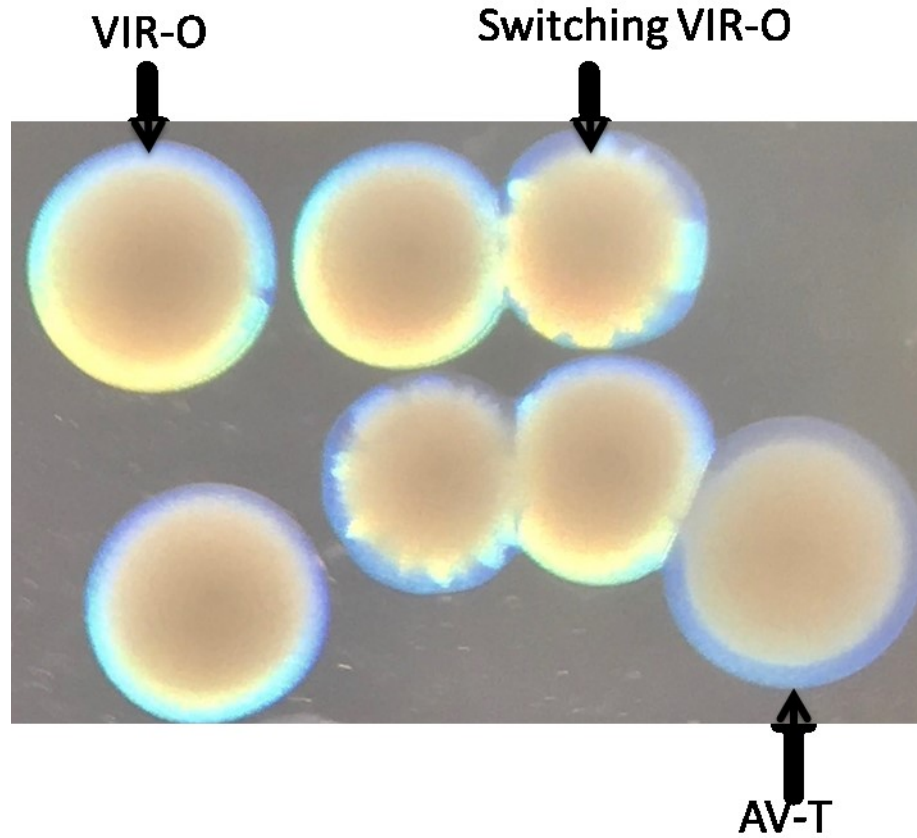


**Figure 2. Examples of translucent (AV-T), opaque (VIR-O), and switching VIR-O colonies.** A 24 hour 0.5X LB agar plate with a mixture of VIR-O, AV-T and VIR-O colonies that are switching to AV-T variants is shown.

## Chapter 5: Discussion

Population heterogeneity is an important strategy for bacterial species to quickly adapt to different environments. Isogenic bacterial strains produce phenotypically distinct subpopulations that are primed for survival in differing environmental conditions, thereby increasing the chance of survival for members of the population should conditions change. This phenomenon is known as bet-hedging (1). In this work we have characterized two distinct forms of population heterogeneity in *Acinetobacter baumannii* AB5075, aminoglycoside heteroresistance and colony opacity variation. We have established that these two forms of heterogeneity are jointly controlled by an antibiotic resistance locus on the plasmid p1AB5075, and that both phenotypes are influenced by variations in copy number of this locus (**Fig. 1**).

Heteroresistance is a type of phenotypic heterogeneity that allows a subpopulation of bacterial cells to actively grow during exposure to a concentration of antibiotic that is inhibitory to the general population (2). This is distinct from the acquisition of stable resistance, as resistant subpopulations in heteroresistant strains are typically unstable (3). It is also distinct from the formation of persisters, which are subpopulations of cells that survive, but do not grow, during antibiotic exposure (4). Heteroresistance has been reported in many bacterial species to a number of antimicrobials (3). Heteroresistance has been reported to occur through unstable mutations, including amplification of resistance genes, as well as through heterogeneous gene expression (5-9). Heteroresistance is thought to contribute to antimicrobial treatment failure (10-17), although the extent of this problem is not well understood.

Colony opacity variation has been reported for several bacterial species (reviewed in Chapter 1). In *A. baumannii*, colony opacity variation appears to be strongly linked to virulence. Virulent opaque (VIR-O) variants of *A. baumannii* predominate during human and animal

infections (18, 19). In contrast to the VIR-O variant, avirulent translucent (AV-T) variants of strain AB5075 are unable to cause disease in animal models (18, 19). While the VIR-O variant appears to be adapted to life in the host, the AV-T variant is proposed to be adapted to life in the external environment, as it forms larger biofilms and exhibits enhanced fitness in nutrient limiting conditions (18). Therefore, opacity variation is likely a bet-hedging mechanism for this opportunistic environmental pathogen to survive in the vastly different environments it encounters during infection and transmission. These variants interconvert at a high frequency under laboratory conditions; methods to measure this switching are detailed in Chapter 4 (5). The mechanism(s) underlying colony opacity variation appear to be highly complex, and are incompletely understood. Switching from VIR-O to AV-T appears to be positively regulated by the ArpAB efflux pump and negatively regulated by the OmpR/EnvZ two-component system (20, 21). The transcriptional regulator ABUW\_1645 is proposed to control maintenance of the AV-T state (18). However, currently a complete understanding of the regulatory network(s) underlying switching is lacking.

This work demonstrates that both heteroresistance to aminoglycosides and colony opacity variation are regulated by copy number of a locus carried on the plasmid p1AB5075. This locus comprises part of a composite integron known as resistance island 2 (RI-2) (22). The locus is annotated to encode five antibiotic resistance genes (*aadB*, *cmlA*, *aadA1*, and *strAB*), which are flanked by two copies of the integrase gene *intI* (22). In Chapter 2, we demonstrated that this locus undergoes spontaneous, high-level, RecA-dependent amplification, which is likely due to homologous recombination between the two *intI* alleles (23). Isolates exhibiting this amplification show elevated expression of *aadB*, which encodes an aminoglycoside adenyltransferase, resulting in increased resistance to the aminoglycosides tobramycin and

gentamicin (23). As with other forms of heteroresistance, these amplifications are unstable (23). Our work in Chapter 2 additionally suggests that a second mechanism of heteroresistance also occurs in AB5075, as a *recA::Tc* mutant still forms colonies with increased resistance that no longer exhibit amplifications of the RI-2 locus (23). In Chapter 3, we demonstrated that these high-level amplifications also result in hyperswitching from VIR-O to AV-T. Furthermore, we found that AB5075 actually forms two other predominant subpopulations of opaque colonies, which exhibit relatively stable differences in copy number of the *intI*-flanked locus. Normal VIR-O colonies, which exhibit two copies of this locus, switch to AV-T at a high frequency. On the other hand, low-switching opaque (LSO) colonies, which exhibit a single copy of the locus, exhibit a dramatic reduction in their frequency of switching to AV-T. We hypothesize that switching is regulated by an sRNA encoded towards the 5' end and upstream of *aadB*. While this putative sRNA is not required for baseline levels of switching in the LSO variant, increases in copy number to two or more result in increased switching. The sRNA is predicted to act on chromosomal target(s), as overexpression of the *aadB* upstream region still stimulates switching in a strain cured of p1AB5075. However, the target(s) of the sRNA remain to be determined. A graphic model for the co-regulation of aminoglycoside heteroresistance and opacity switching in AB5075 is presented in **Fig. 1**.

This work adds to a growing body of evidence that spontaneous gene duplications and amplifications (GDAs) are an important source of phenotypic heterogeneity in bacteria. Although the role of unstable genetic changes in phenotypic heterogeneity has long been appreciated, much of the focus in the literature has been on the phase variation mechanisms of slipped-strand mispairing and DNA inversion (24). Typically these two mechanisms function as an on/off switch for genes, or in the case of inversions, as a switch between the expression of

different alleles of the same gene (24). In contrast, GDA allows for changes in the dose of a gene product (25). GDA appears to occur quite frequently. The genome-wide frequency of tandem duplications has been measured in *Salmonella enterica* Typhimurium, and was found to be quite high, between  $10^{-5}$  and  $10^{-2}$  per cell per generation (25-28). Rapid acquisition of high-copy gene amplifications has also been reported to occur under selective pressure in species including *S. Typhimurium* and *Escherichia coli* (29-31). In some cases these amplifications were found to be RecA-dependent, similar to what was observed for the high-level amplifications reported in Chapter 2 (23, 29, 31). For a variety of bacteria, subpopulations exhibiting GDAs have been shown to exhibit enhanced survival during nutrient limitation (27, 32-35), growth *in vivo* (36, 37), and antibiotic exposure (6, 38-51).

While several reports have described strains exhibiting unstable amplifications of antibiotic resistance genes, most of these studies exhibit key differences from ours. Many studies have reported on clinical isolates that exhibit increased resistance through GDAs that appeared to occur during infection (39, 40, 43, 47-50). However, these reports do not provide information about the frequency of amplifications in the original infecting population, nor the mechanism by which the amplifications were selected, so it is unclear whether these strains would be classified as heteroresistant. Still other studies have selected for increased resistance *in vitro* using step-wise increases in drug concentration, allowing for the gradual accumulation of GDAs (41, 43, 51). Strains exhibiting GDAs following step-wise selection are likely not heteroresistant, as the resistant subpopulation in heteroresistant strains is thought to be preexisting prior to selection. A few studies have demonstrated unstable GDAs following selection in a single concentration of antibiotic *in vitro*, including in *Proteus mirabilis* (chloramphenicol) (44), *E. coli* (tetracycline, chloramphenicol, and norfloxacin; sulfathiazole)

(45, 46), *S. Typhimurium* (colistin) (6), and *Bacillus subtilis* (tetracycline) (42), although in most of these cases prolonged exposure to the antibiotics was used to select for the resistant variants (6, 45, 46). Our study in Chapter 2 was the first to demonstrate aminoglycoside heteroresistance due to a spontaneous GDA. We isolated resistant colonies containing high-level amplifications of *aadB* following a single overnight *in vitro* selection step (23), strongly suggesting that this resistant subpopulation was present prior to selection.

Following publication of our work in Chapter 2, a more broad study was published examining mechanisms of heteroresistance to a variety of antimicrobials in *E. coli*, *S. Typhimurium*, *Klebsiella pneumoniae*, and *A. baumannii* (7). This study documented aminoglycoside heteroresistance due to GDA in *E. coli* and *K. pneumoniae*. GDAs also resulted in heteroresistance to trimethoprim/sulfamethoxazole in *K. pneumoniae* and *A. baumannii*, tetracycline in *S. Typhimurium*, and cephalosporins in *S. Typhimurium*. Taken together with our work in Chapter 2, this study suggests that GDA is a widespread underlying mechanism of heteroresistance in bacteria.

Our work in Chapter 3 demonstrates a novel role for a gene duplication in regulating *A. baumannii* colony morphology and virulence. Previous studies have implicated GDAs in virulence, including in *Vibrio cholerae* and *Haemophilus influenzae* (36, 37). In both of these cases, GDAs involving genes encoding known virulence factors (cholera toxin and capsule, respectively) have been shown to be selected for *in vivo* (36, 37). In Chapter 3, the duplication described does not encompass known virulence factors, but likely increases the copy number of a proposed sRNA that appears to be involved in regulating virulence factors. Furthermore, the duplication described in Chapter 3 was not isolated by selection *in vivo*, but instead was found to preexist in our wild-type populations grown *in vitro*. Our work in Chapter 3 is, to our

knowledge, the second report linking a DNA duplication to variations in colony opacity. The mushroom pathogen *Pseudomonas tolaasii* switches between smooth, virulent, opaque colonies and rough, avirulent, translucent colonies (52). This switch is mediated via a duplication that occurs internal to the *pheN* master regulator gene, which is required for the smooth phenotype. The duplication results in reversible inactivation of *pheN*, resulting in the rough colony type (52). This obviously differs from the mechanism reported in Chapter 3 in several ways. The duplication in Chapter 3 does not disrupt any genes, and is instead hypothesized to increase the copy number of the proposed sRNA. Furthermore, this duplication does not cause the switch from the VIR-O to AV-T phenotype. Instead, the duplication increases the frequency of the VIR-O to AV-T switch. In addition, it is interesting that the duplication reported here is quite stable. While LSO and normal VIR-O colonies do interconvert, normal VIR-O populations appear to only lose the duplication at a rate of 4% after 24 h. It has been reported that duplications are typically lost at a very high frequency in the absence of selection (28), but that does not seem to be the case here.

Taken together, the results in Chapters 2 and 3 have some interesting implications for the role of the duplicated locus during infection and treatment. Based on our results, AB5075 should want to maintain a low number of duplications of this locus *in vivo*. The presence of at least two copies of this locus appears to be important for virulence, so the normal VIR-O is likely to be the predominant infecting form of AB5075. High-level amplification of the locus, as seen in the isolate hetR-O2, is likely to be selected against *in vivo*, as this leads to hyperswitching to the avirulent AV-T state. Indeed, our preliminary mouse experiments indicate that hetR-O2 is less virulent than the normal VIR-O (CY Chin, unpublished data). However, high-level amplifications may still be selected for during treatment with aminoglycosides. More work is

needed to determine whether this is the case, and whether aminoglycoside treatment leads to decreased *in vivo* fitness (even in highly resistant isolates) as a result.

It is unclear whether coupling aminoglycoside heteroresistance and the rate of VIR-O to AV-T switching is advantageous for AB5075. The normal VIR-O variant exhibits a slight increase in aminoglycoside resistance over the LSO variant, along with heightened virulence. The normal VIR-O form would be expected to be favored *in vivo*, and it is possible that coupling two sources of selective pressure (increased virulence and increased aminoglycoside resistance) helps maintain this form during infection. It is also possible that coupling hyperswitching to AV-T with high-level tobramycin resistance helps select for the AV-T form in the environment. Many antibiotics, including tobramycin, are naturally produced by members of the saprophytic genus *Streptomyces* (53). It is possible that aminoglycosides in the soil environment could help select for the AV-T form of AB5075, which is hypothesized to be more fit outside of the host (18). It is also conceivable that the co-regulation of these two processes is coincidental, but does not cause sufficient decreases in fitness to be selected against.

As discussed in Chapter 3, the prevalence of the system described here in different *A. baumannii* strains remains to be determined. RI-2 has been identified in two other sequenced *A. baumannii* strains, although in both strains it is carried on plasmids distinct from p1AB5075 (54, 55). However, as mentioned in Chapter 3, a BLAST search of the first 300 nt of the *aadB* transcript, which is hypothesized to encode the putative sRNA, yields over one hundred full or partial hits to different *A. baumannii* genomes, suggesting that this sRNA or similar transcripts may be widespread. These hits map to both plasmid-borne and chromosomal resistance islands. Our results in Chapter 3 suggest that horizontal acquisition and duplication of this element, possibly either through acquisition of a plasmid or through incorporation of the element into the

chromosome, would likely lead to increased virulence, suggesting that this element is likely to be selected for in the *A. baumannii* genome. Furthermore, as this element is genetically linked to aminoglycoside resistance genes, aminoglycosides are likely to provide a further selective pressure to ensure against loss of this element.

There are additional unanswered questions from both Chapters 2 and 3 that could be addressed in future experiments. The most intriguing question from Chapter 2 concerns the occurrence of colonies with unstably increased resistance that form in a *recA::Tc* strain. These resistant colonies do not exhibit amplifications in the *aadB* region, demonstrating that AB5075 exhibits a second mechanism of aminoglycoside heteroresistance. Future work should identify whether these colonies form through the acquisition of unstable mutations, RecA-independent GDAs, heterogeneous expression of resistance genes in the absence of mutation, or another unknown mechanism.

Several unanswered questions remain from our work in Chapter 3. Most importantly, the sequence of the proposed sRNA, its mechanism of production, and its functional target(s) remain to be determined. We are currently carrying out work to determine the sequence of the sRNA. We have obtained AB5075 sRNA sequencing results from our collaborators at the University of South Florida, which reveal a high frequency of terminating RNA reads approximately 300 nt into the *aadB* transcript (L. Shaw, *et al*, unpublished data). This matches the expected size of the sRNA reported in Chapter 3. Future studies will validate this endpoint through 5'-RACE and additional Northern blotting. We are also characterizing a number of ribonuclease mutants to determine whether any of these genes are required for production of the sRNA. Identification of the sRNA target(s) could be accomplished by a number of methods. Indirect identification of targets could be achieved using transcriptomics or proteomics in an sRNA deletion or

overexpression strain (56-61). However, such a method could potentially reveal a large pool of potential targets, many of which would likely be indirectly regulated by the sRNA, so further experimentation to confirm sRNA binding to putative targets would be required (58, 60). This method is also complicated by the fact that sRNAs can act as both positive and negative regulators (62), which could complicate the interpretation of the transcriptomics/proteomics results. Targets could instead be predicted by bioinformatic analyses (63-65), although since regions of homology between sRNAs and their targets are often quite small (66), this approach also has limitations. Methods have also been developed to purify and sequence RNA targets bound to tagged sRNAs *in vivo*, which would allow for the direct, experimental determination of targets (67). Identification of the target(s) of the proposed sRNA will be critical for understanding how the sRNA fits into the larger regulation of opacity switching and virulence in AB5075.

Future studies should also confirm the mechanism(s) underlying the decreased virulence of the LSO variant. While our RNA-seq results in Chapter 3 indicate that this variant exhibits decreased expression of known virulence genes, the role of these genes in contributing to decreased virulence in the LSO variant remains to be experimentally confirmed. The RNA-seq results should first be experimentally verified through qRT-PCR. Virulence of normal VIR-O and LSO variants exhibiting deletions (or overexpression) of these genes should then be examined to determine which gene(s) actually are responsible for the decreased virulence observed in the LSO variant.

In conclusion, this work has established a novel mechanism of co-regulation for colony opacity, virulence, and antimicrobial heteroresistance in *A. baumannii*. We have added to the understanding of a key virulence switch in *A. baumannii*, which has important implications for

the future development of virulence-targeted therapeutics for this pathogen. Our findings also have interesting implications for the effect of aminoglycoside antibiotics on virulence in *A. baumannii*. Finally, this work also underscores the importance of phenotypic heterogeneity, and in particular of gene duplications and amplifications, in bacterial populations.

## References

1. Grimbergen AJ, Siebring J, Solopova A, Kuipers OP. 2015. Microbial bet-hedging: the power of being different. *Curr Opin Microbiol* 25:67-72.
2. El-Halfawy OM, Valvano MA. 2015. Antimicrobial heteroresistance: an emerging field in need of clarity. *Clin Microbiol Rev* 28:191-207.
3. Andersson DI, Nicoloff H, Hjort K. 2019. Mechanisms and clinical relevance of bacterial heteroresistance. *Nat Rev Microbiol* doi:10.1038/s41579-019-0218-1.
4. Shah D, Zhang Z, Khodursky A, Kaldalu N, Kurg K, Lewis K. 2006. Persisters: a distinct physiological state of *E. coli*. *BMC Microbiol* 6:53.
5. Anderson SE, Rather PN. 2019. Distinguishing Colony Opacity Variants and Measuring Opacity Variation in *Acinetobacter baumannii*. *Methods Mol Biol* 1946:151-157.
6. Hjort K, Nicoloff H, Andersson DI. 2016. Unstable tandem gene amplification generates heteroresistance (variation in resistance within a population) to colistin in *Salmonella enterica*. *Mol Microbiol* 102:274-289.
7. Nicoloff H, Hjort K, Levin BR, Andersson DI. 2019. The high prevalence of antibiotic heteroresistance in pathogenic bacteria is mainly caused by gene amplification. *Nat Microbiol* 4:504-514.
8. Sanchez-Romero MA, Casadesus J. 2014. Contribution of phenotypic heterogeneity to adaptive antibiotic resistance. *Proc Natl Acad Sci U S A* 111:355-60.
9. El Meouche I, Siu Y, Dunlop MJ. 2016. Stochastic expression of a multiple antibiotic resistance activator confers transient resistance in single cells. *Sci Rep* 6:19538.

10. Band VI, Crispell EK, Napier BA, Herrera CM, Tharp GK, Vavikolanu K, Pohl J, Read TD, Bosinger SE, Trent MS, Burd EM, Weiss DS. 2016. Antibiotic failure mediated by a resistant subpopulation in *Enterobacter cloacae*. *Nat Microbiol* 1:16053.
11. Band VI, Satola SW, Burd EM, Farley MM, Jacob JT, Weiss DS. 2018. Carbapenem-Resistant *Klebsiella pneumoniae* Exhibiting Clinically Undetected Colistin Heteroresistance Leads to Treatment Failure in a Murine Model of Infection. *mBio* 9.
12. Fusco DN, Alexander EL, Weisenberg SA, Mediavilla JR, Kreiswirth BN, Schuetz AN, Jenkins SG, Rhee KY. 2009. Clinical failure of vancomycin in a dialysis patient with methicillin-susceptible vancomycin-heteroresistant *S. aureus*. *Diagn Microbiol Infect Dis* 65:180-183.
13. Lin S-Y, Chen T-C, Chen F-J, Chen Y-H, Lin Y-I, Kristopher Siu L, Lu P-L. 2012. Molecular epidemiology and clinical characteristics of hetero-resistant vancomycin intermediate *Staphylococcus aureus* bacteremia in a Taiwan Medical Center. *J Microbiol Immunol Infect* 45:435-441.
14. Sola C, Lamberghini RO, Ciarlantini M, Egea AL, Gonzalez P, Diaz EG, Huerta V, Gonzalez J, Corso A, Vilaro M, Petiti JP, Torres A, Vindel A, Bocco JL. 2011. Heterogeneous vancomycin-intermediate susceptibility in a community-associated methicillin-resistant *Staphylococcus aureus* epidemic clone, in a case of Infective Endocarditis in Argentina. *Ann Clin Microbiol Antimicrob* 10:15.
15. Charles PGP, Ward PB, Johnson PDR, Howden BP, Grayson ML. 2004. Clinical Features Associated with Bacteremia Due to Heterogeneous Vancomycin-Intermediate *Staphylococcus aureus*. *Clin Infect Dis* 38:448-451.

16. Casapao AM, Davis SL, McRoberts JP, Lagnf AM, Patel S, Kullar R, Levine DP, Rybak MJ. 2014. Evaluation of vancomycin population susceptibility analysis profile as a predictor of outcomes for patients with infective endocarditis due to methicillin-resistant *Staphylococcus aureus*. *Antimicrob Agents Chemother* 58:4636-41.
17. Claeys KC, Lagnf AM, Hallesy JA, Compton MT, Gravelin AL, Davis SL, Rybak MJ. 2016. Pneumonia Caused by Methicillin-Resistant *Staphylococcus aureus*: Does Vancomycin Heteroresistance Matter? *Antimicrob Agents Chemother* 60:1708-1716.
18. Chin CY, Tipton KA, Farokhyfar M, Burd EM, Weiss DS, Rather PN. 2018. A high-frequency phenotypic switch links bacterial virulence and environmental survival in *Acinetobacter baumannii*. *Nat Microbiol* 3:563-569.
19. Tipton KA, Dimitrova D, Rather PN. 2015. Phase-Variable Control of Multiple Phenotypes in *Acinetobacter baumannii* Strain AB5075. *J Bacteriol* 197:2593-9.
20. Tipton KA, Farokhyfar M, Rather PN. 2016. Multiple roles for a novel RND-type efflux system in *Acinetobacter baumannii* AB5075. *Microbiologyopen* doi:10.1002/mbo3.418.
21. Tipton KA, Rather PN. 2016. An ompR/envZ Two-Component System Ortholog Regulates Phase Variation, Osmotic Tolerance, Motility, and Virulence in *Acinetobacter baumannii* strain AB5075. *J Bacteriol* doi:10.1128/jb.00705-16.
22. Gallagher LA, Ramage E, Weiss EJ, Radey M, Hayden HS, Held KG, Huse HK, Zurawski DV, Brittnacher MJ, Manoil C. 2015. Resources for Genetic and Genomic Analysis of Emerging Pathogen *Acinetobacter baumannii*. *J Bacteriol* 197:2027-35.
23. Anderson SE, Sherman EX, Weiss DS, Rather PN. 2018. Aminoglycoside Heteroresistance in *Acinetobacter baumannii* AB5075. *mSphere* 3.

24. Phillips ZN, Tram G, Seib KL, Attack JM. 2019. Phase-variable bacterial loci: how bacteria gamble to maximise fitness in changing environments. *Biochem Soc Trans* 47:1131-1141.
25. Andersson DI, Hughes D. 2009. Gene amplification and adaptive evolution in bacteria. *Annu Rev Genet* 43:167-95.
26. Anderson P, Roth J. 1981. Spontaneous tandem genetic duplications in *Salmonella typhimurium* arise by unequal recombination between rRNA (*rrn*) cistrons. *Proc Natl Acad Sci U S A* 78:3113-7.
27. Sonti RV, Roth JR. 1989. Role of gene duplications in the adaptation of *Salmonella typhimurium* to growth on limiting carbon sources. *Genetics* 123:19-28.
28. Pettersson ME, Sun S, Andersson DI, Berg OG. 2009. Evolution of new gene functions: simulation and analysis of the amplification model. *Genetica* 135:309-24.
29. Andersson DI, Slechta ES, Roth JR. 1998. Evidence that gene amplification underlies adaptive mutability of the bacterial *lac* operon. *Science* 282:1133-5.
30. Tlsty TD, Albertini AM, Miller JH. 1984. Gene amplification in the *lac* region of *E. coli*. *Cell* 37:217-24.
31. Edlund T, Normark S. 1981. Recombination between short DNA homologies causes tandem duplication. *Nature* 292:269-71.
32. Ghosal D, You IS. 1988. Gene duplication in haloaromatic degradative plasmids pJP4 and pJP2. *Can J Microbiol* 34:709-15.
33. Rangnekar VM. 1988. Variation in the ability of *Pseudomonas* sp. strain B13 cultures to utilize meta-chlorobenzoate is associated with tandem amplification and deamplification of DNA. *J Bacteriol* 170:1907-12.

34. Reams AB, Neidle EL. 2003. Genome plasticity in *Acinetobacter*: new degradative capabilities acquired by the spontaneous amplification of large chromosomal segments. *Mol Microbiol* 47:1291-304.
35. Straus DS. 1975. Selection for a large genetic duplication in *Salmonella typhimurium*. *Genetics* 80:227-37.
36. Mekalanos JJ. 1983. Duplication and amplification of toxin genes in *Vibrio cholerae*. *Cell* 35:253-63.
37. Cerquetti M, Cardines R, Ciofi Degli Atti ML, Giufre M, Bella A, Sofia T, Mastrantonio P, Slack M. 2005. Presence of multiple copies of the capsulation b locus in invasive *Haemophilus influenzae* type b (Hib) strains isolated from children with Hib conjugate vaccine failure. *J Infect Dis* 192:819-23.
38. Baylay AJ, Ivens A, Piddock LJ. 2015. A novel gene amplification causes upregulation of the PatAB ABC transporter and fluoroquinolone resistance in *Streptococcus pneumoniae*. *Antimicrob Agents Chemother* 59:3098-108.
39. Chirakul S, Somprasong N, Norris MH, Wuthiekanun V, Chantratita N, Tuanyok A, Schweizer HP. 2019. *Burkholderia pseudomallei* acquired ceftazidime resistance due to gene duplication and amplification. *Int J Antimicrob Agents* 53:582-588.
40. Schechter LM, Creely DP, Garner CD, Shortridge D, Nguyen H, Chen L, Hanson BM, Sodergren E, Weinstock GM, Dunne WM, Jr., van Belkum A, Leopold SR. 2018. Extensive Gene Amplification as a Mechanism for Piperacillin-Tazobactam Resistance in *Escherichia coli*. *MBio* 9.

41. Sun S, Berg OG, Roth JR, Andersson DI. 2009. Contribution of gene amplification to evolution of increased antibiotic resistance in *Salmonella typhimurium*. *Genetics* 182:1183-95.
42. Wannarat W, Motoyama S, Masuda K, Kawamura F, Inaoka T. 2014. Tetracycline tolerance mediated by gene amplification in *Bacillus subtilis*. *Microbiology* 160:2474-80.
43. McGann P, Courvalin P, Snesrud E, Clifford RJ, Yoon EJ, Onmus-Leone F, Ong AC, Kwak YI, Grillot-Courvalin C, Lesho E, Waterman PE. 2014. Amplification of Aminoglycoside Resistance Gene *aphA1* in *Acinetobacter baumannii* Results in Tobramycin Therapy Failure. *mBio* 5.
44. Hashimoto H, Rownd RH. 1975. Transition of the R factor NR1 and *Proteus mirabilis*: level of drug resistance of nontransitioned and transitioned cells. *J Bacteriol* 123:56-68.
45. Nichols BP, Guay GG. 1989. Gene amplification contributes to sulfonamide resistance in *Escherichia coli*. *Antimicrob Agents Chemother* 33:2042-8.
46. Nicoloff H, Perreten V, Levy SB. 2007. Increased genome instability in *Escherichia coli lon* mutants: relation to emergence of multiple-antibiotic-resistant (Mar) mutants caused by insertion sequence elements and large tandem genomic amplifications. *Antimicrob Agents Chemother* 51:1293-303.
47. Brochet M, Couve E, Zouine M, Poyart C, Glaser P. 2008. A naturally occurring gene amplification leading to sulfonamide and trimethoprim resistance in *Streptococcus agalactiae*. *J Bacteriol* 190:672-80.
48. Hammond DS, Schooneveldt JM, Nimmo GR, Huygens F, Giffard PM. 2005. *bla(SHV)* Genes in *Klebsiella pneumoniae*: different allele distributions are associated with different promoters within individual isolates. *Antimicrob Agents Chemother* 49:256-63.

49. Bertini A, Poirel L, Bernabeu S, Fortini D, Villa L, Nordmann P, Carattoli A. 2007. Multicopy *blaOXA-58* gene as a source of high-level resistance to carbapenems in *Acinetobacter baumannii*. *Antimicrob Agents Chemother* 51:2324-8.
50. Hansen KH, Andreasen MR, Pedersen MS, Westh H, Jelsbak L, Schonning K. 2019. Resistance to piperacillin/tazobactam in *Escherichia coli* resulting from extensive IS26-associated gene amplification of *blaTEM-1*. *J Antimicrob Chemother* doi:10.1093/jac/dkz349.
51. Seoane A, Sanchez E, Garcia-Lobo JM. 2003. Tandem amplification of a 28-kilobase region from the *Yersinia enterocolitica* chromosome containing the *blaA* gene. *Antimicrob Agents Chemother* 47:682-8.
52. Han B, Pain A, Johnstone K. 1997. Spontaneous duplication of a 661 bp element within a two-component sensor regulator gene causes phenotypic switching in colonies of *Pseudomonas tolaasii*, cause of brown blotch disease of mushrooms. *Mol Microbiol* 25:211-8.
53. Kharel MK, Basnet DB, Lee HC, Liou K, Woo JS, Kim BG, Sohng JK. 2004. Isolation and characterization of the tobramycin biosynthetic gene cluster from *Streptomyces tenebrarius*. *FEMS Microbiol Lett* 230:185-90.
54. Mabrouk A, Grosso F, Botelho J, Achour W, Ben Hassen A, Peixe L. 2017. GES-14-Producing *Acinetobacter baumannii* Isolates in a Neonatal Intensive Care Unit in Tunisia Are Associated with a Typical Middle East Clone and a Transferable Plasmid. *Antimicrob Agents Chemother* 61:e00142-17.

55. Bonnin RA, Nordmann P, Potron A, Lecuyer H, Zahar J-R, Poirel L. 2011. Carbapenem-Hydrolyzing GES-Type Extended-Spectrum  $\beta$ -Lactamase in *Acinetobacter baumannii*. *Antimicrob Agents Chemother* 55:349-354.
56. Eyraud A, Tattevin P, Chabelskaya S, Felden B. 2014. A small RNA controls a protein regulator involved in antibiotic resistance in *Staphylococcus aureus*. *Nucleic Acids Res* 42:4892-905.
57. Landt SG, Lesley JA, Britos L, Shapiro L. 2010. CrfA, a small noncoding RNA regulator of adaptation to carbon starvation in *Caulobacter crescentus*. *J Bacteriol* 192:4763-75.
58. Ellis MJ, Trussler RS, Charles O, Haniford DB. 2017. A transposon-derived small RNA regulates gene expression in *Salmonella Typhimurium*. *Nucleic Acids Res* 45:5470-5486.
59. Frohlich KS, Forstner KU, Gitai Z. 2018. Post-transcriptional gene regulation by an Hfq-independent small RNA in *Caulobacter crescentus*. *Nucleic Acids Res* 46:10969-10982.
60. Frohlich KS, Papenfort K, Fekete A, Vogel J. 2013. A small RNA activates CFA synthase by isoform-specific mRNA stabilization. *Embo j* 32:2963-79.
61. Loh E, Dussurget O, Gripenland J, Vaitkevicius K, Tiensuu T, Mandin P, Repoila F, Buchrieser C, Cossart P, Johansson J. 2009. A trans-acting riboswitch controls expression of the virulence regulator PrfA in *Listeria monocytogenes*. *Cell* 139:770-9.
62. Dutta T, Srivastava S. 2018. Small RNA-mediated regulation in bacteria: A growing palette of diverse mechanisms. *Gene* 656:60-72.
63. Busch A, Richter AS, Backofen R. 2008. IntaRNA: efficient prediction of bacterial sRNA targets incorporating target site accessibility and seed regions. *Bioinformatics* 24:2849-56.

64. Tjaden B. 2012. Computational identification of sRNA targets. *Methods Mol Biol* 905:227-34.
65. King AM, Vanderpool CK, Degan PH. 2019. sRNA Target Prediction Organizing Tool (SPOT) Integrates Computational and Experimental Data To Facilitate Functional Characterization of Bacterial Small RNAs. *mSphere* 4.
66. Kunne T, Swarts DC, Brouns SJ. 2014. Planting the seed: target recognition of short guide RNAs. *Trends Microbiol* 22:74-83.
67. Carrier MC, Morin C, Masse E. 2018. On the Prowl: An In Vivo Method to Identify RNA Partners of a sRNA. *Methods Enzymol* 612:251-268.

Figure 1

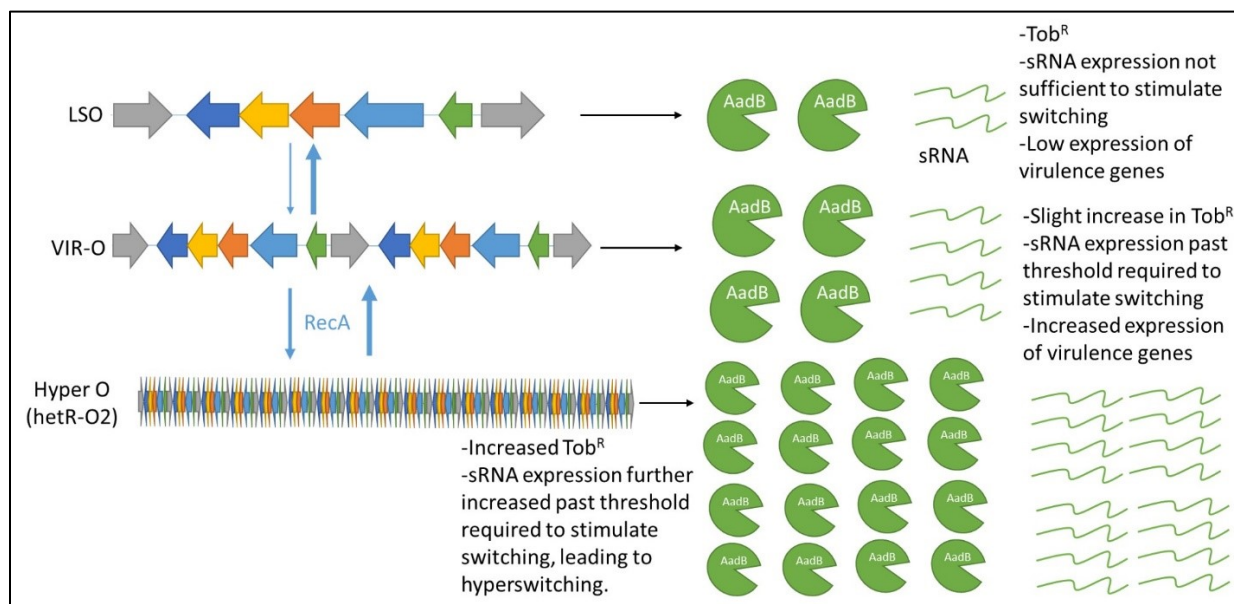


**Figure 1. A model of the mechanism of co-regulation of aminoglycoside heteroresistance**

**and opacity variation in AB5075.** The LSO variant encodes one copy of the *intI*-flanked

interval within RI-2. This interval encodes two *intI* alleles (grey arrows), *strB* (dark blue arrow), *strA* (yellow arrow), *aadA1* (orange arrow), *cmlA* (light blue arrow), and *aadB* (green arrow). In

this state, baseline levels of AadB are produced, leading to baseline levels of tobramycin

resistance. Baseline levels of the proposed ~300 nt sRNA are also produced, which are not

sufficient to stimulate switching to AV-T. The LSO variant also exhibits decreased expression of virulence genes, although the mechanism underlying this repression has yet to be determined.

The LSO variant is able to undergo a tandem duplication, presumably mediated through

homologous recombination between the two *intI* alleles, to generate the normal **VIR-O** variant.

This duplication is unstable, and will revert back to the LSO variant at a higher frequency than it is formed, as determined in Chapter 3. In the normal VIR-O state, the duplication leads to an

increase in AadB production, leading to a small increase in tobramycin resistance relative to the

LSO, as observed in Chapter 3. This also leads to increased expression of the putative sRNA,

resulting in increased switching to AV-T. The normal VIR-O state also exhibits increased expression of virulence genes relative to the LSO. In a RecA-dependent manner, the normal VIR-O variant is able to undergo further amplification of this locus to yield a **hyperswitching opaque** (hyper O) phenotype, as exemplified by the hetR-O2 isolate characterized in Chapters 2 and 3. This amplification is highly unstable. In this state, dramatic increases in copy number lead to increased expression of *aadB* and increased resistance to tobramycin and gentamicin, as described in Chapter 2. This also leads to increased putative sRNA production, resulting in hyperswitching to the AV-T state.